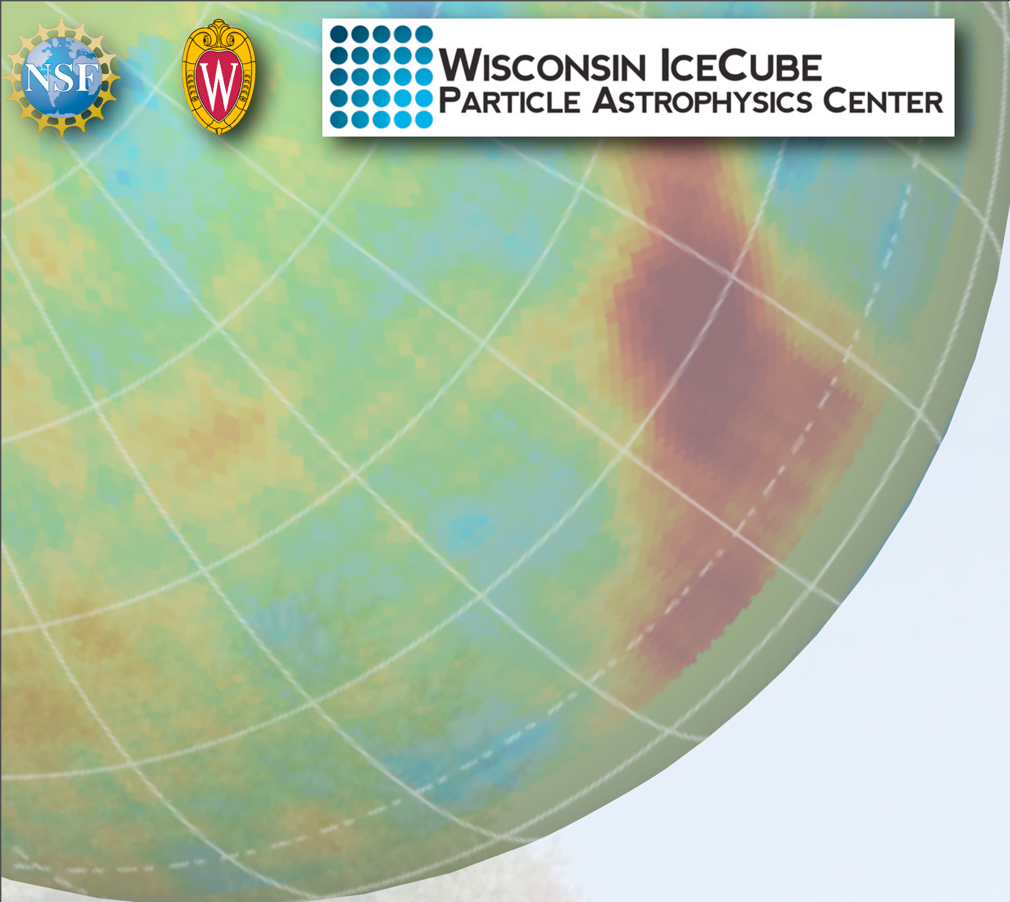

TeV cosmic ray anisotropy and the heliospheric magnetic field

Paolo Desiati[1,2] <desiati@wipac.wisc.edu>

Alexander Lazarian[2]

[1] WIPAC - Wisconsin IceCube Particle Astrophysics Center
[2] Department of Astronomy

University of Wisconsin - Madison

RUB November 8, 2013

cosmic rays
spectrum

Gaisser, Stanev, Tilav, 2013 - arXiv:1303.3565

- cosmic rays produced in the **Galaxy** below 10^8-10^9 GeV
- **spectral features** from acceleration mechanisms & propagation effects
- **source distribution** in Galaxy and our neighborhood
- **magnetic field** configurations in local interstellar medium
- cosmic ray **anisotropy**

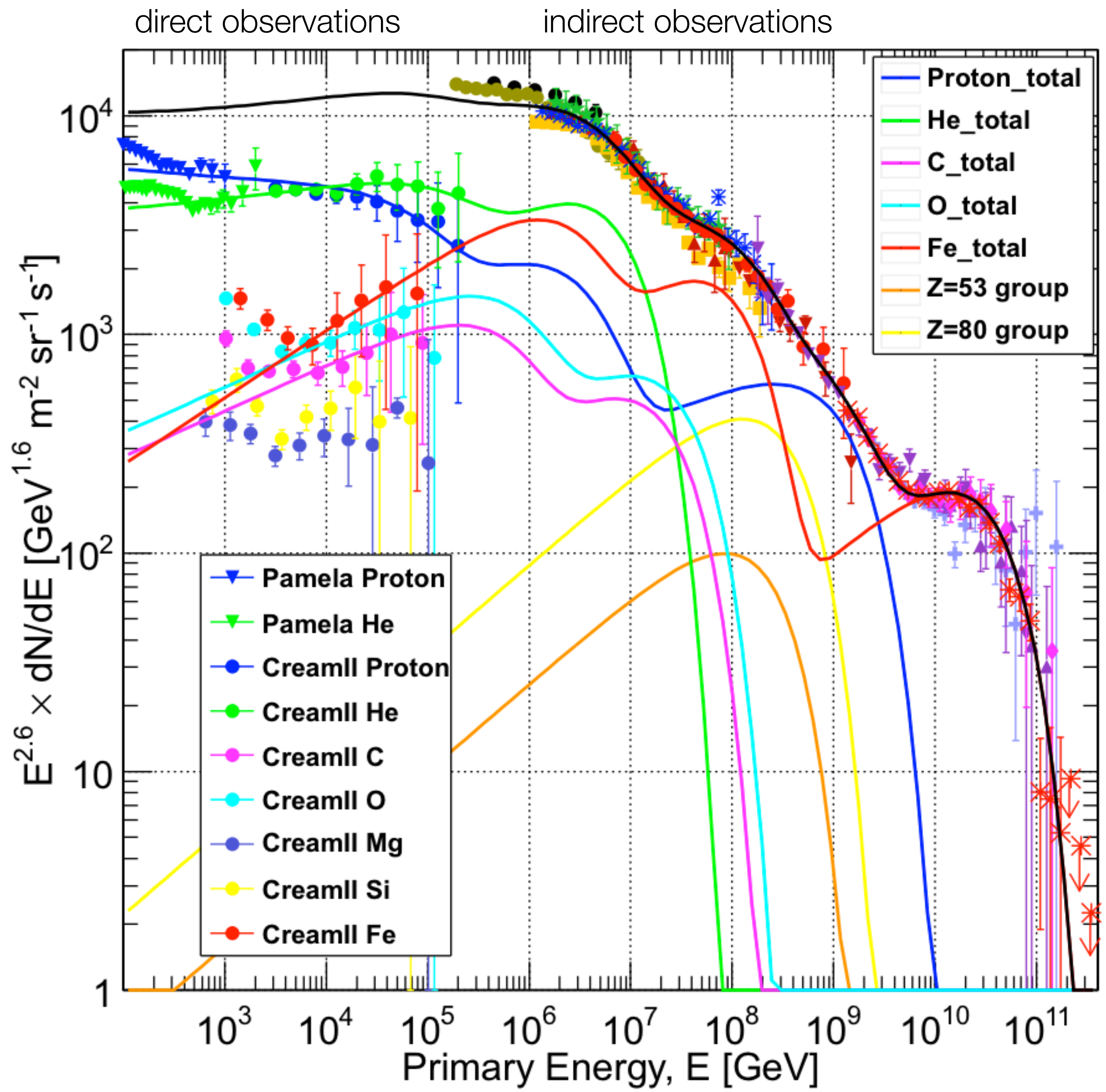

cosmic rays

composition

- varying mass composition vs energy

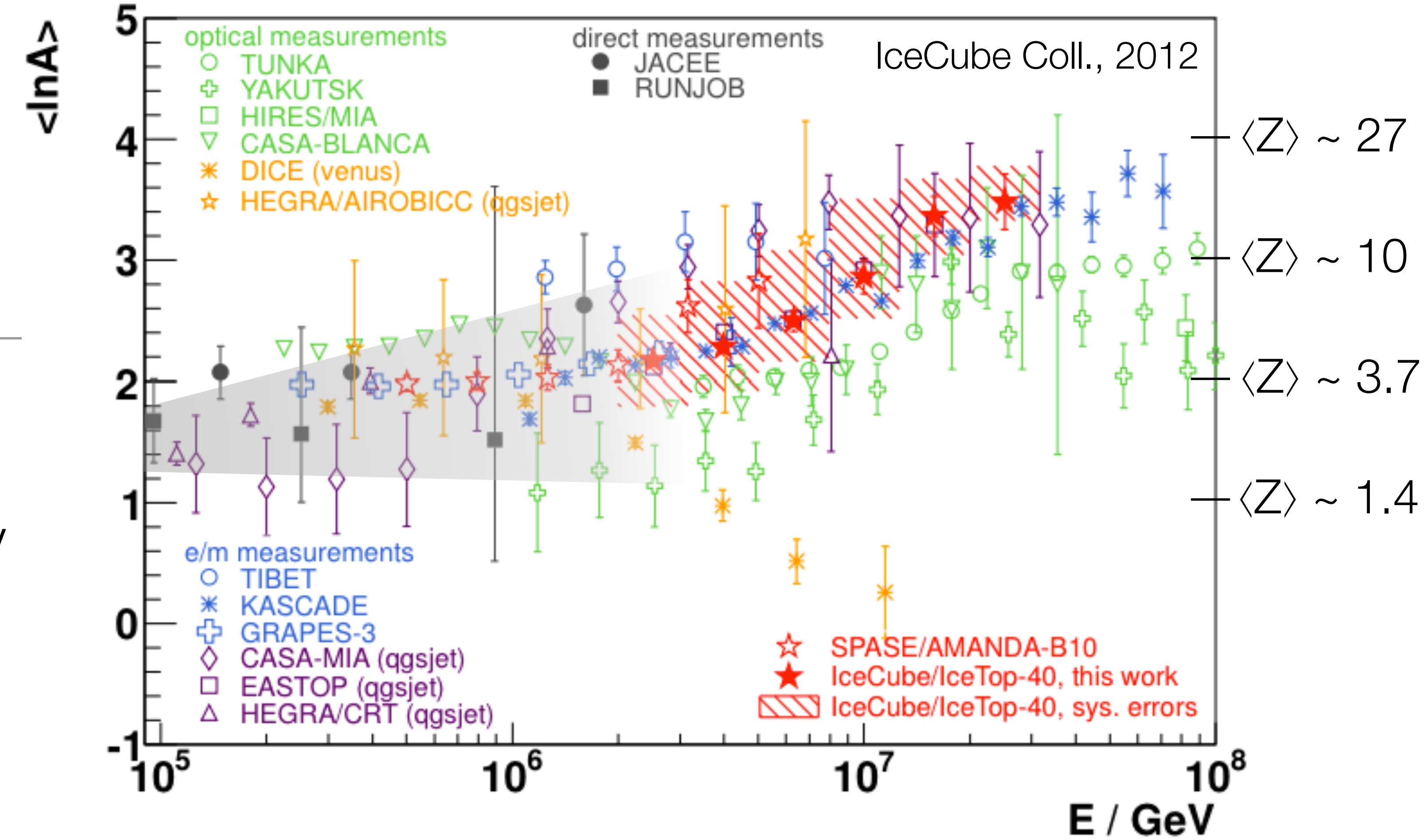

- rigidity dependent gyro-radius

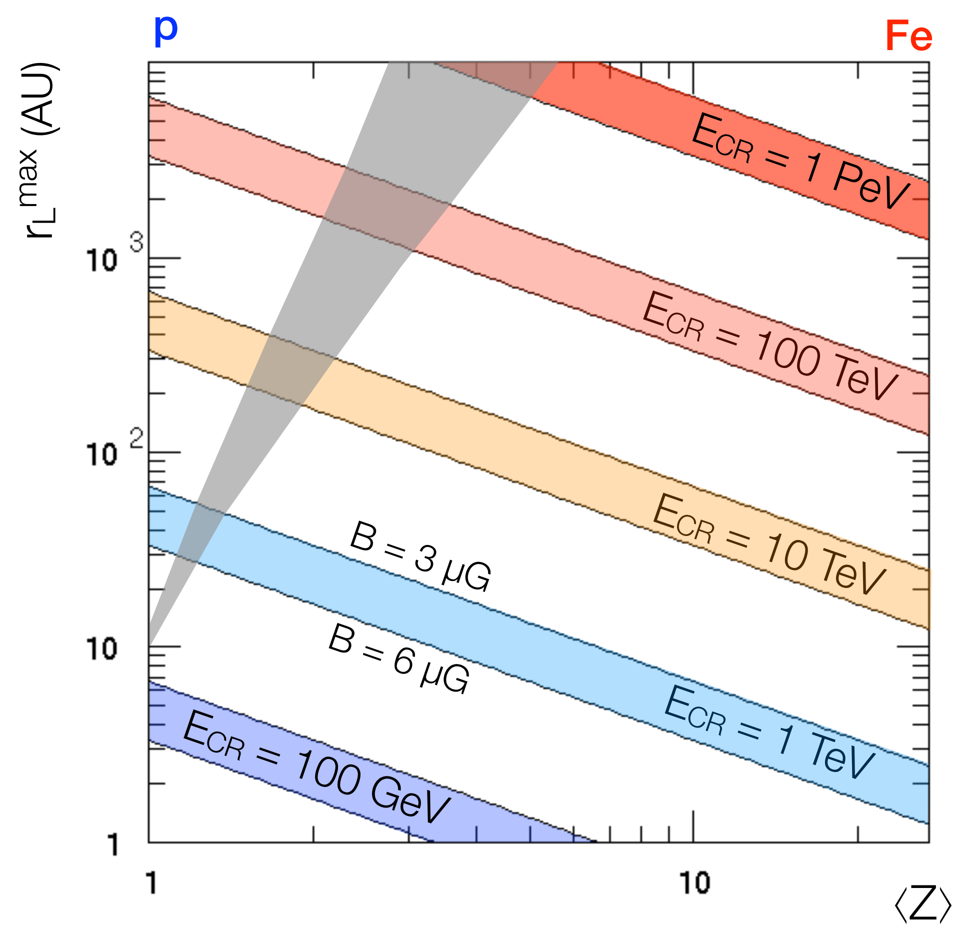

gyro-radius

$$r_L = \frac{p_\perp}{ZeB} = \frac{p}{ZeB}\sqrt{1-\mu^2}$$

$$r_L^{max} \approx \frac{200}{Z}\left(\frac{E}{TeV}\right)\left(\frac{\mu G}{B}\right) AU$$

- gyro-radius depends on mean CR charge (i.e. composition)

cosmic rays
anisotropy

equatorial coordinates

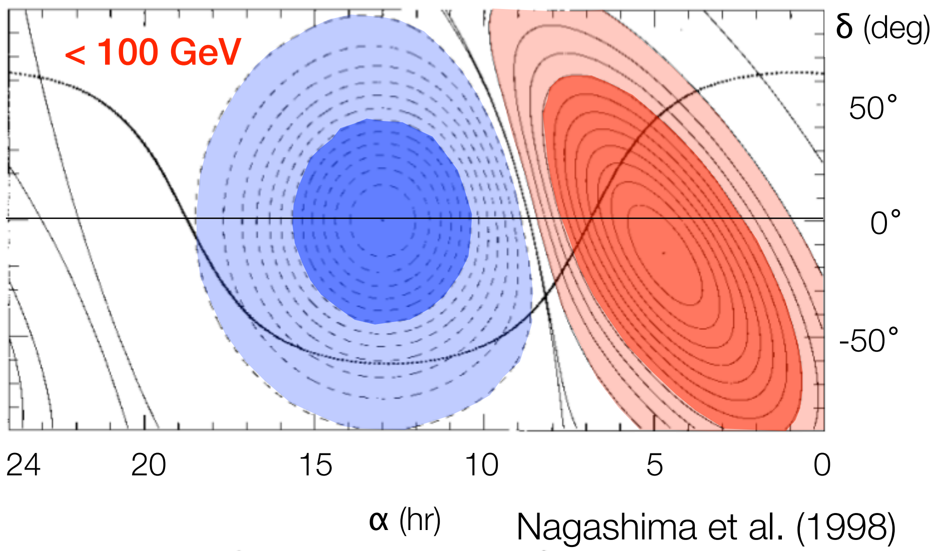

Nagashima et al. (1998)
Hall et al. (1999)

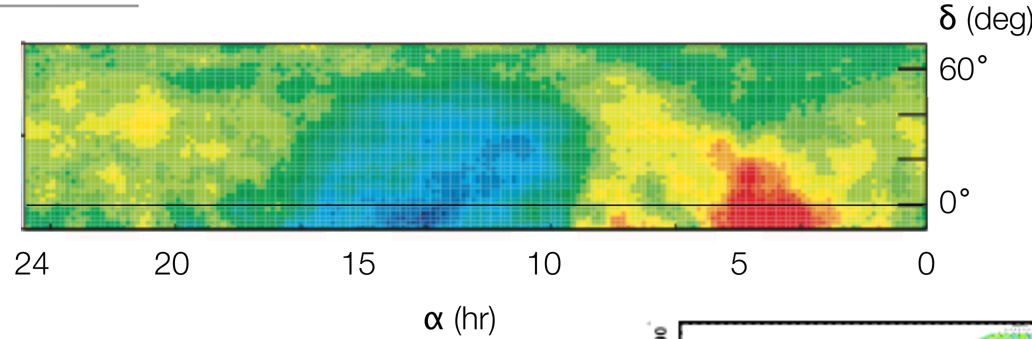

4 TeV
Tibet ASγ
Amenomori et al. (2006)

tail-in excess

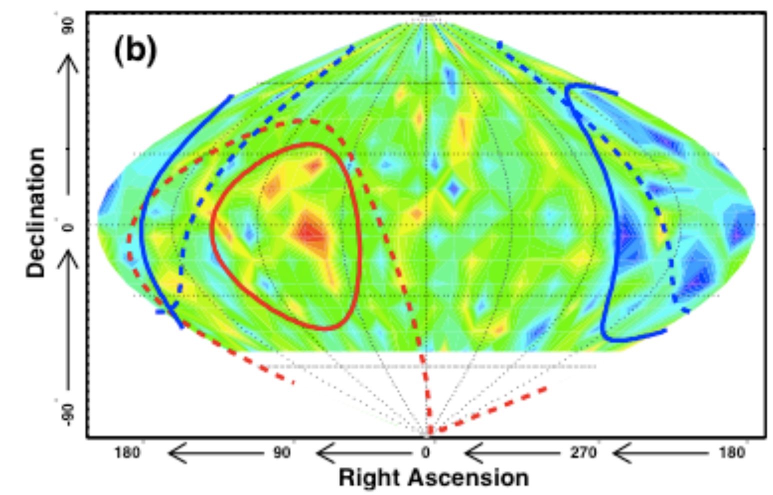

10 TeV
Super Kamiokande
Guillian et al. (2007)

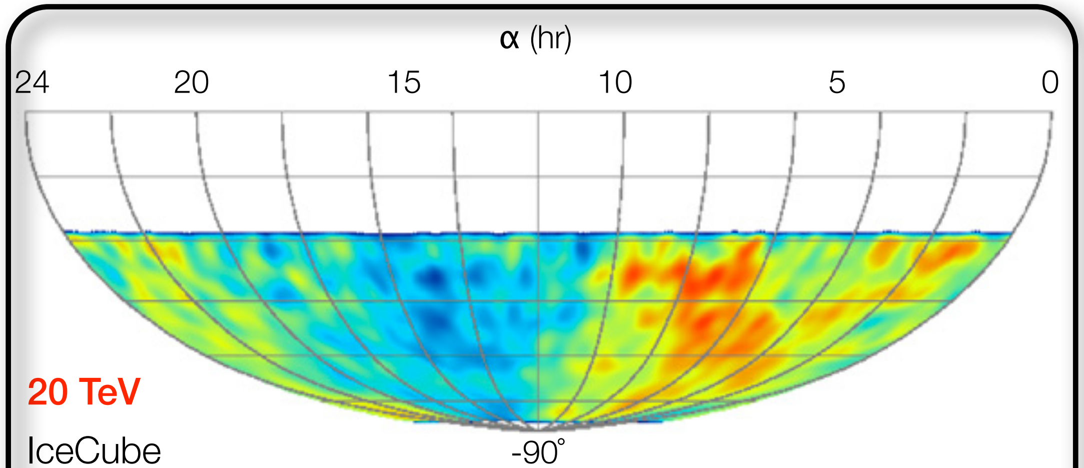

20 TeV
IceCube
Abbasi et al. (2010)

4 TeV
ARGO-YBJ
Zhang et al. (2009)

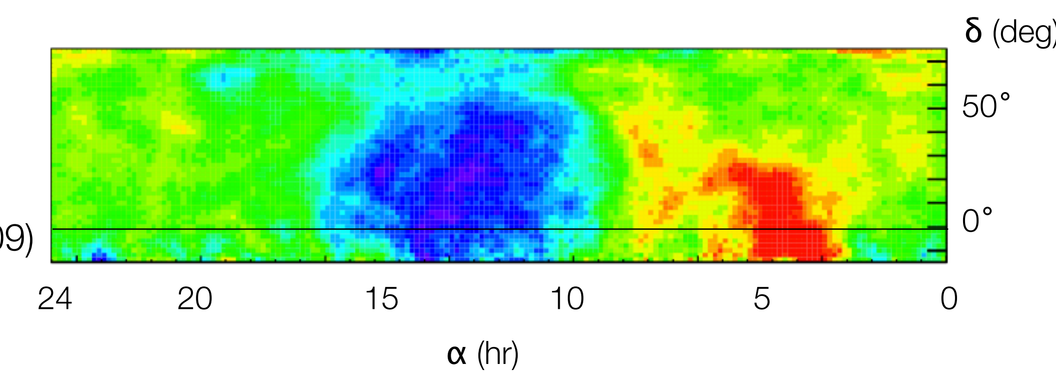

5 TeV
Milagro
Abdo et al. (2009)

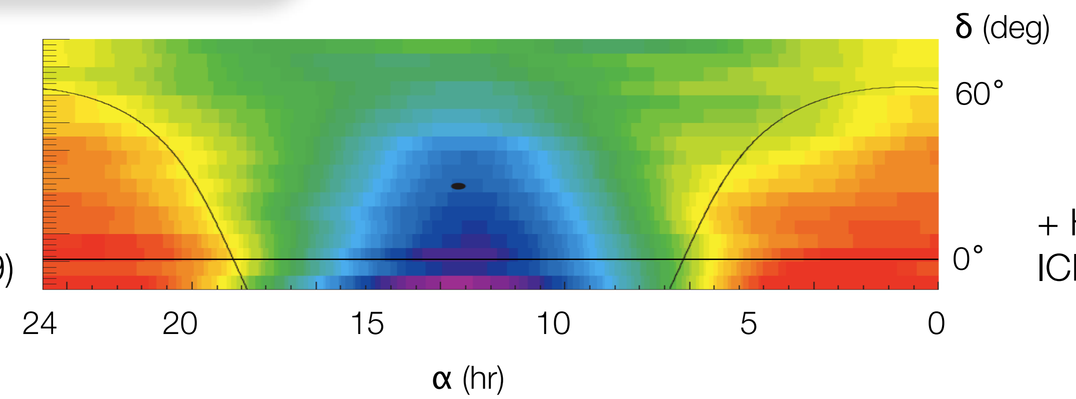

+ HAWC
ICRC 2013

cosmic ray anisotropy

structural complexity

- significant **small angular scale** features ~10x smaller amplitude over global anisotropy
- the **tail-in excess region** composed of smaller structures above TeV energy
- observation of **spectral anomalies** associated to localized excess regions (Milagro, ARGO-YBJ)

Tibet-III (global fit) Amenomori et al. (2006)

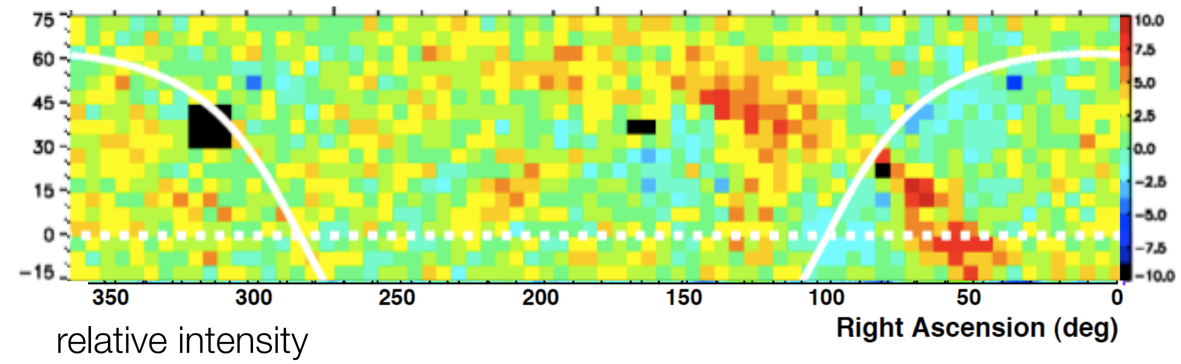

relative intensity

Milagro (direct integration) Abdo et al. (2008)

+ HAWC

ICRC 2013

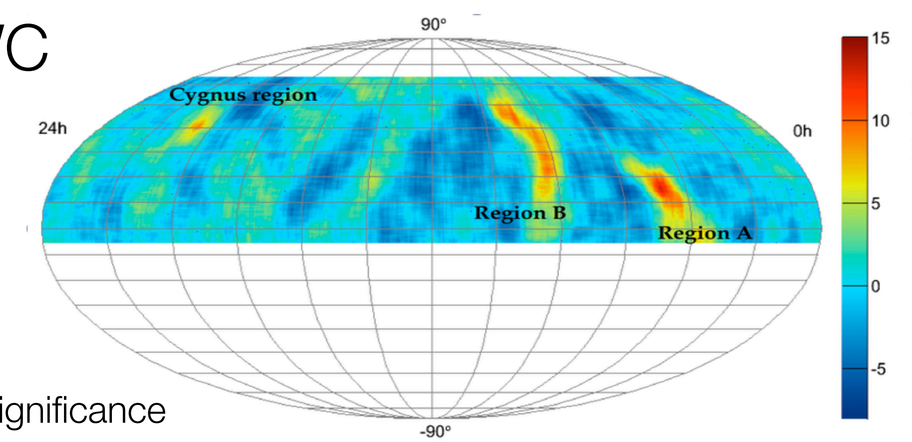

statistical significance

ARGO-YBJ (time scrambling) Vernetto et al. (2009) Iuppa et al. (2011)

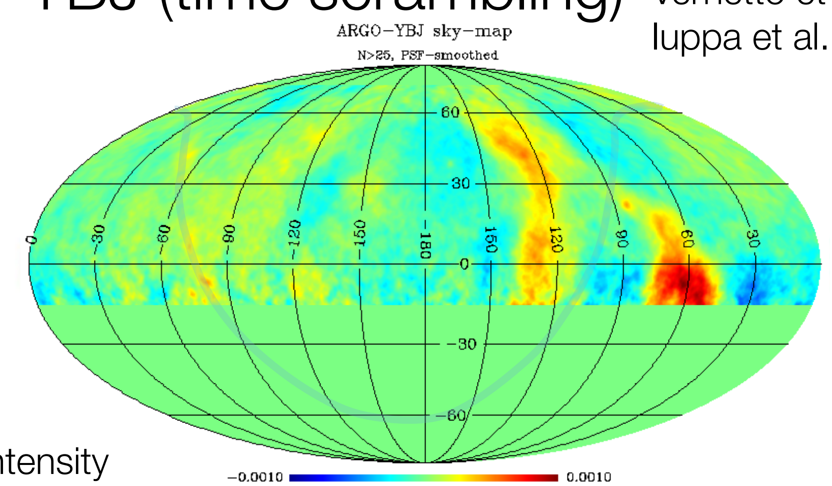

relative intensity

cosmic ray anisotropy large scale

Abbasi et al., ApJ, **718**, L194, 2010
Abbasi et al., ApJ, **746**, 33, 2012
Aartsen et al., ApJ, **765**, 55, 2013

relative intensity equatorial coordinates

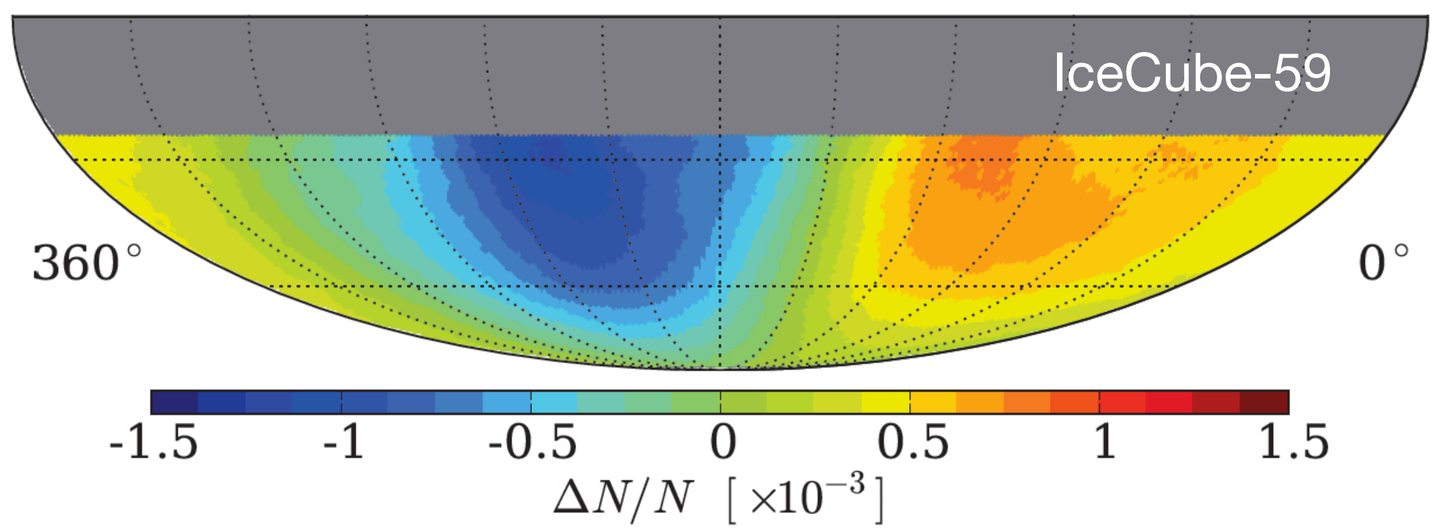

20 TeV

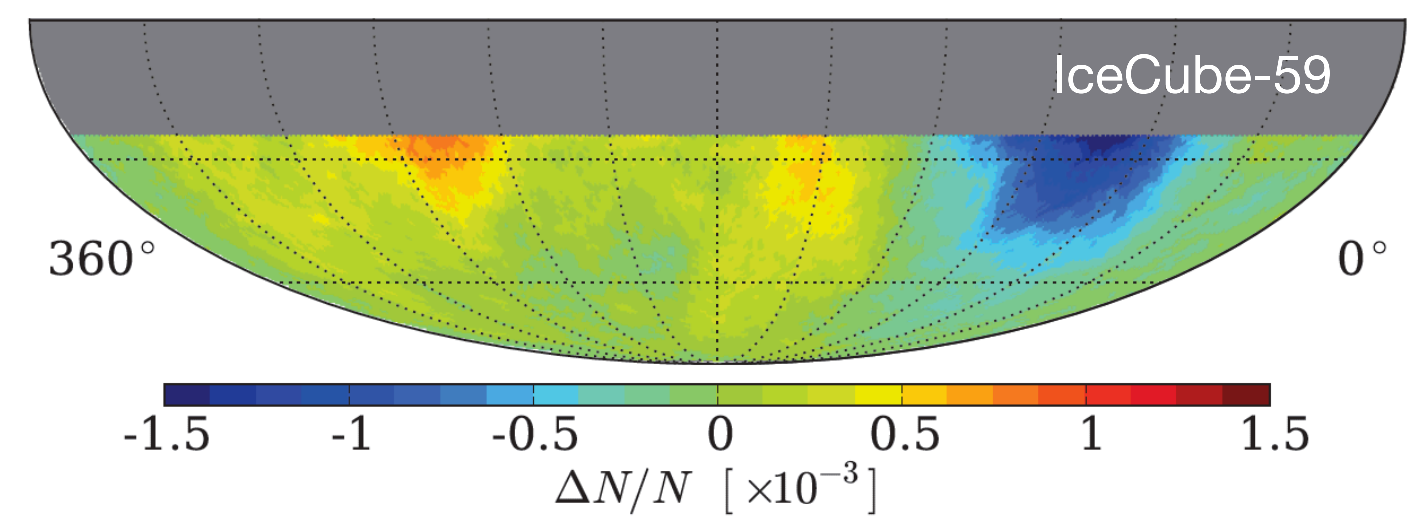

400 TeV

deficit
6.3 σ

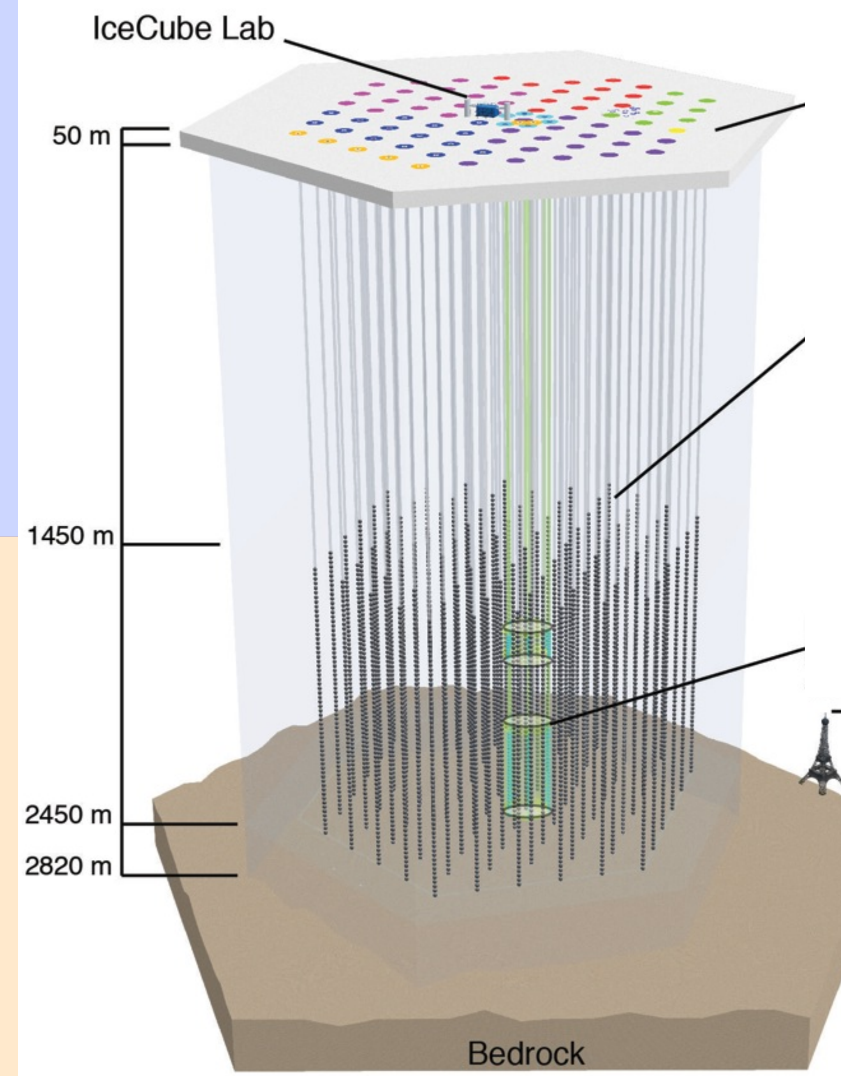

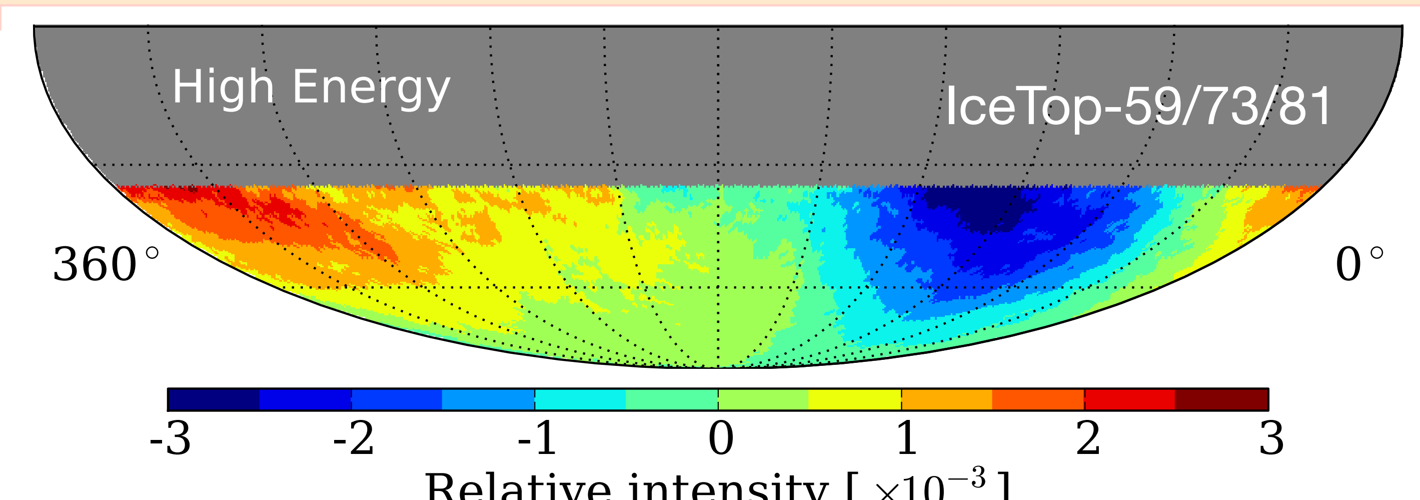

2 PeV

deficit
7 σ

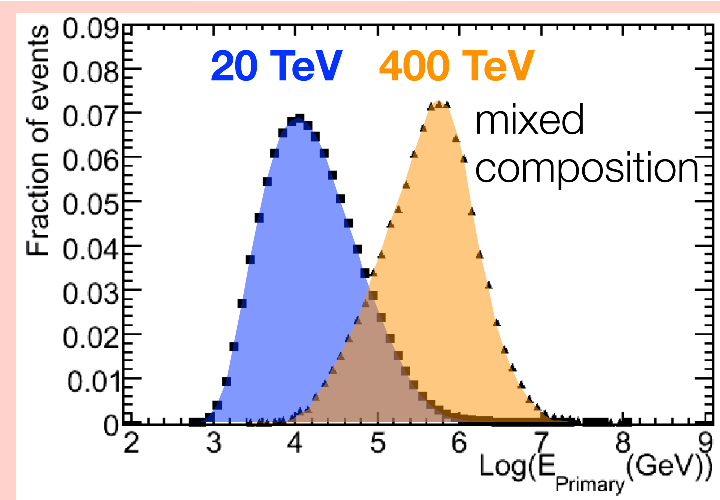

cosmic ray anisotropy large scale

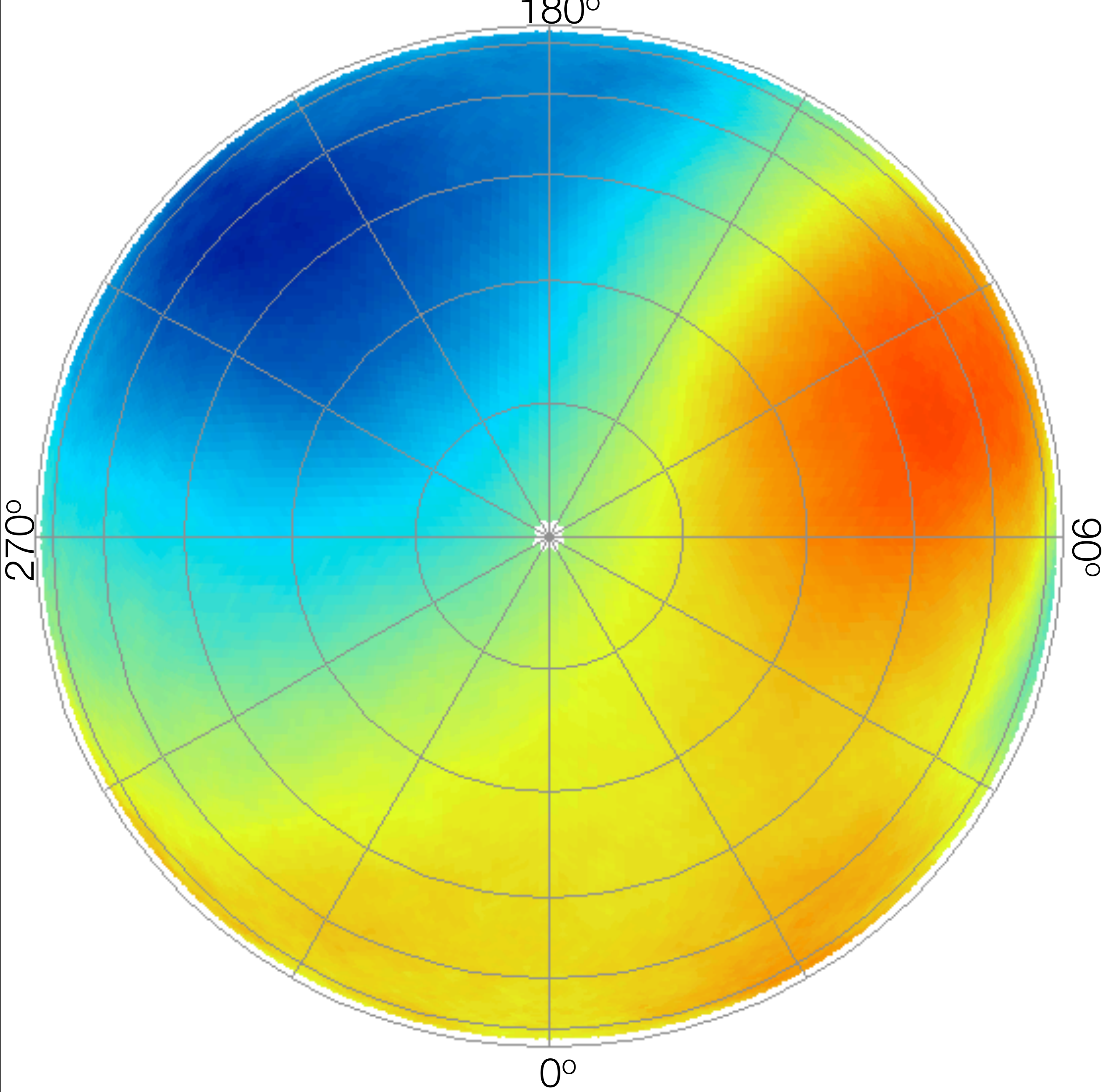

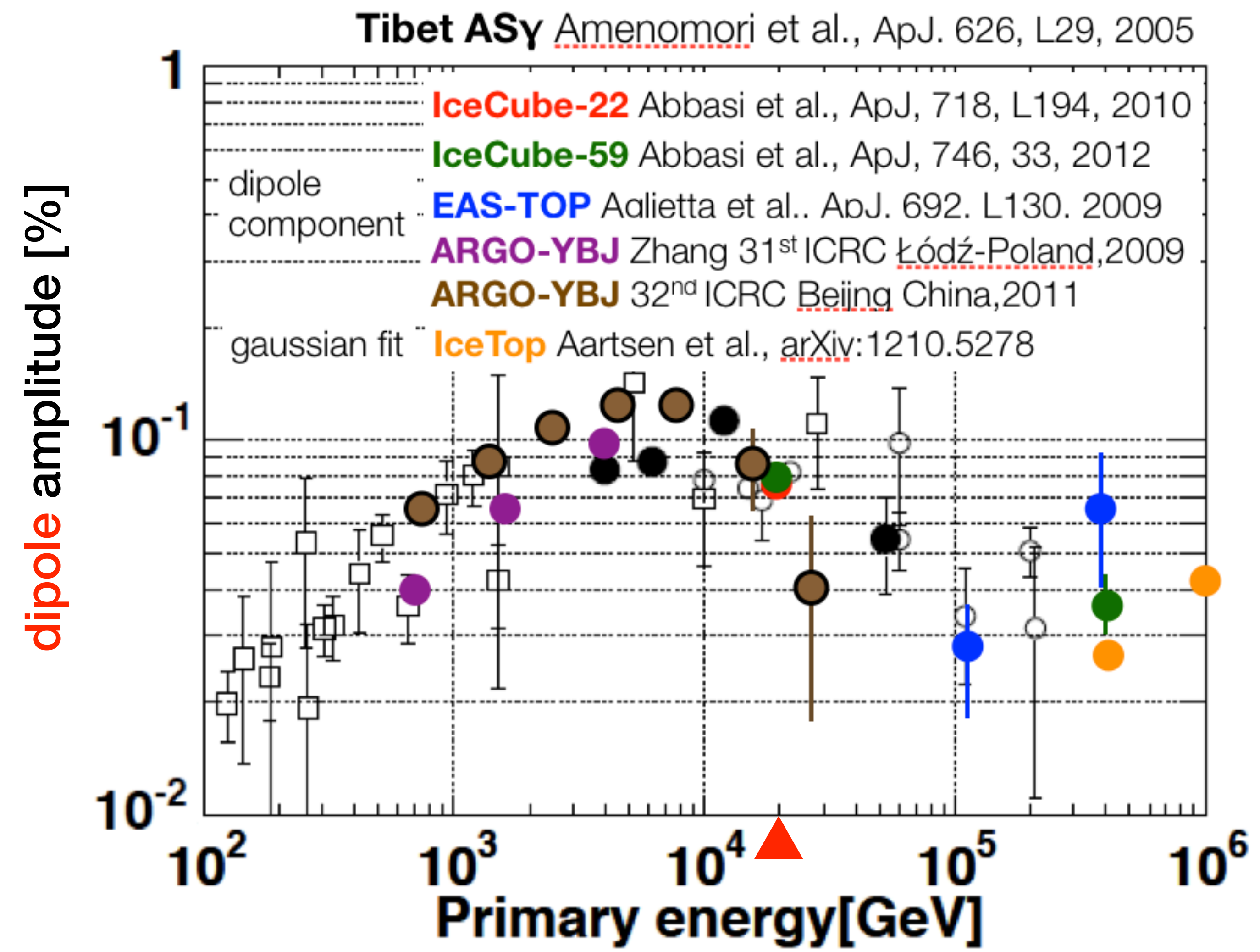

- NOT a dipole change of **phase**
- BUT a structural **modification**

cosmic ray anisotropy large scale

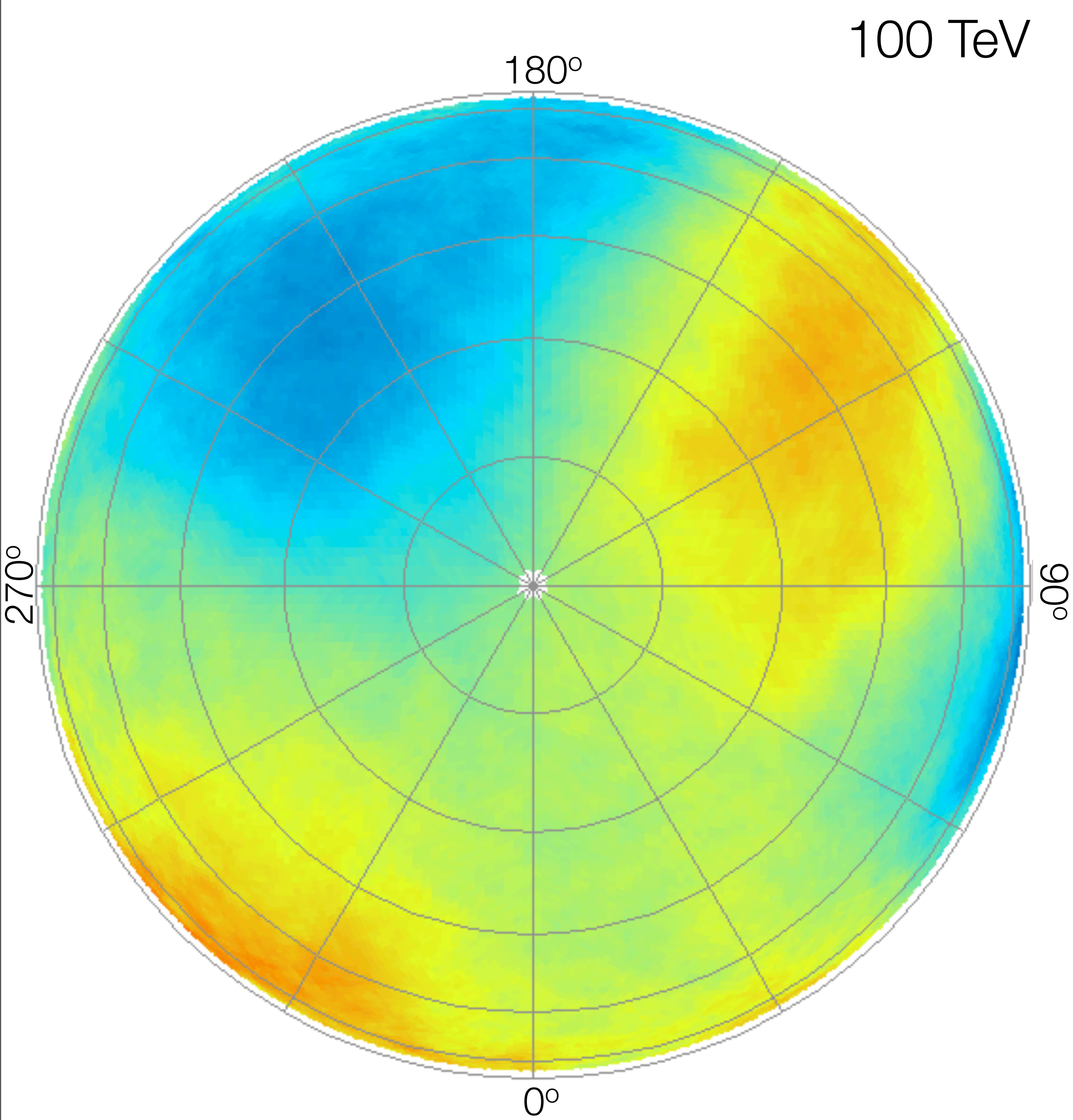

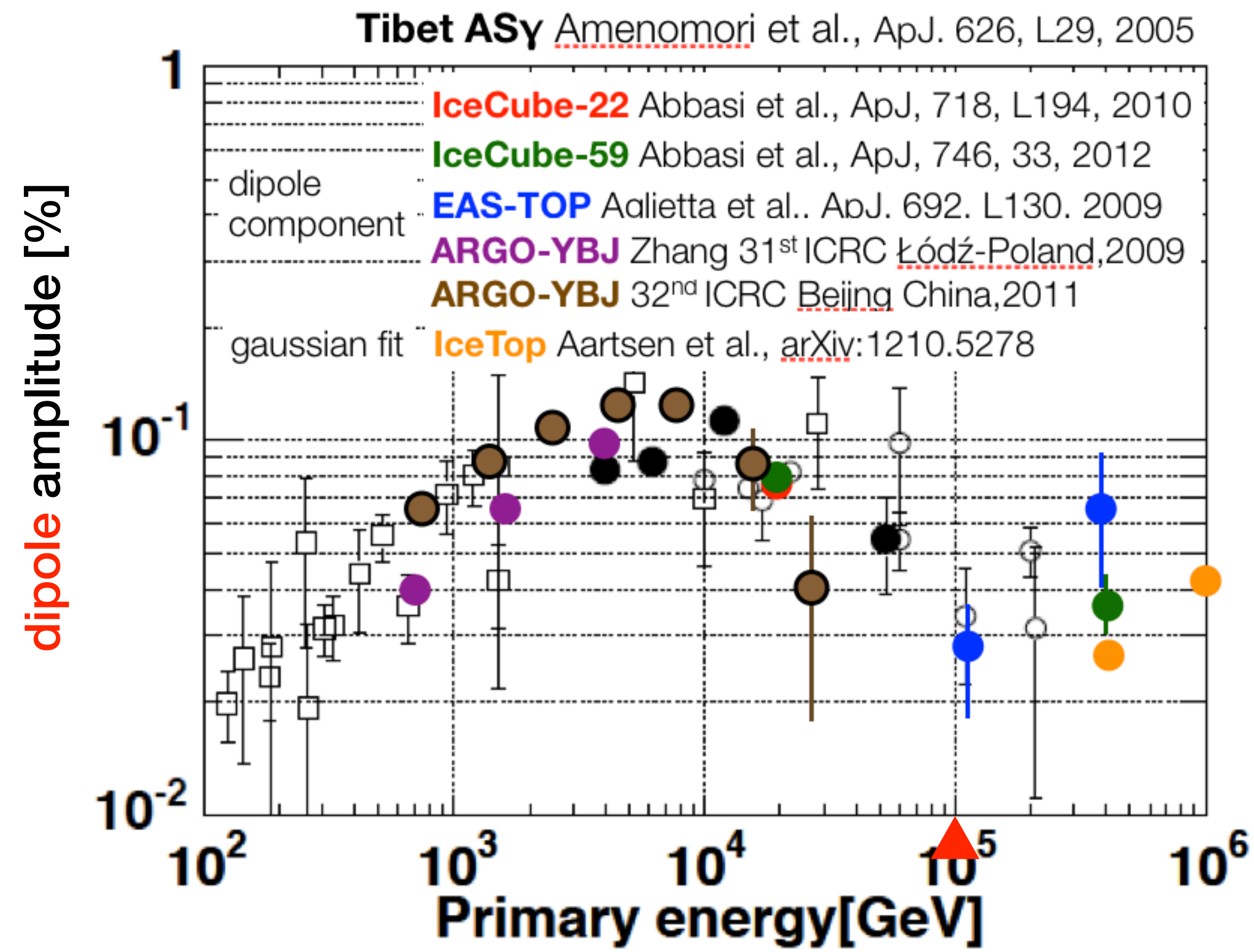

- NOT a dipole change of **phase**
- BUT a structural **modification**

cosmic ray anisotropy large scale

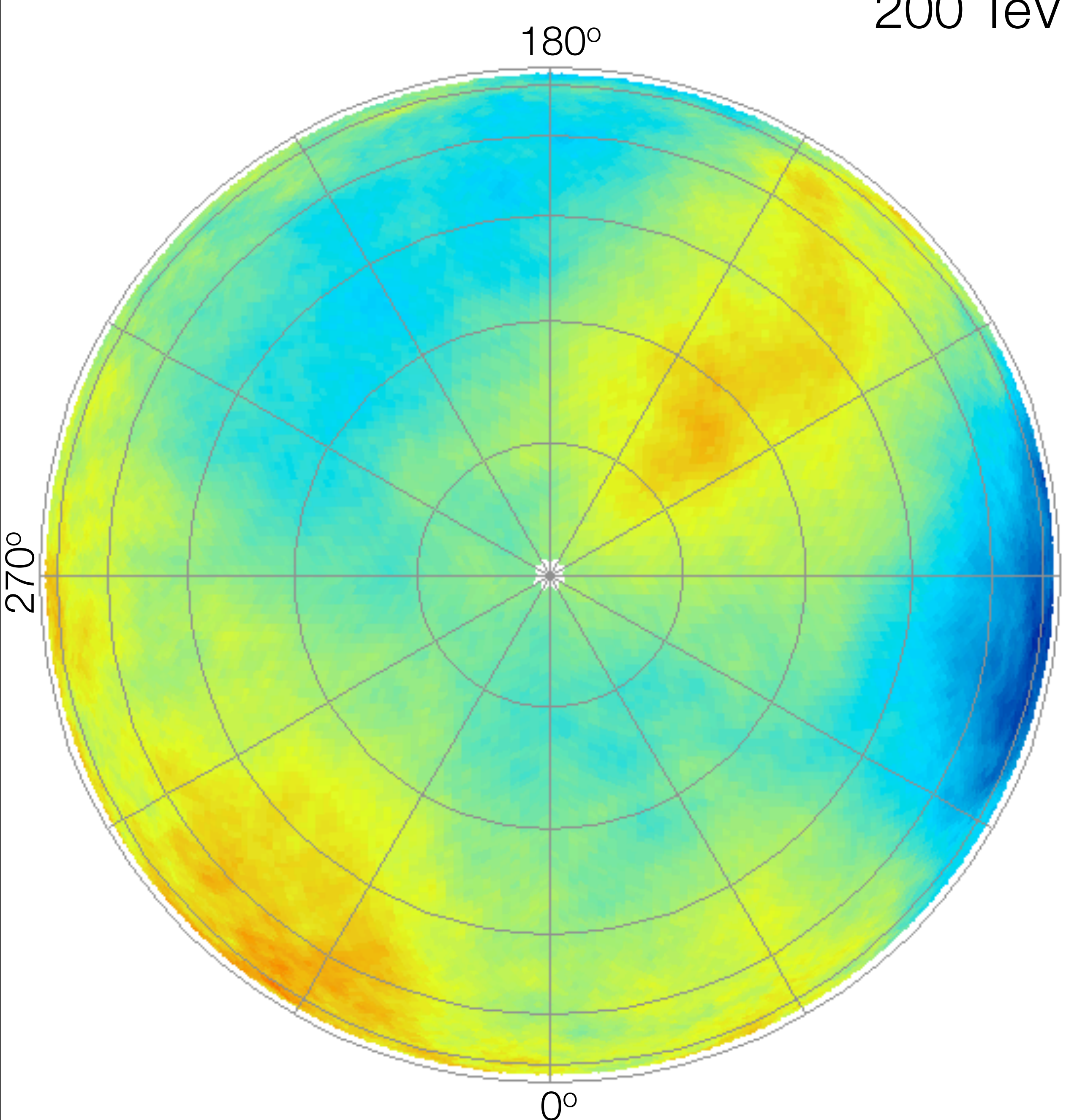

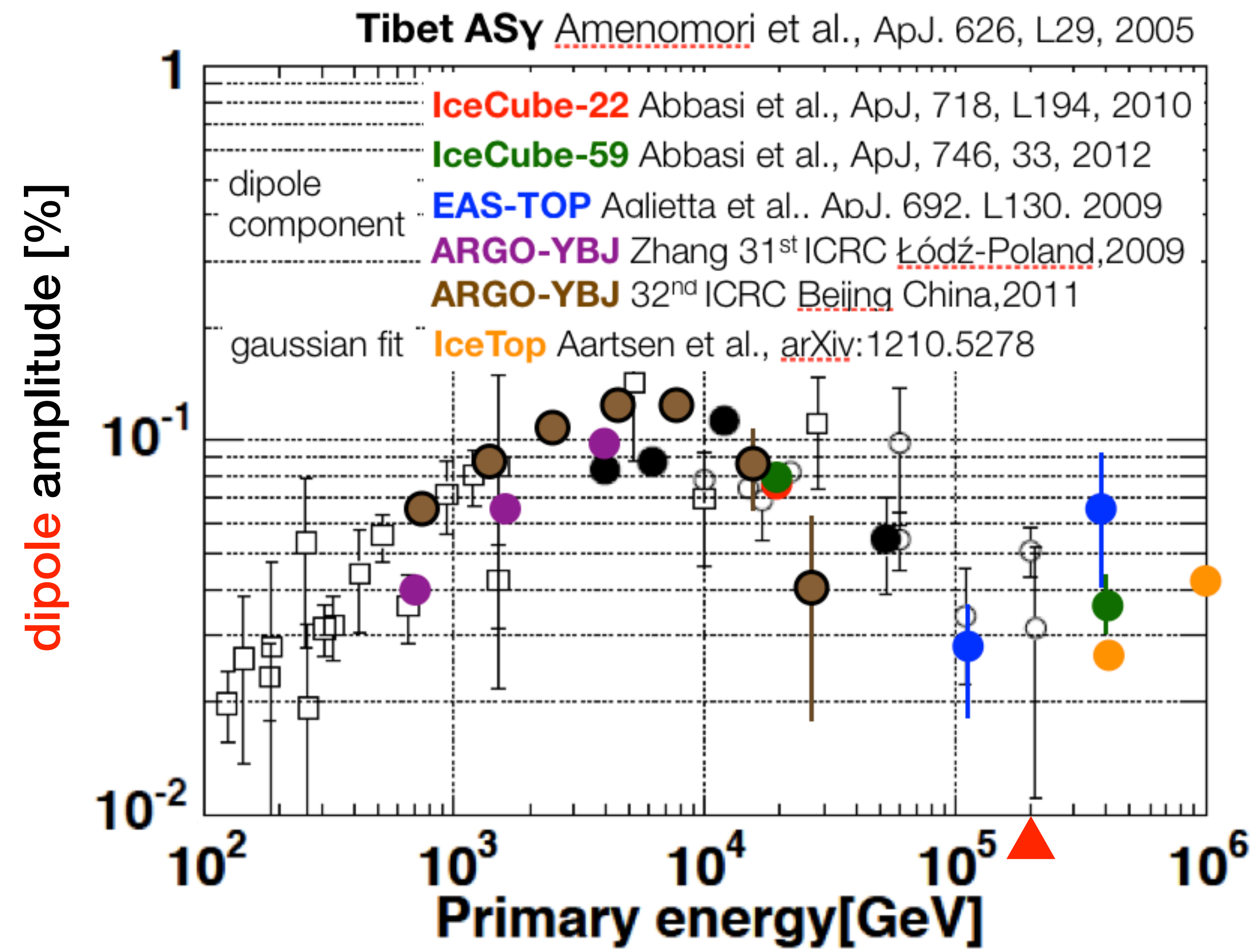

- NOT a dipole change of **phase**
- BUT a structural **modification**

cosmic ray anisotropy large scale

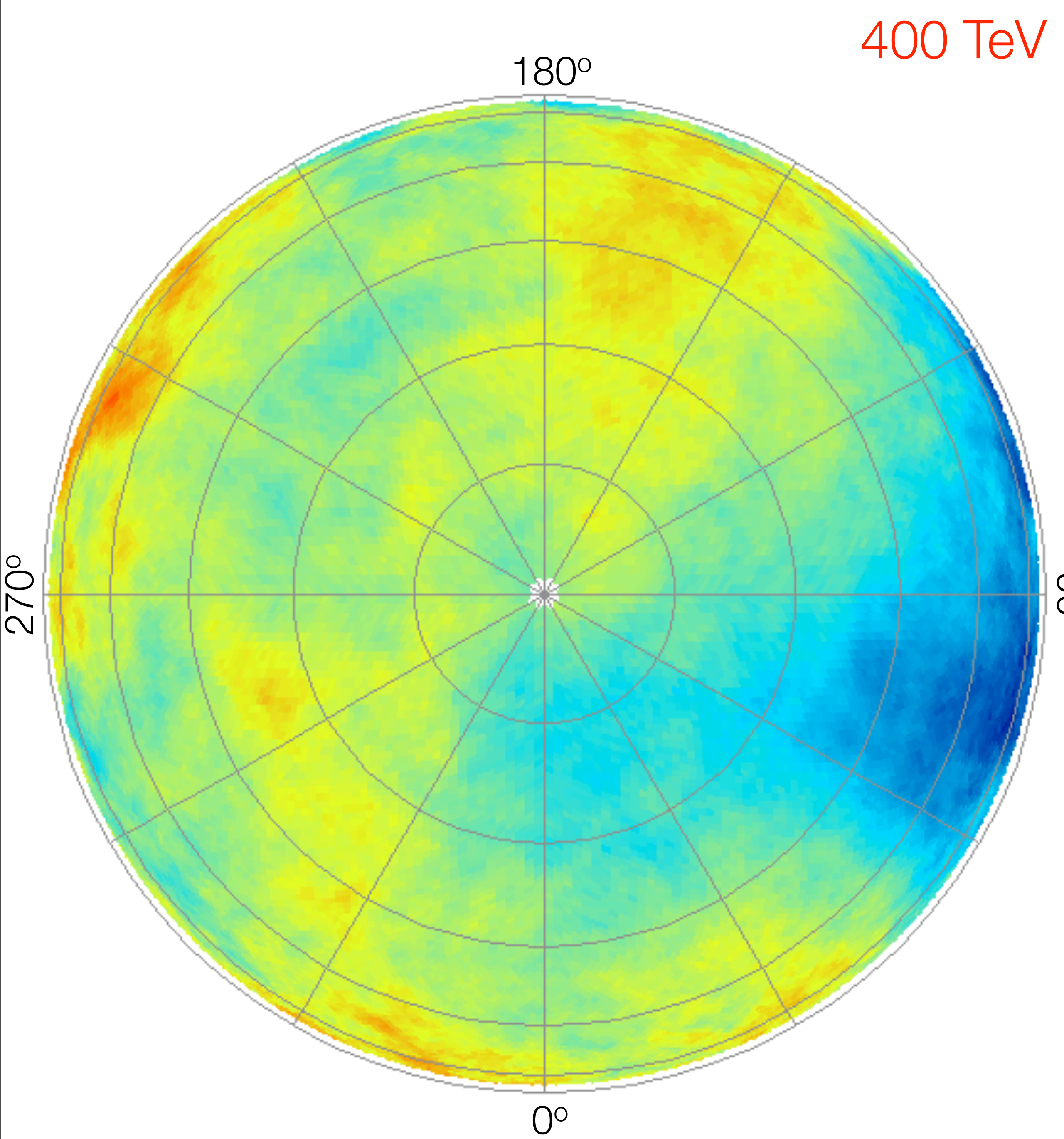

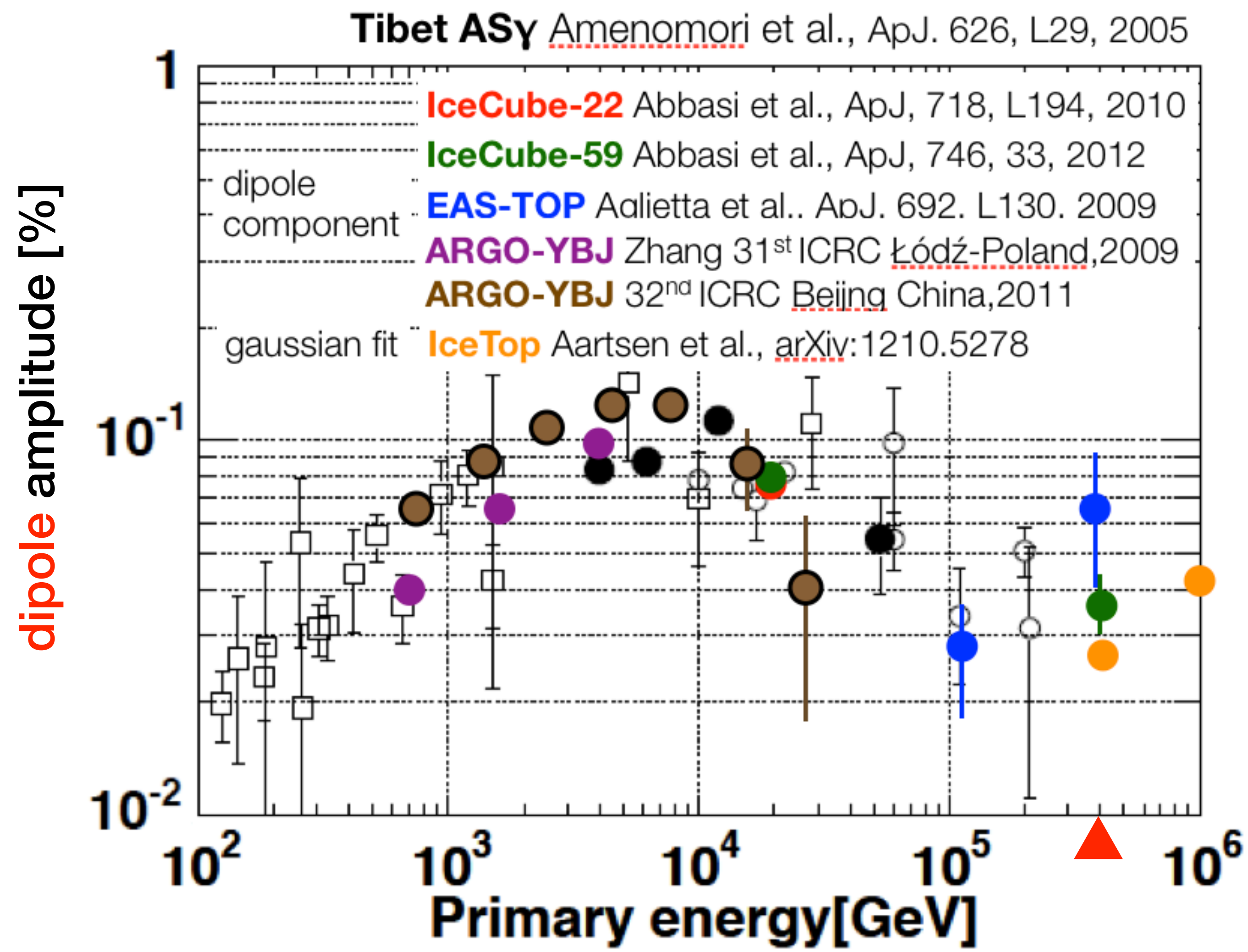

- **NOT** a dipole change of **phase**
- **BUT** a structural **modification**

cosmic ray anisotropy large scale

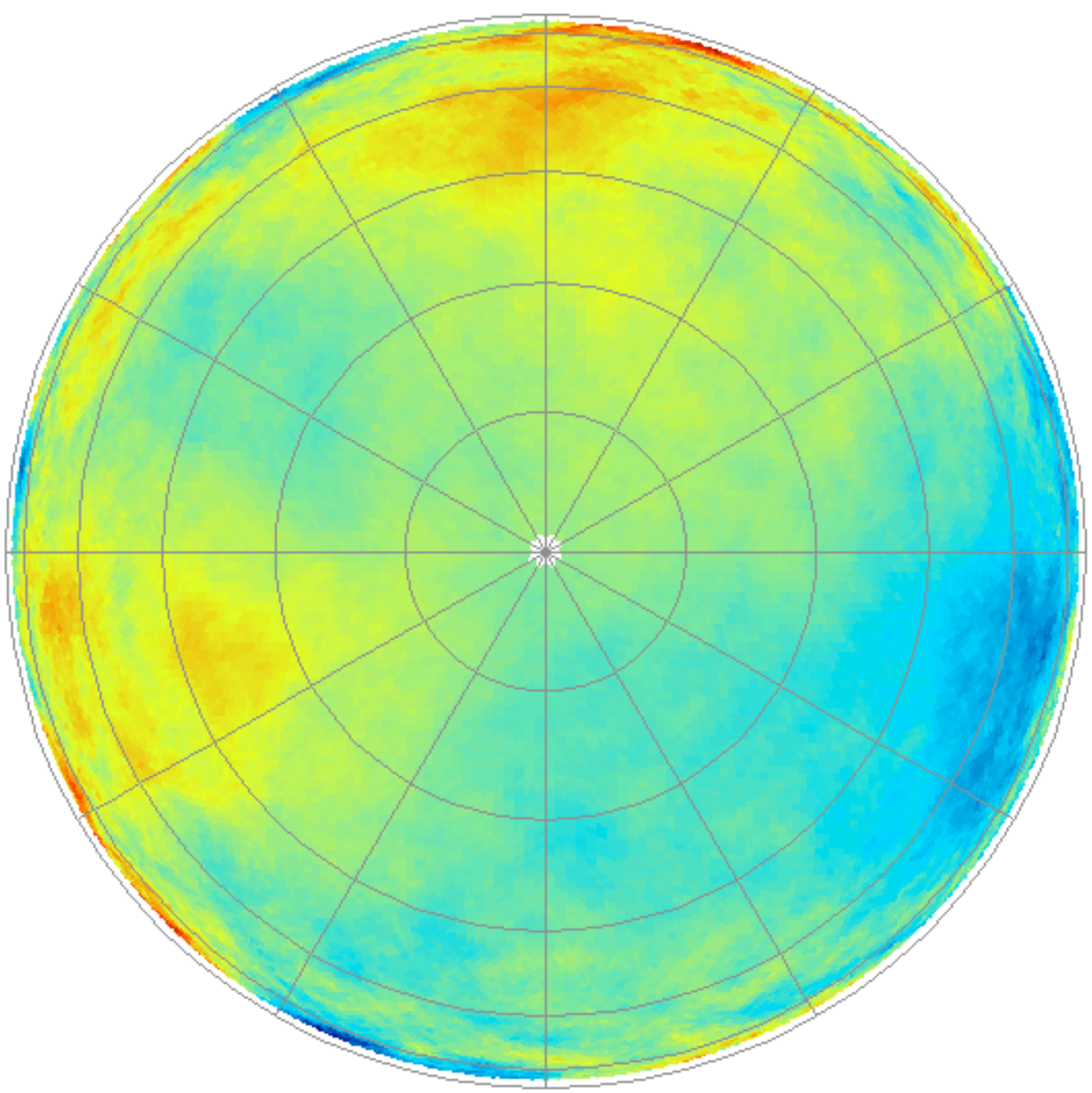

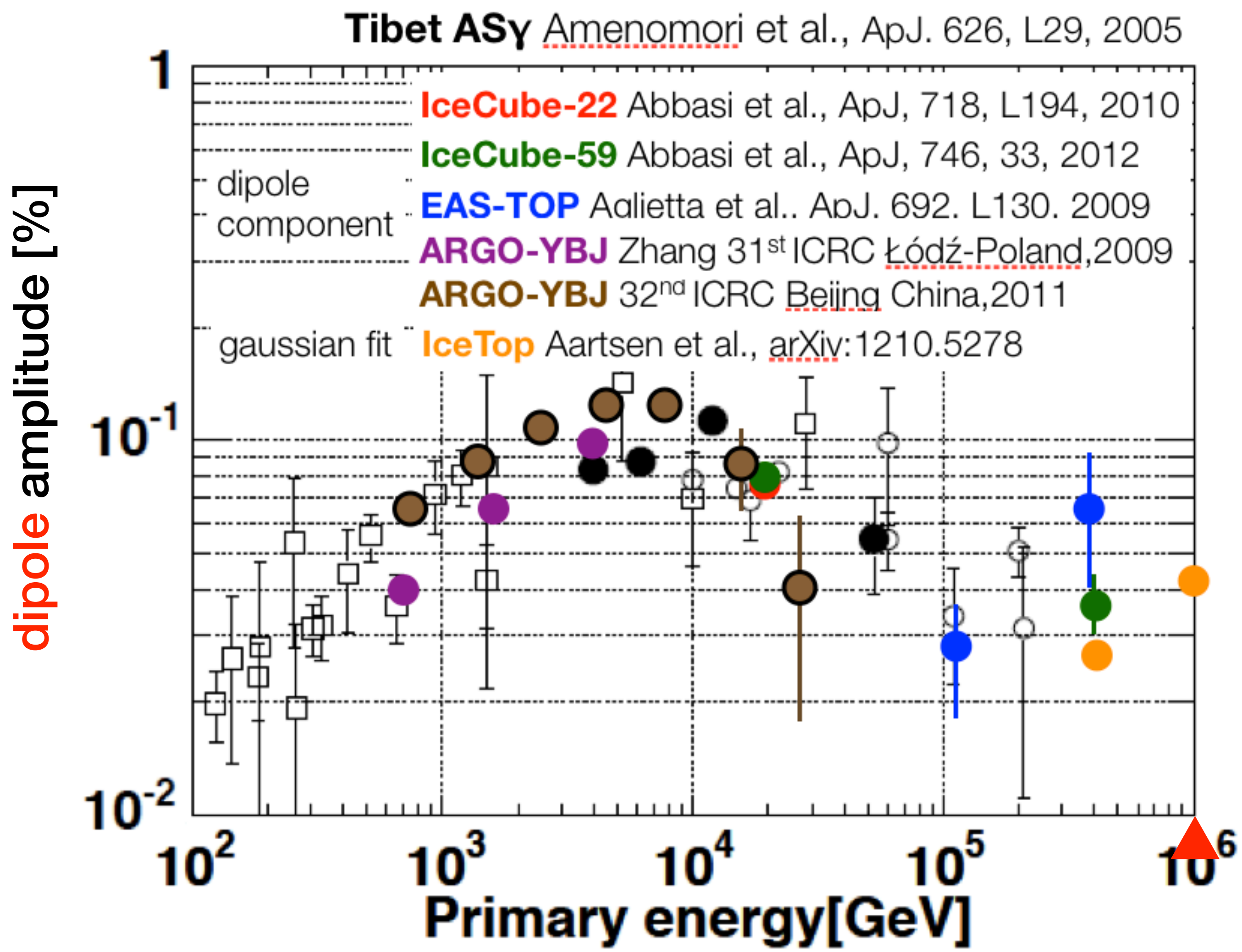

- NOT a dipole change of **phase**
- BUT a structural **modification**

cosmic ray anisotropy large scale → small scale

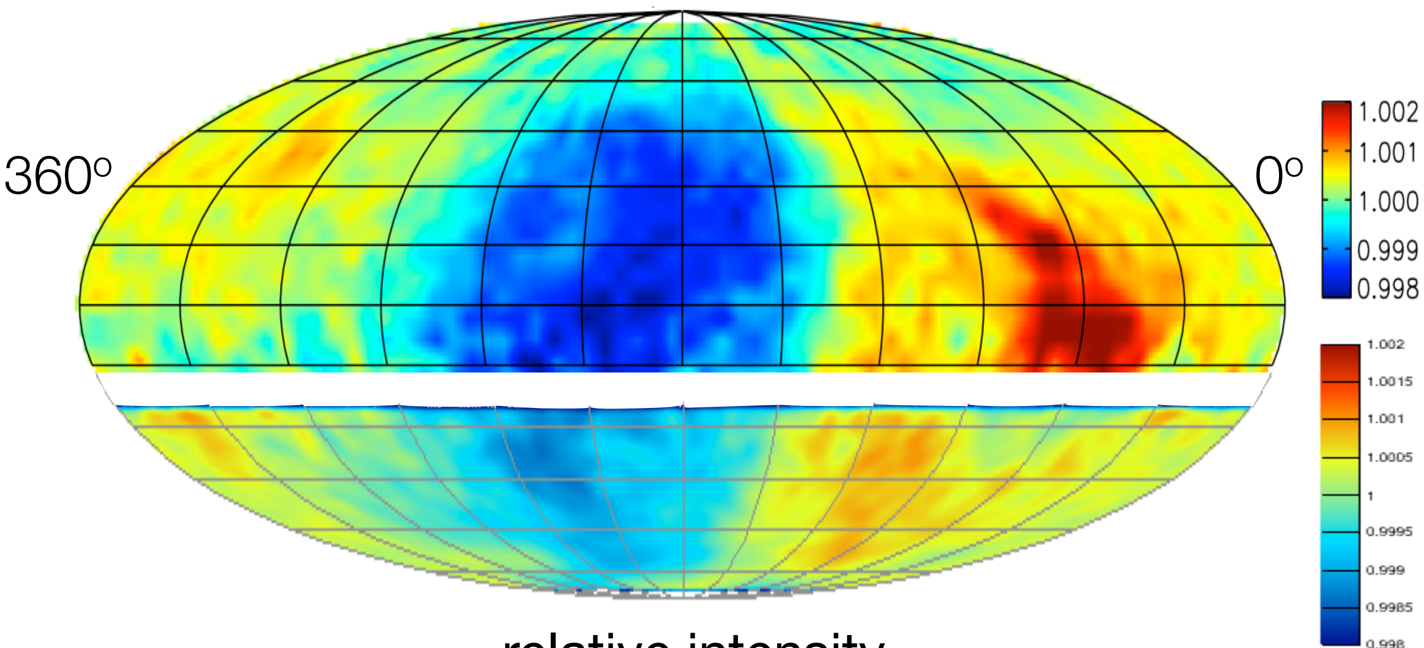

relative intensity

Tibet-III 5 TeV
Amenomori et al., ICRC 2011

equatorial coordinates

IceCube-59 20 TeV
Abbasi et al., ApJ, **746**, 33, 2012

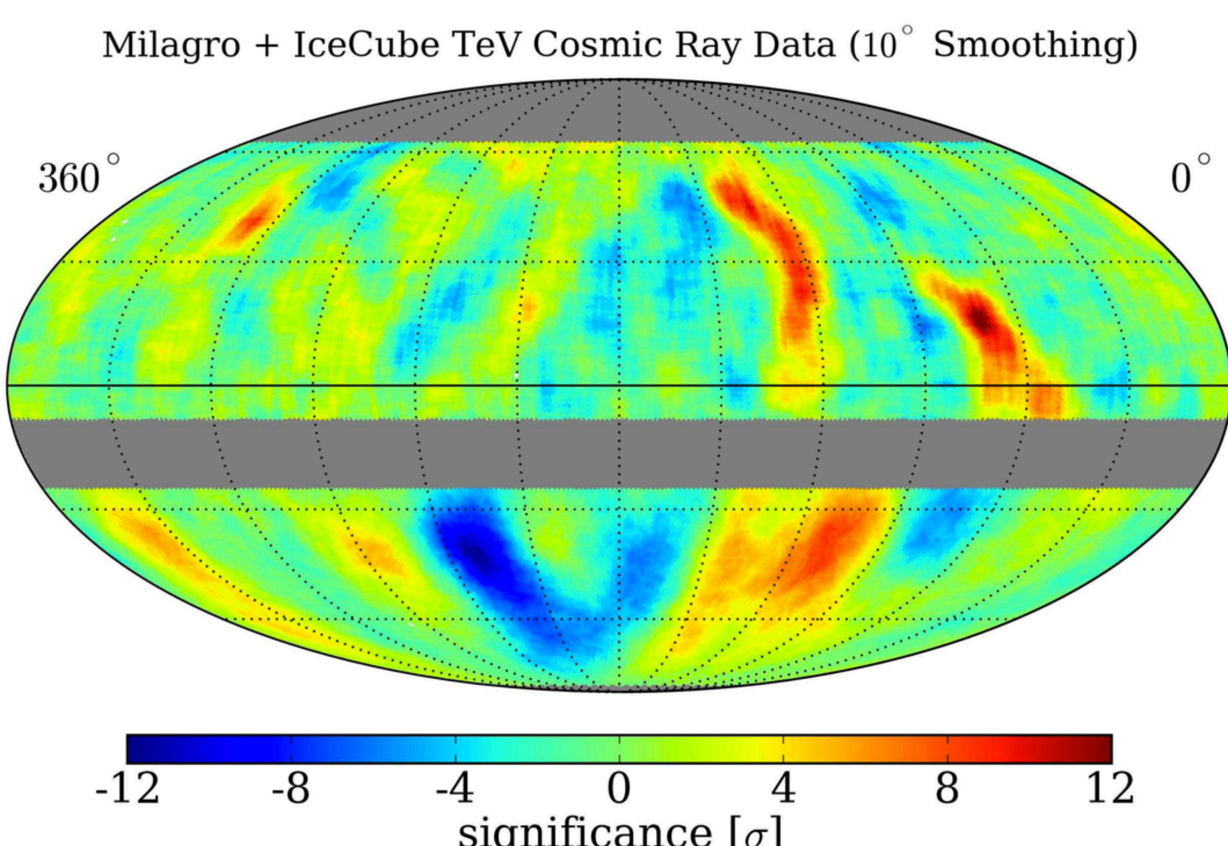

Milagro 1 TeV
Abdo et al., PRL, **101**, 221101, 2008

IceCube 20 TeV
Abbasi et al., ApJ, **740**, 16, 2011

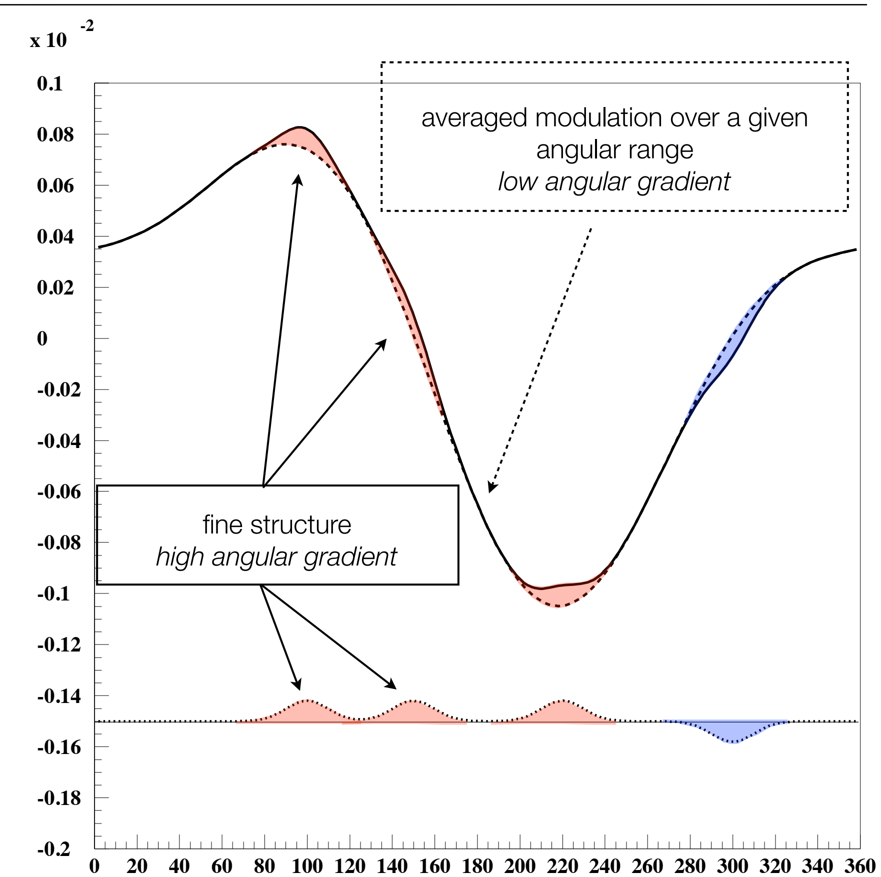

cosmic ray propagation
interstellar medium

- gyro-radius $R_L \approx \frac{200}{Z} \frac{E_{TeV}}{B_{\mu G}} [AU]$

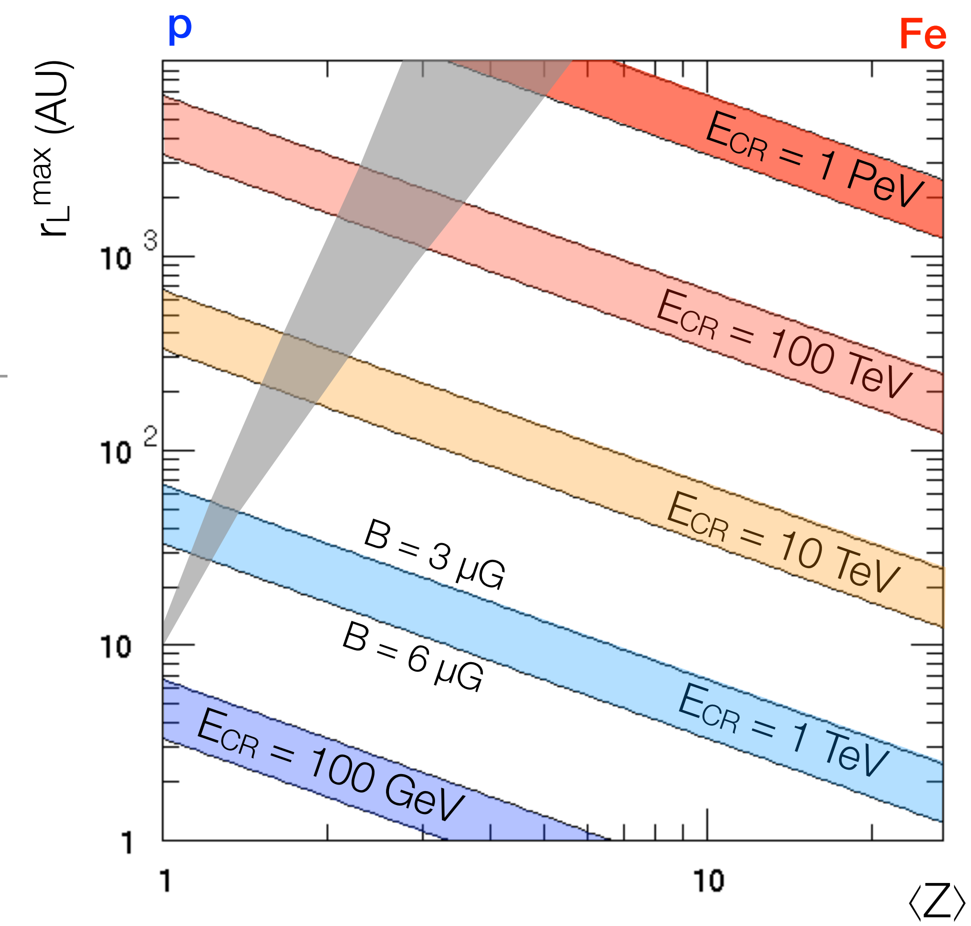

- mean free path in ISM

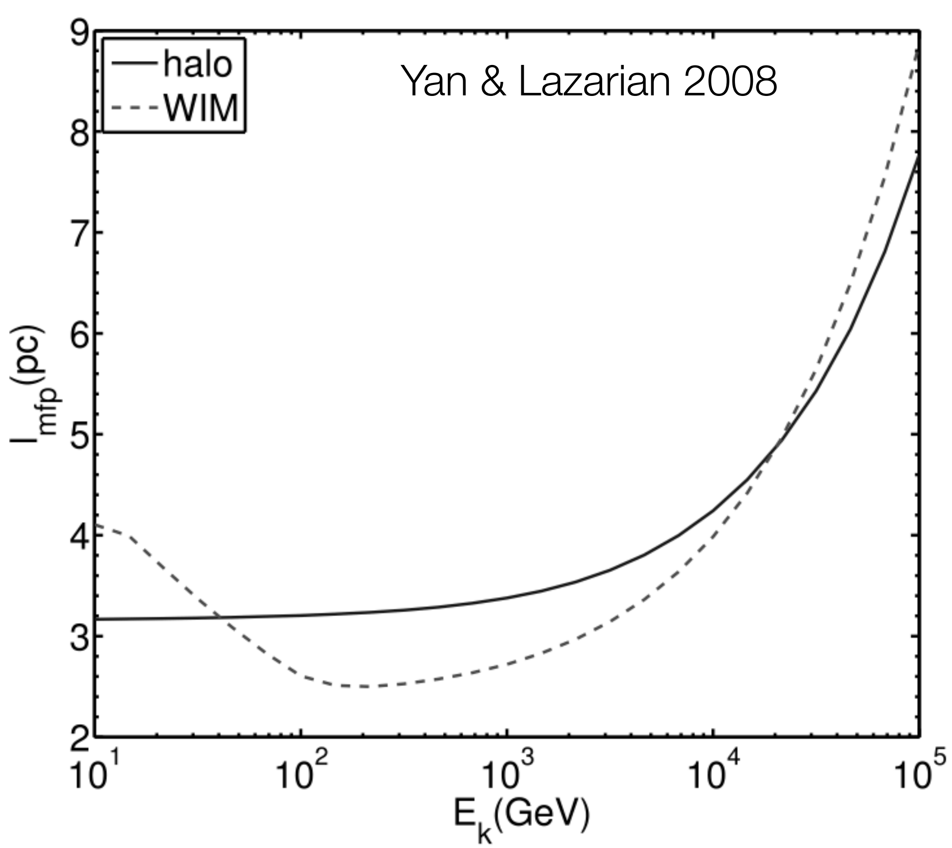

- **non-diffusive** effects < mean free path

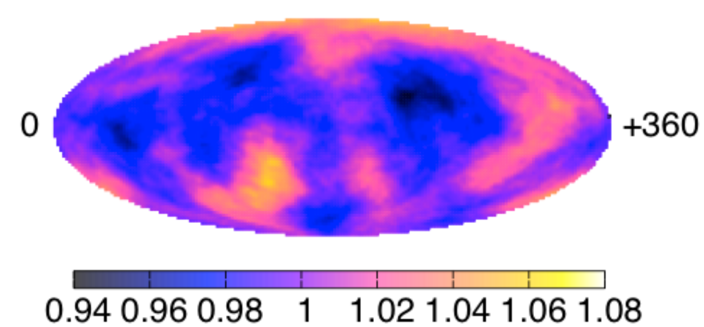

E/Z = 10 PeV

for random realization of B field

Giacinti & Sigl 2011, arXiv:1111.2536
Biermann+, 2012
Ahlers, 2013

cosmic ray propagation

heliosphere

- heliosphere as a 500-700 AU perturbation of the Local Interstellar Magnetic Field
- long tail down stream IS flow

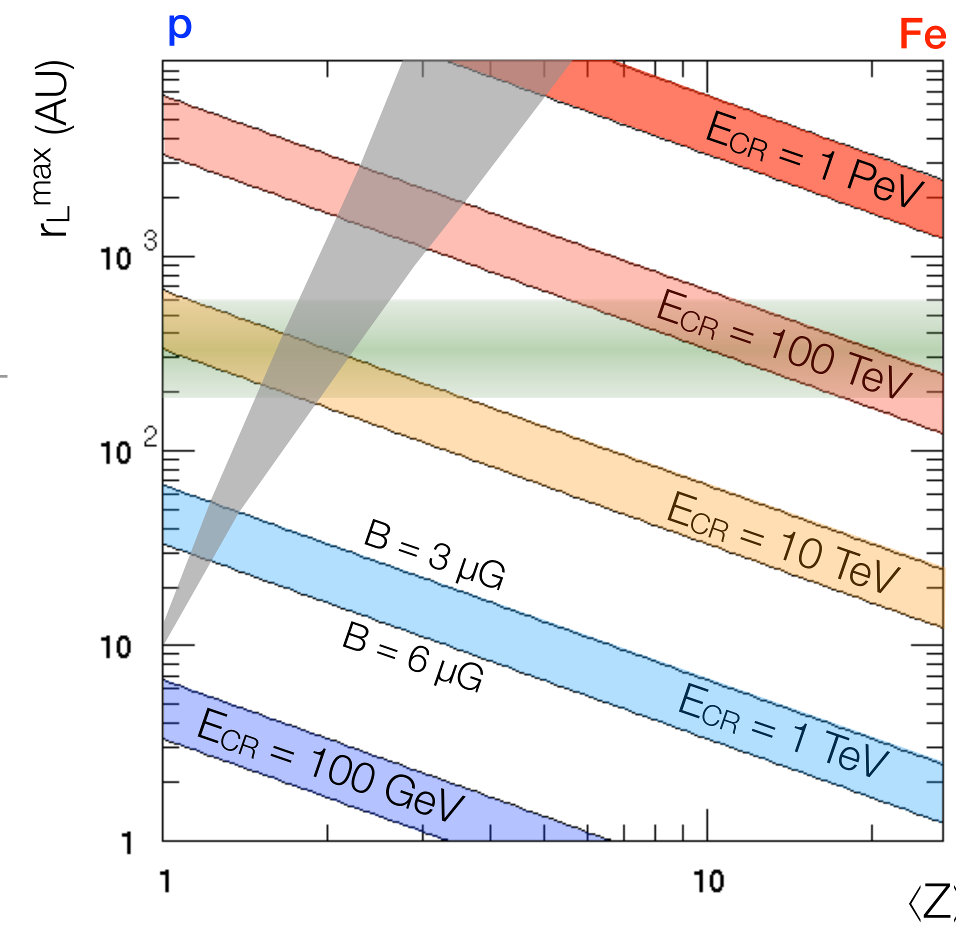

- resonate with O(10) TeV CR

Pogorelov+ 2011

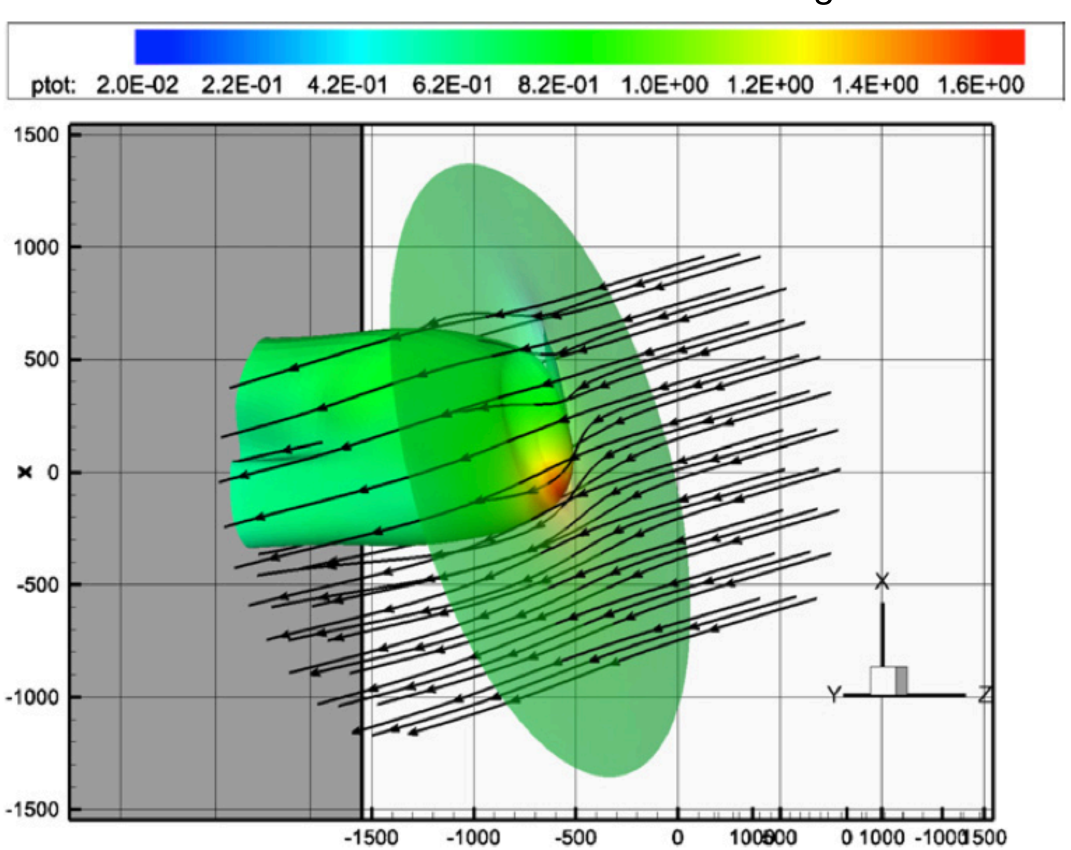

heliospheric perturbations
heliopause instabilities

- Rayleigh-Taylor instabilities driven and mediated by interstellar neutral atoms

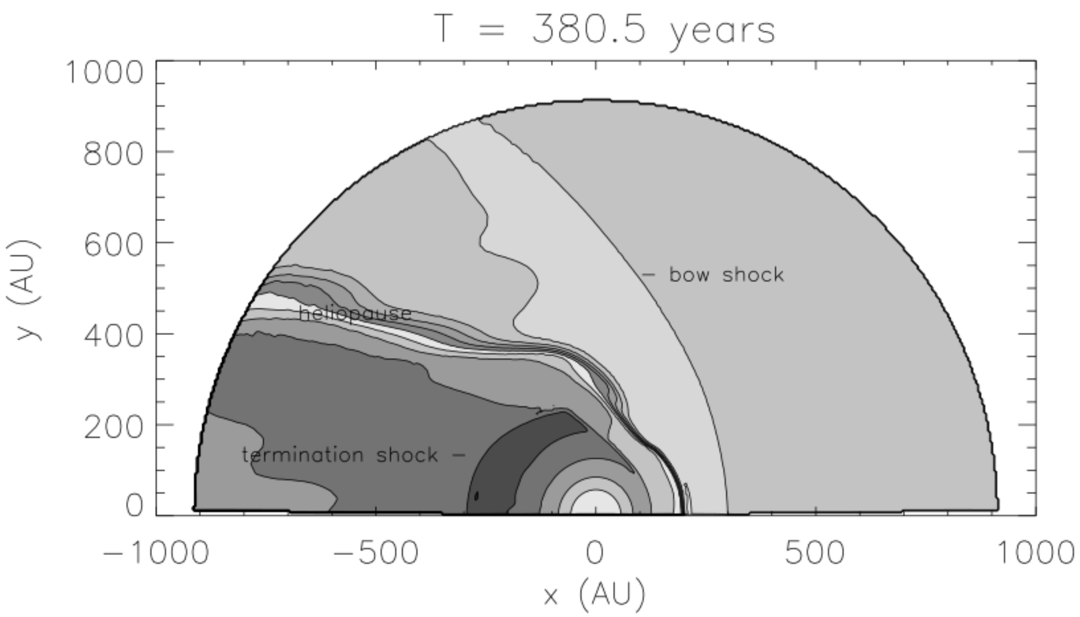

Liewer+ 1996
Zank+ 1996

- plasma-fluid instabilities at the flank of HP by charge exchange processes

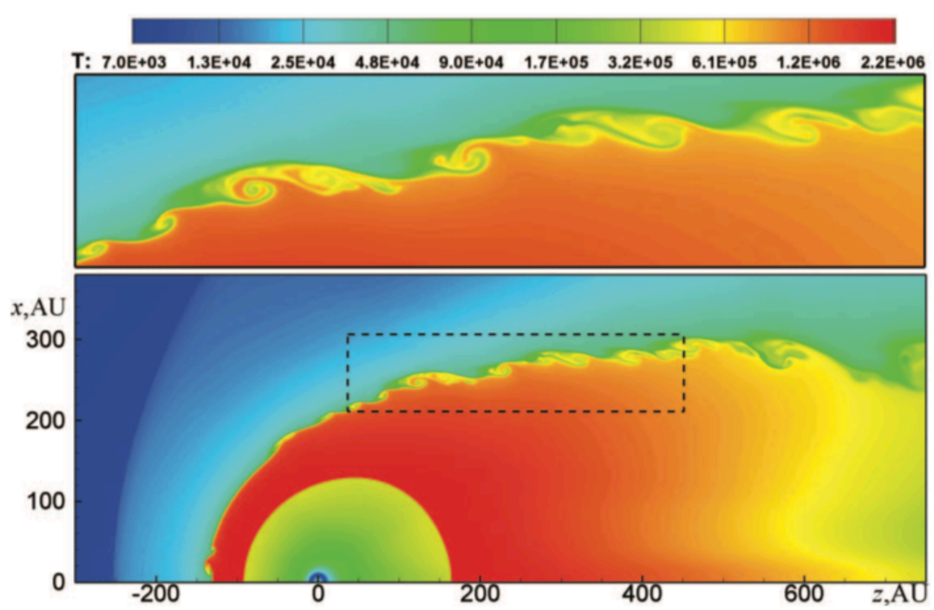

Zank 1999
Florinski+ 2005
Borovikov+ 2008
Zank 2009
Shaikh & Zank 2010

heliospheric perturbations
heliopause instabilities

- effect of Solar Cycles on inner and outer heliosphere
- perturbations on the flanks

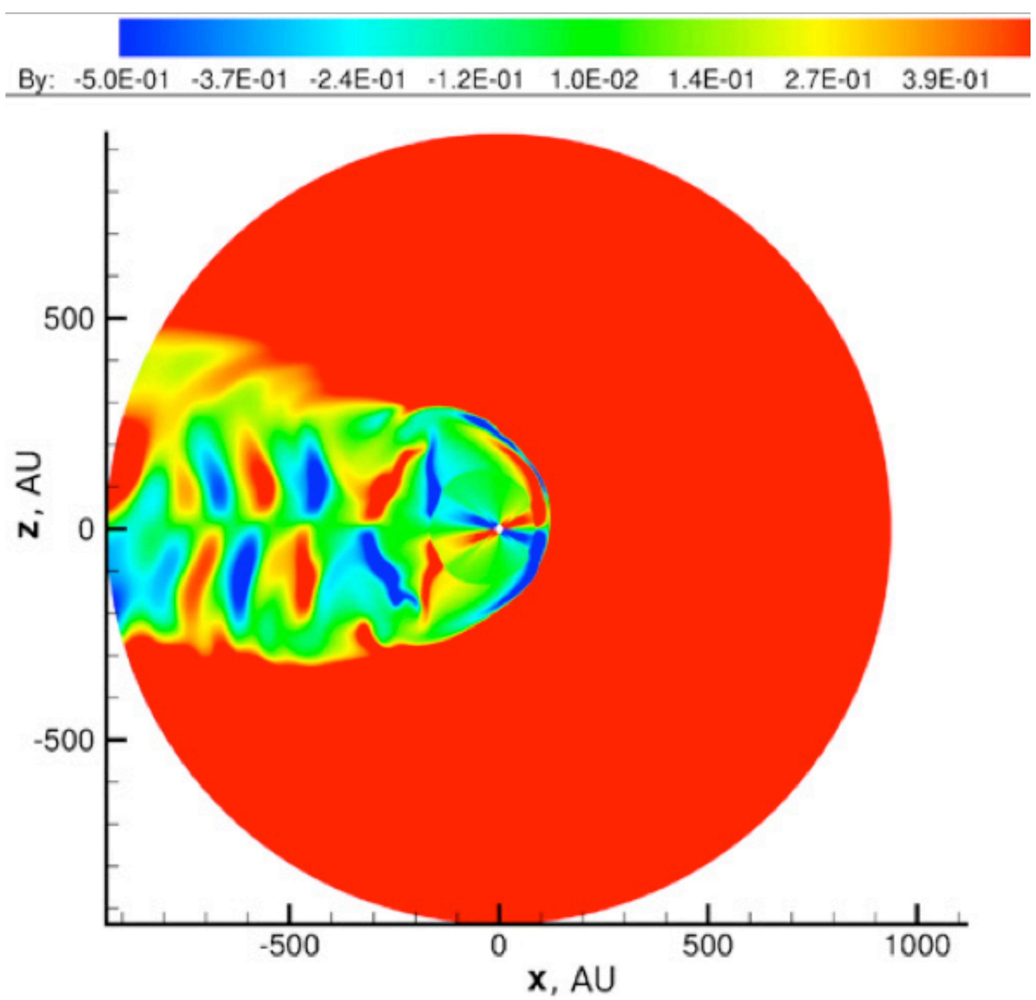

Pogorelov+ 2009

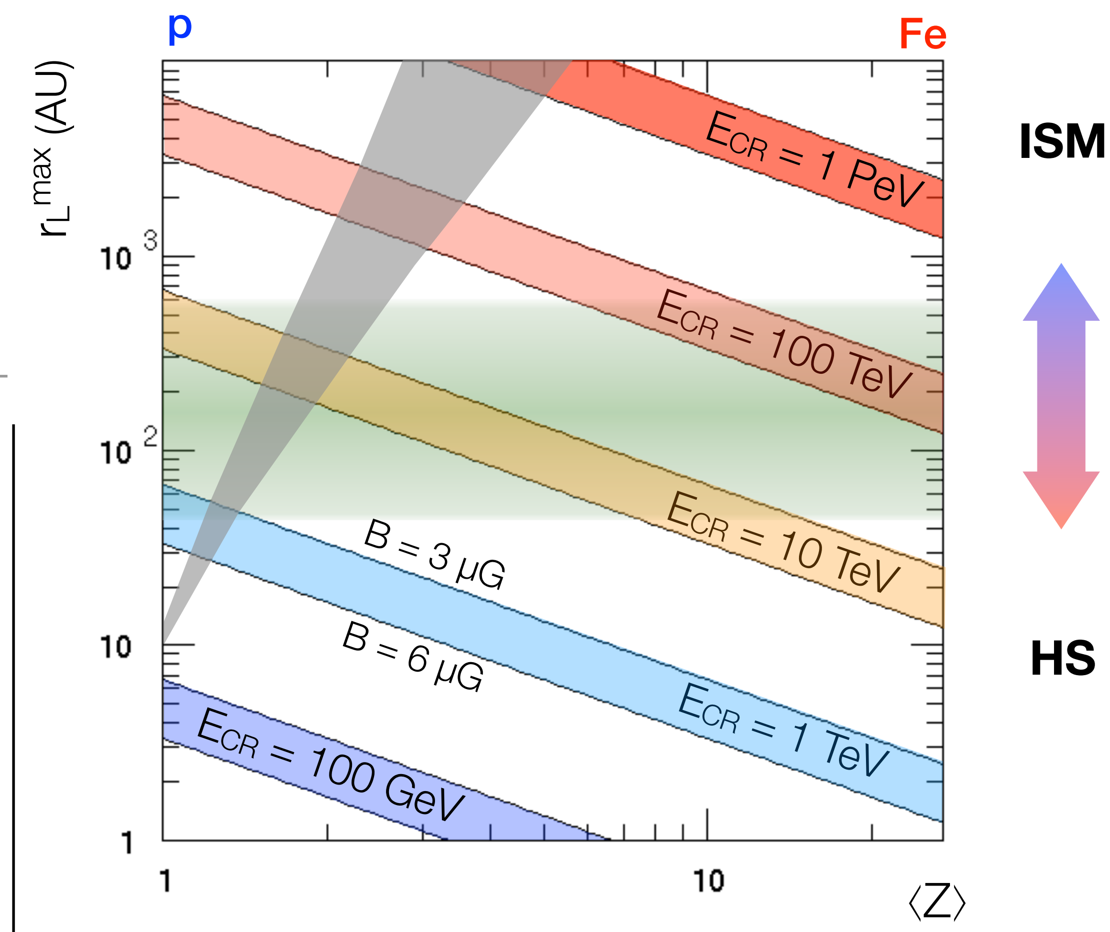

- resonate with multi-TeV CR
- 10 TeV as a transition scale

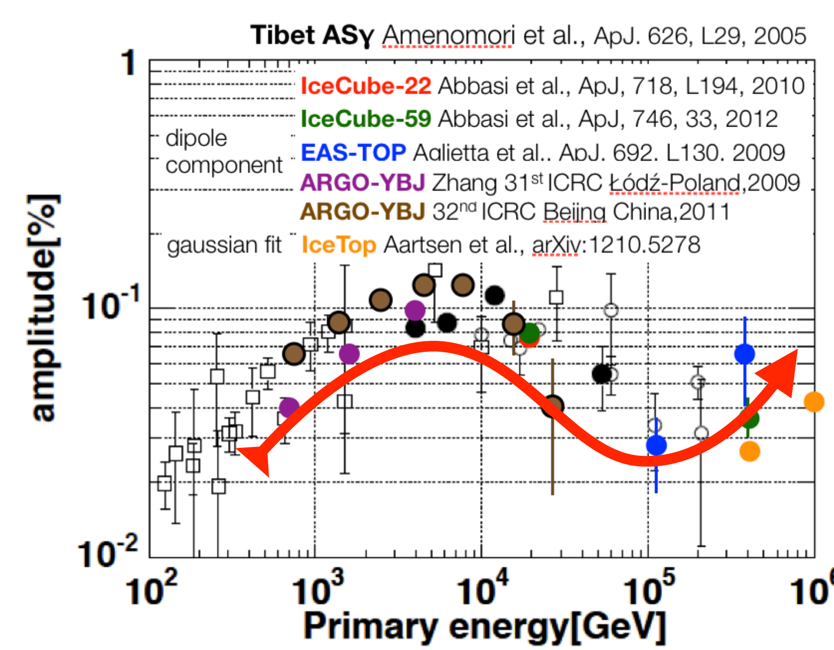

cosmic ray anisotropy

heliosphere

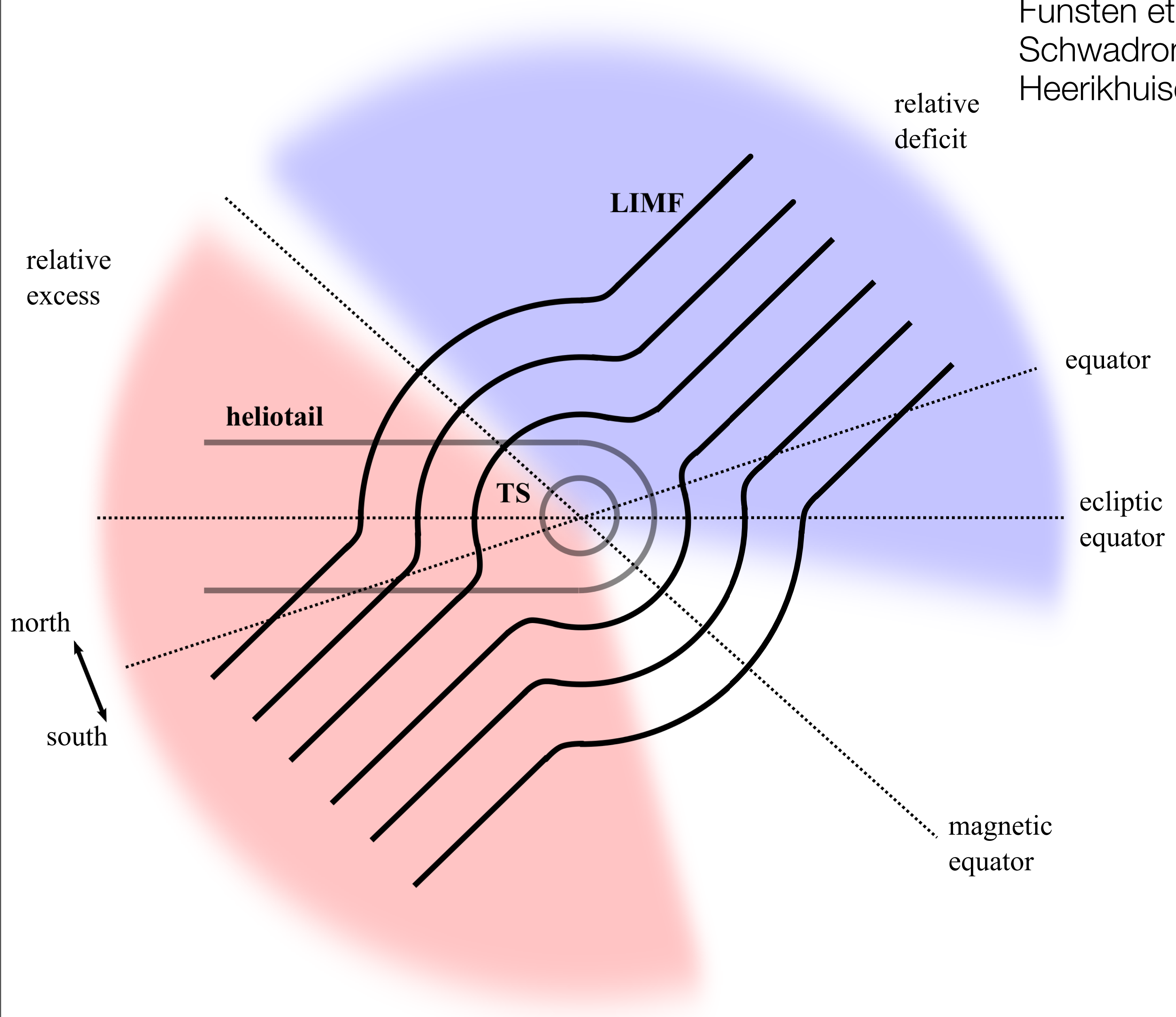

Funsten et al. (2009)
Schwadron et al. (2009)
Heerikhuisen et al. (2010)

PD & Lazarian 2013, arXiv:1111.3075

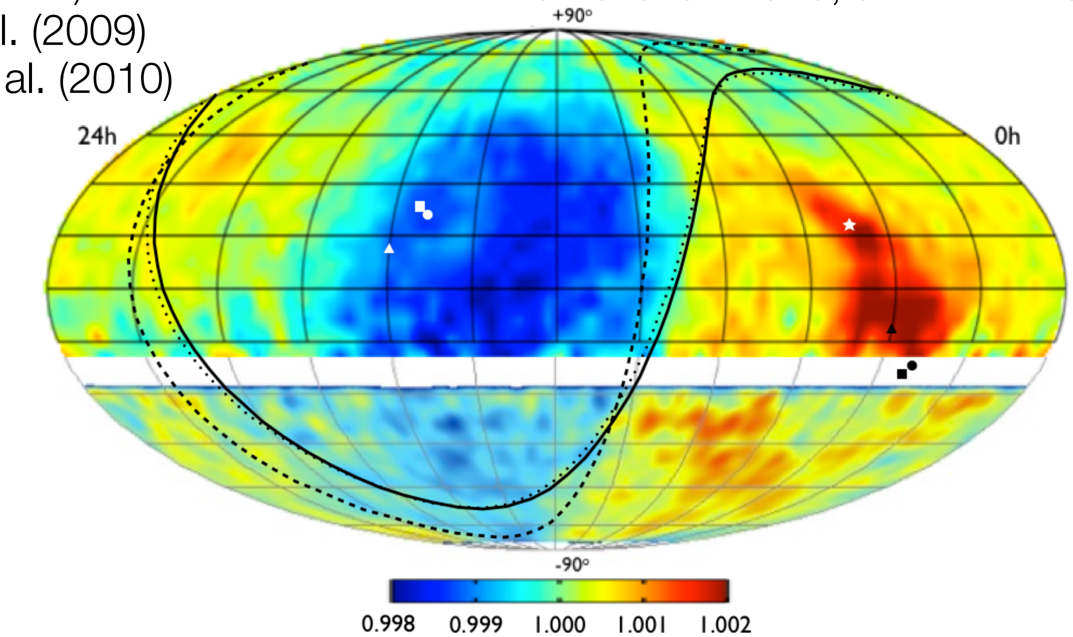

equatorial coordinates

magnetic equator

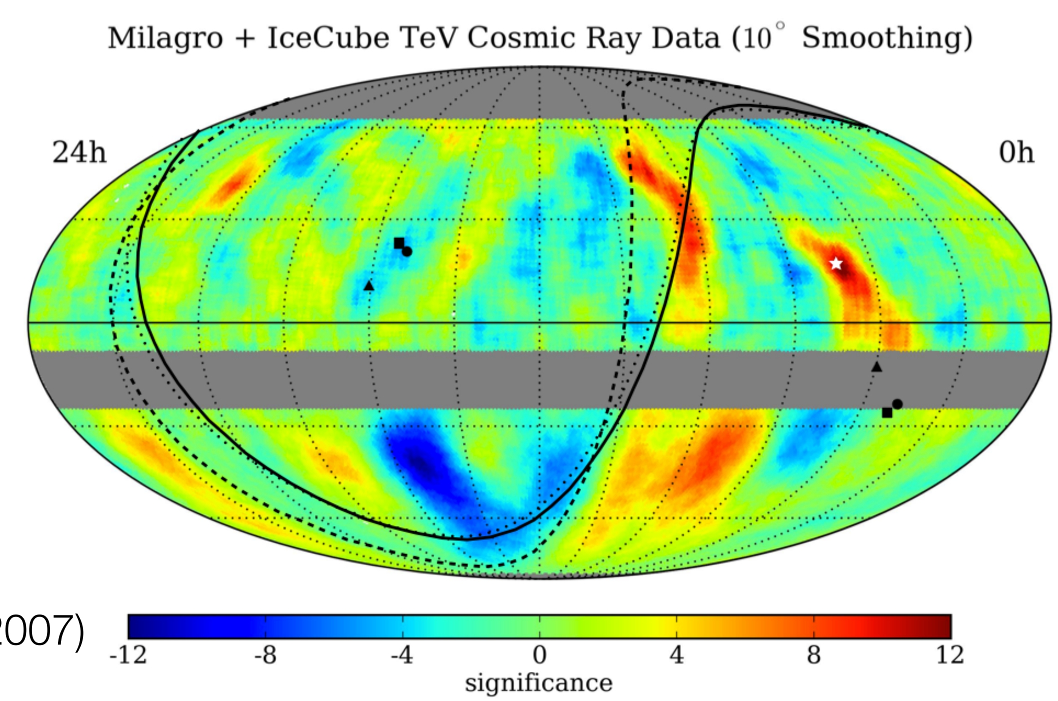

LIMF direction compatible with

- Ca II absorption & H I lines, Frisch (1996)
- radio emission from inner heliosheath, Lallement et al. (2005), Opher et al. (2007)
- polarization measurements, Frisch (2010)

cosmic ray anisotropy
heliosphere

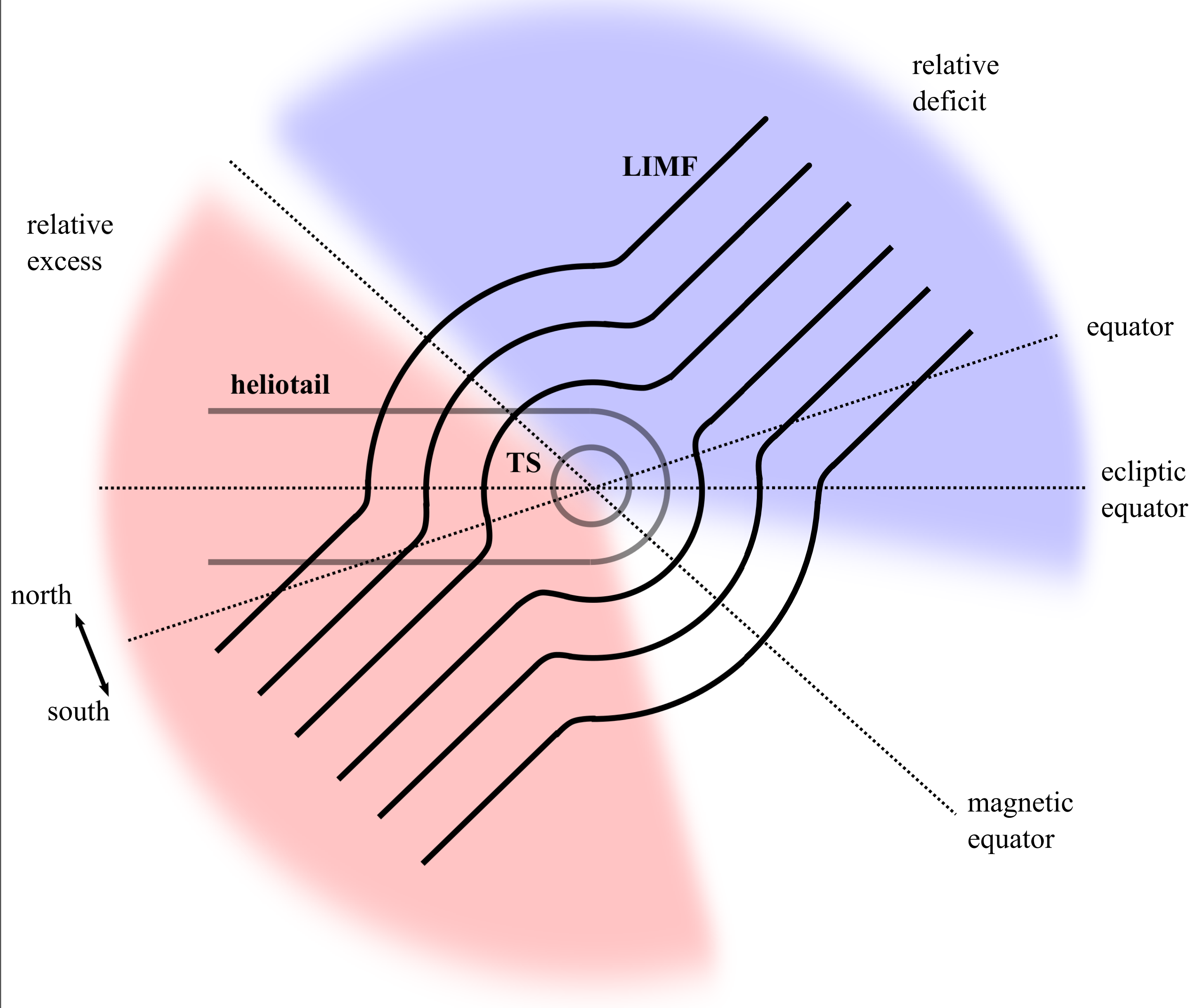

PD & Lazarian 2013, arXiv:1111.3075

1-10 TeV

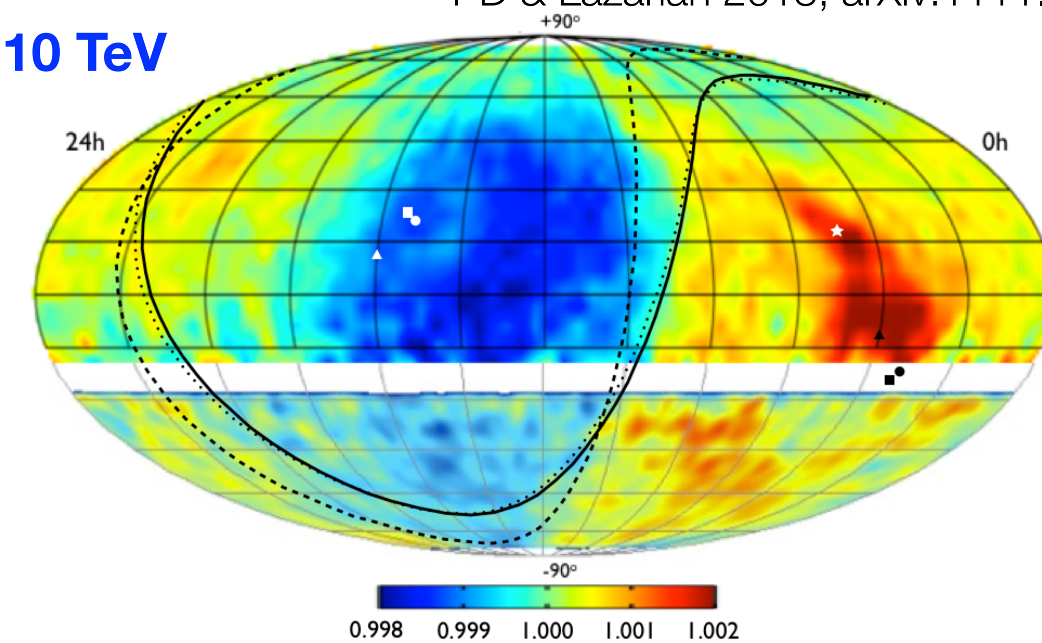

equatorial coordinates

magnetic equator

>100 TeV @ large distance, O(7000) AU

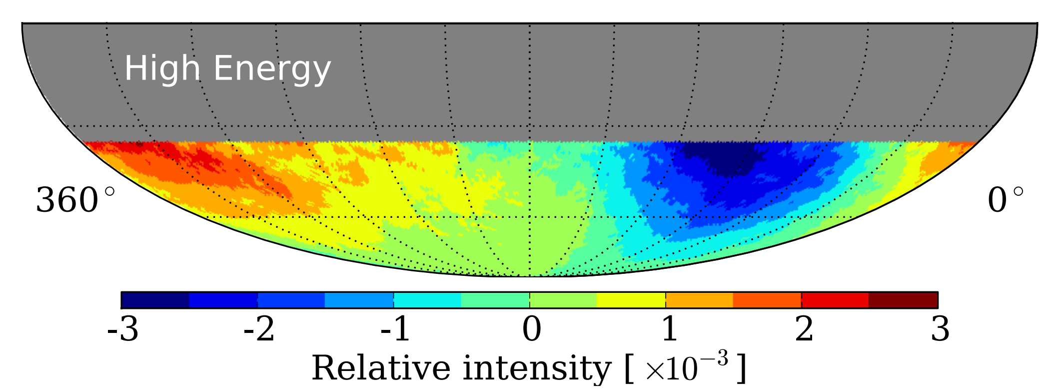

scattering at heliospheric boundary

heuristic model

- resonant scattering to **re-direct** CR distribution
- **back-scattering** @ flanks back from downstream

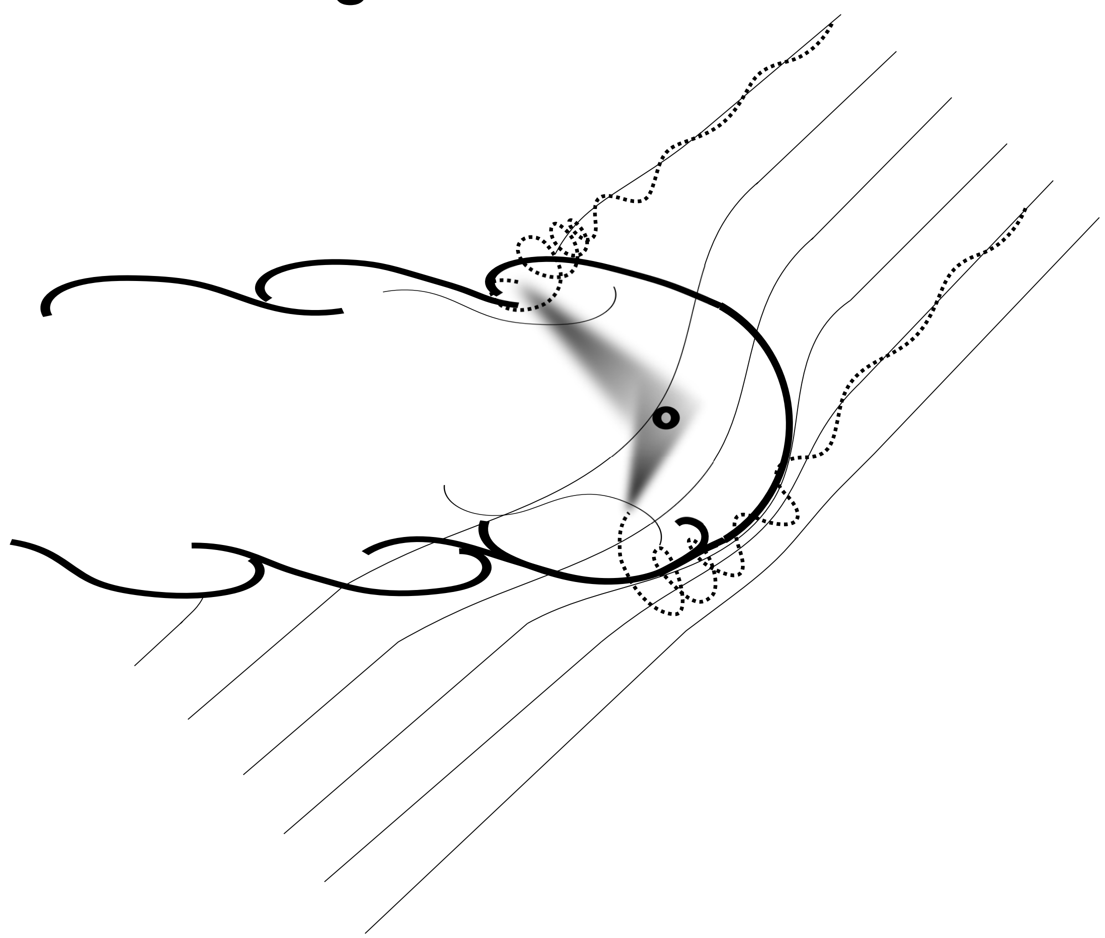

- global anisotropy with **large edge gradients**
- particle trajectory integration in heliospheric model

PD & Lazarian 2013, arXiv:1111.3075

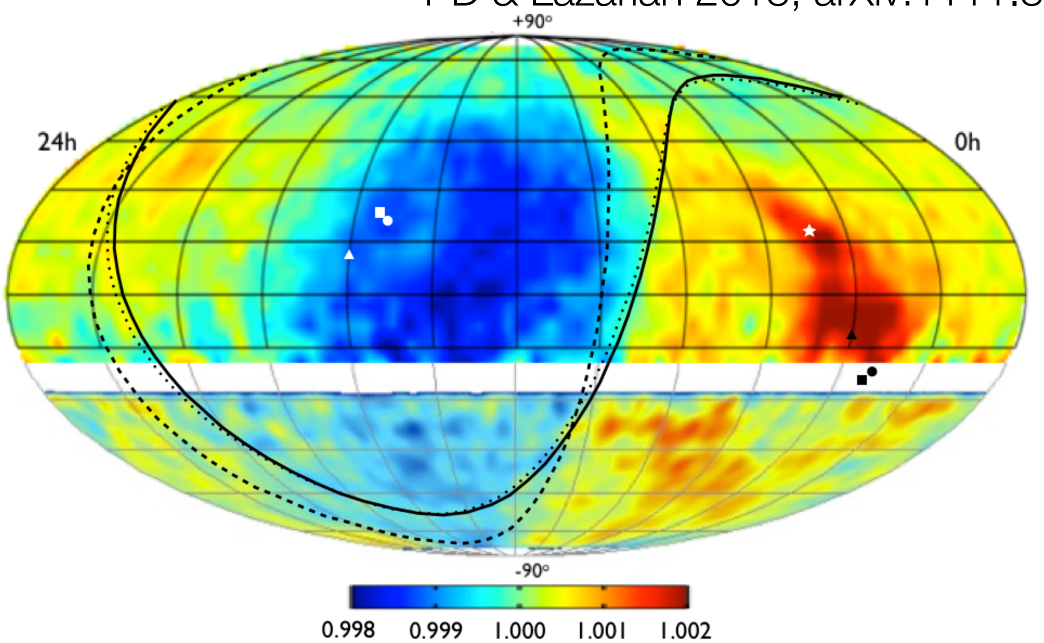

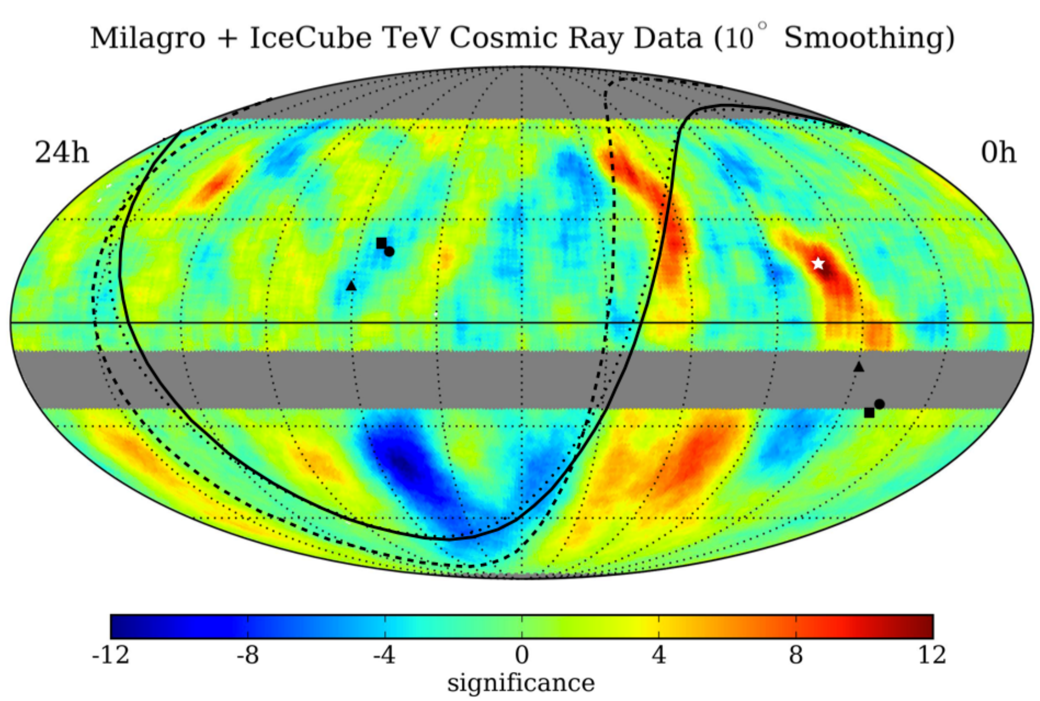

scattering on heliospheric boundary

toy model

PD & Lazarian, ApJ, **762**, 44, 2013

$$N_b = n_{\rm CR}\, P_s\, R_E^2 \int_{R_H}^{R_H+dR_H} dr \int_0^{2\pi r} dl \int_0^{\infty} \frac{dz}{z^2+r^2}$$

$$= n_{\rm CR}\, P_s\, \pi^2\, R_E^2\, dR_H,$$

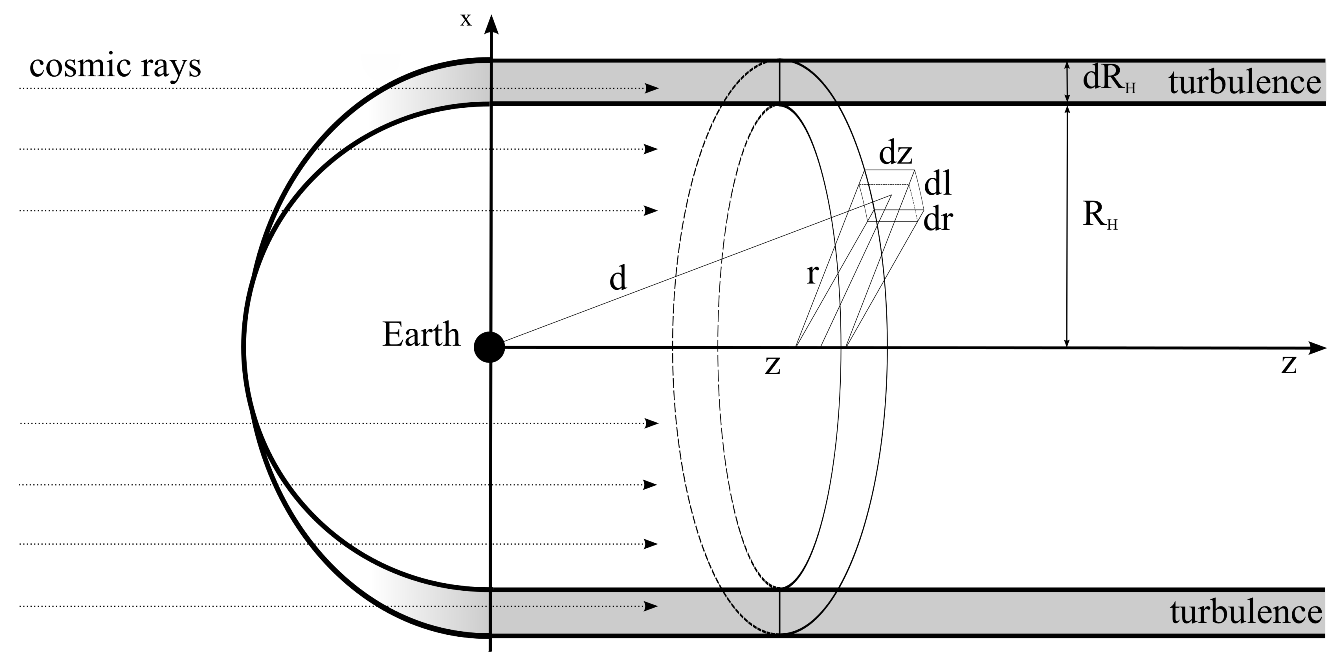

$$N_d = n_{\rm CR}\, 4\pi\, R_E^2\, c\,\tau.$$

$$\delta = \frac{N_b - N_d}{N_b + N_d} = \frac{N_b/N_d - 1}{N_b/N_d + 1},$$

$$\frac{N_b}{N_d} = \frac{3\pi}{4}\, P_s\, \frac{dR_H}{c\,\tau}.$$

$$\delta \gtrsim 0,$$

$$dR_H \gtrsim (10-100)/P_s$$

cosmic ray anisotropy
spectral hardening

- relatively harder than average spectrum observed toward the heliotail

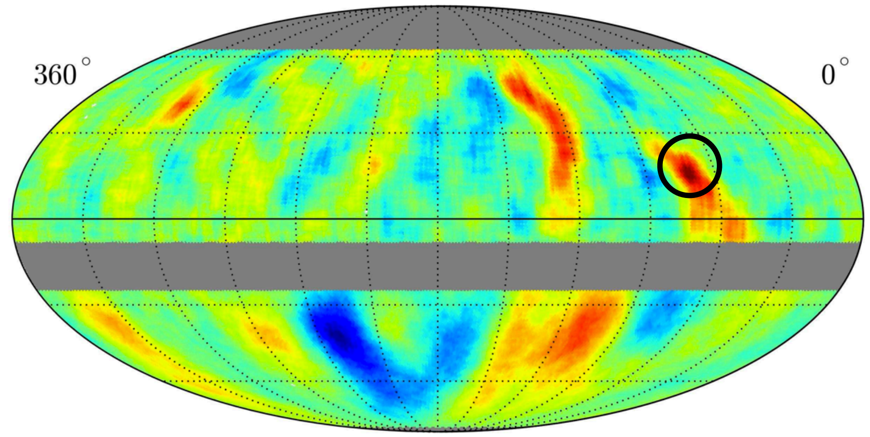

Milagro observation Abdo+ 2008

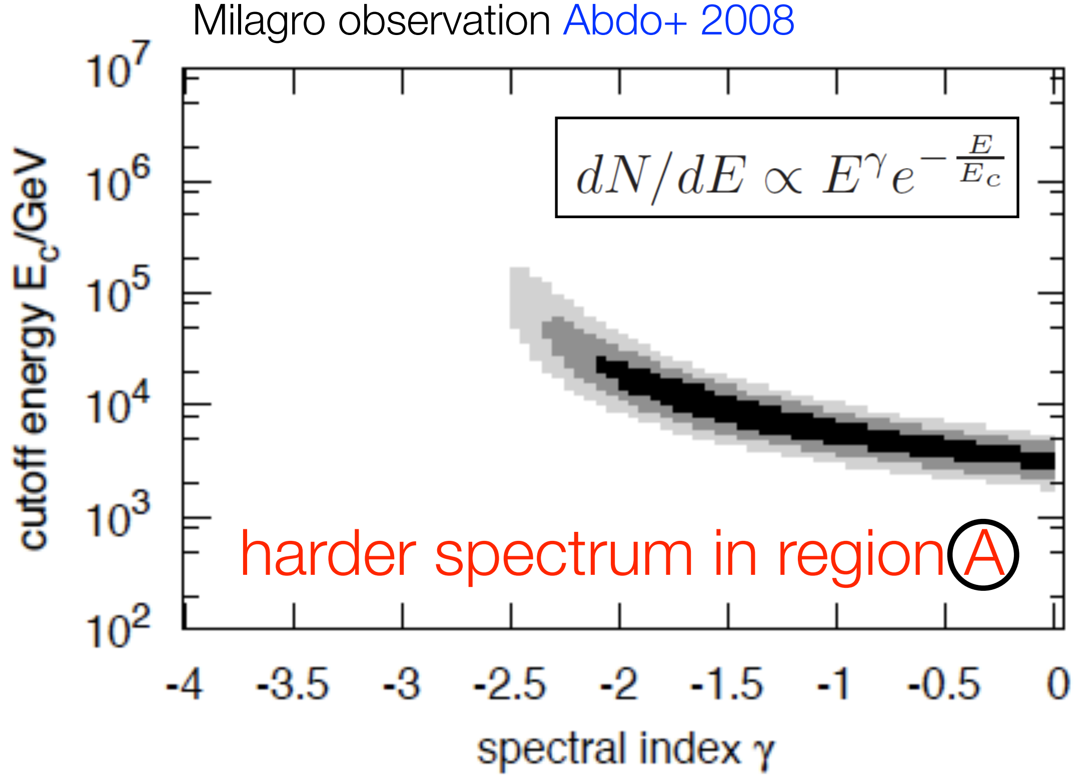

$\gamma < \gamma_{elsewhere}$ at 4.6 σ level
E_C = 3 - 25 TeV

ARGO-YBJ observation Di Sciascio+ 2013

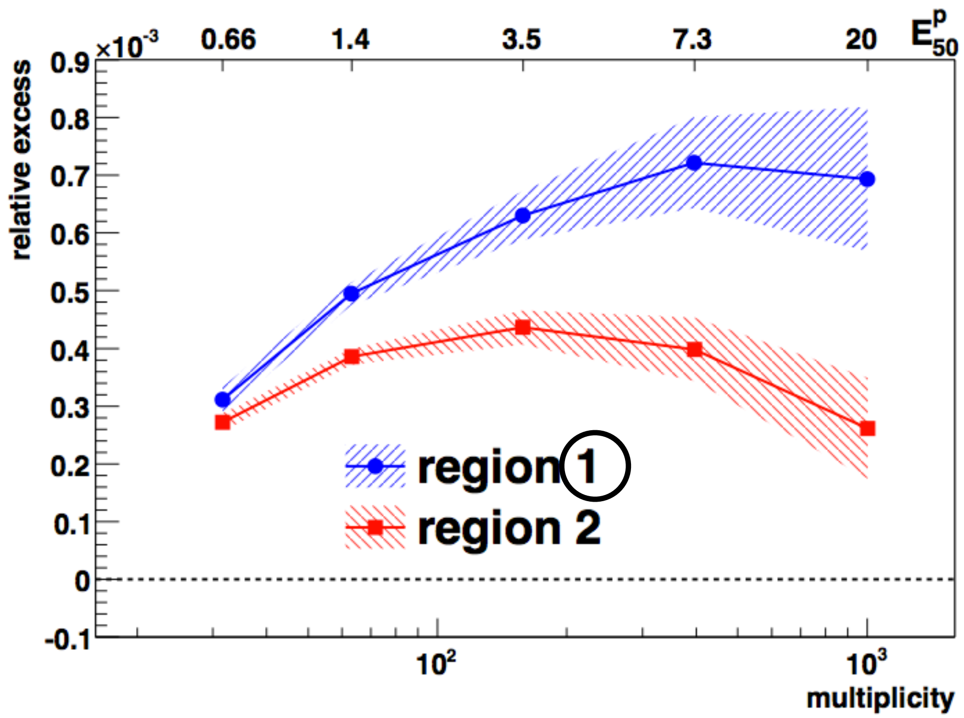

cosmic ray anisotropy
stochastic magnetic reconnection in the heliotail

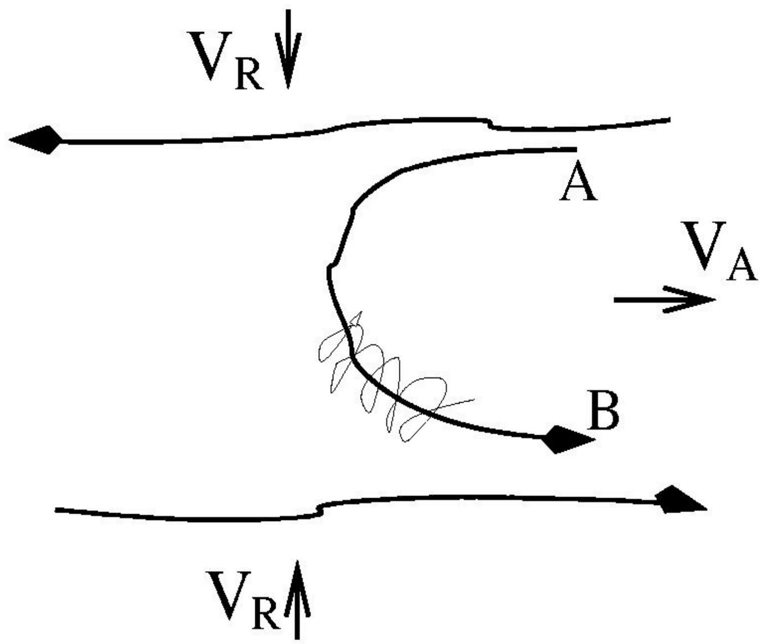

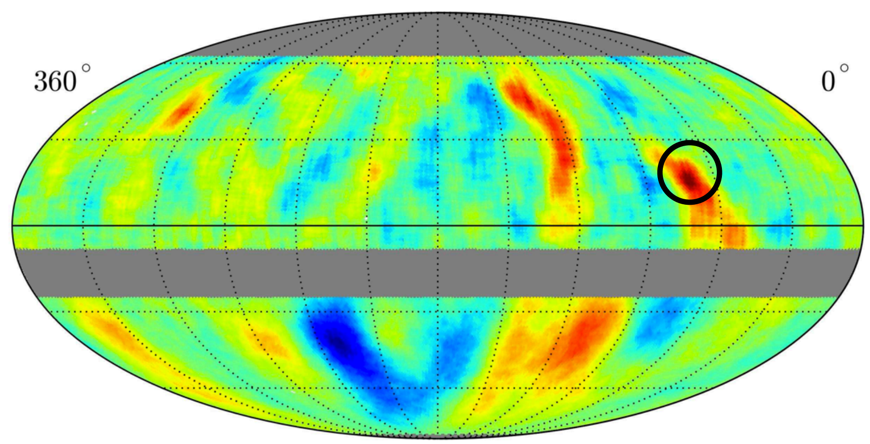

turbulent reconnection Lazarian & Vishniac 1999

1st order Fermi acceleration de Gouveia dal Pino & Lazarian 2003, 2005

$$N(E)\,dE \sim E^{-5/2}\,dE$$

$$E_{max} \approx 0.5 \left(\frac{B}{1\,\mu G}\right)\left(\frac{L_{zone}}{100\,AU}\right) TeV \approx 0.5 - 6\,TeV$$

Lazarian, PD 2010 - PD, Lazarian 2012

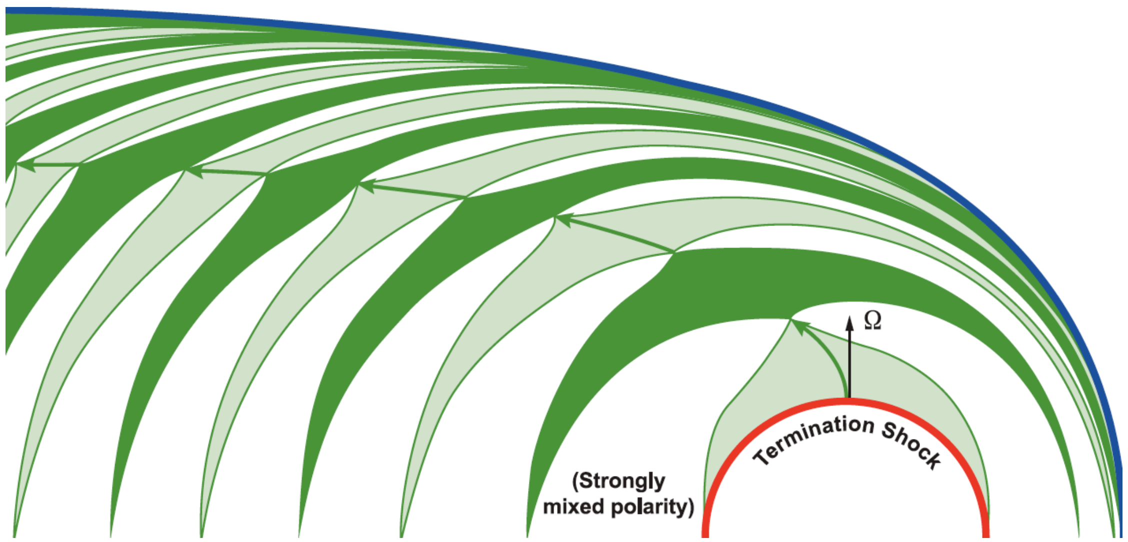

Nerney & Suess 1995

conclusions

- heliospheric perturbations could explain TeV CR anisotropy: no effect above 100 TeV

- **scattering** with perturbation on heliopause

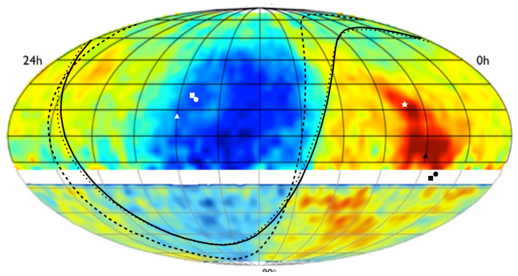

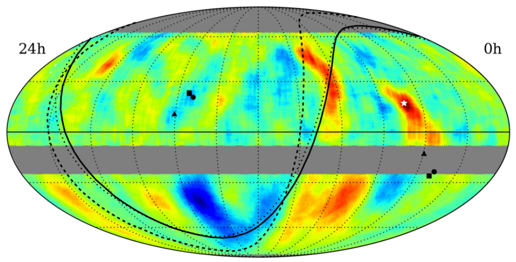

- **re-acceleration** mechanism from heliotail

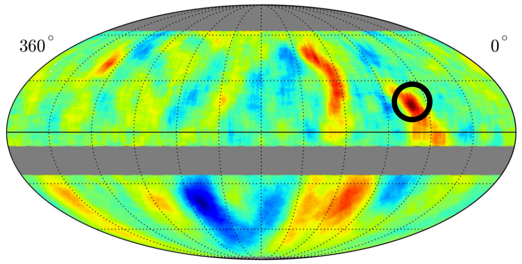

Lazarian & PD, 2010
PD & Lazarian, 2012

- heliospheric modeling extended along **heliotail** with fine resolution: turbulence & global structure. Particle trajectory integration studies with heliospheric model → predictive

- observations in wider energy range, in correlation with CR mass and spectral structures

- probe short/long time variabilities related to heliosphere still exist in the TeV range

thank you

backup

$$R_g \approx \frac{200}{Z}\left(\frac{E}{1\,TeV}\right)\left(\frac{\mu G}{B}\right) AU$$

from the Galaxy to our local interstellar medium

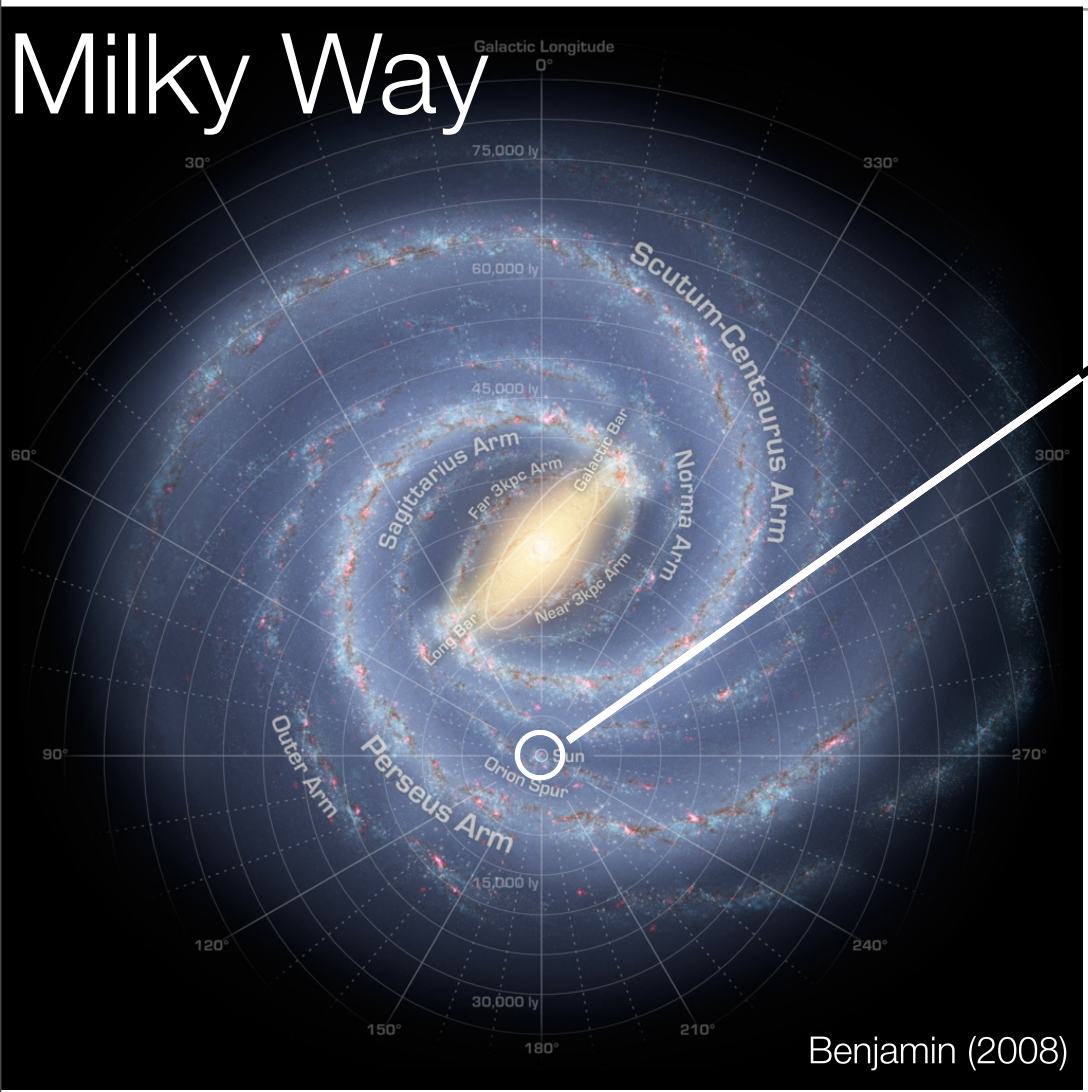

< 30,000 pc > (80 EeV)

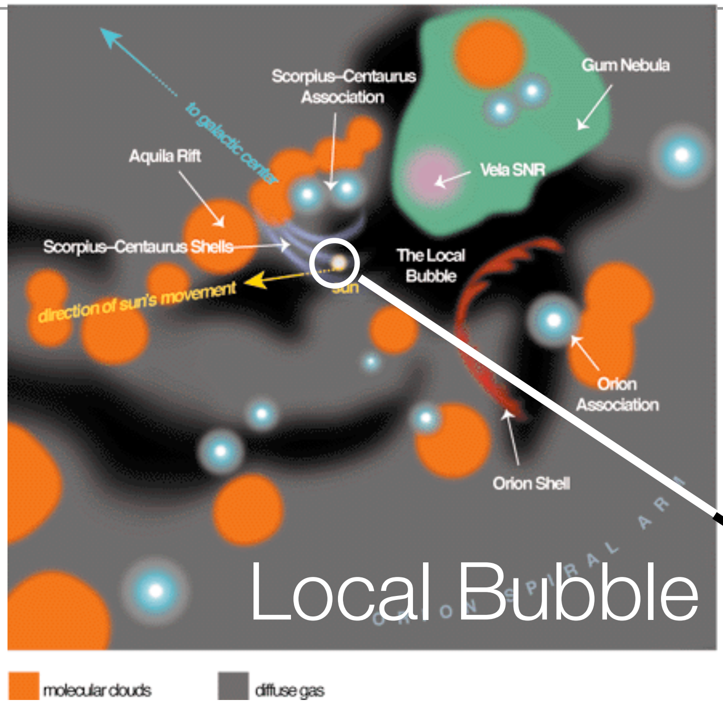

Frisch

< 500 pc > (1.4 EeV)

Frisch

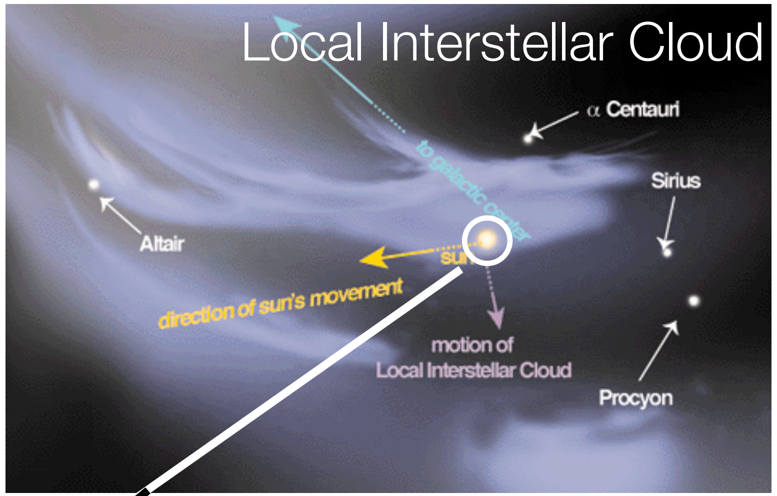

< 10-50 pc >

(30 PeV - 140 PeV)

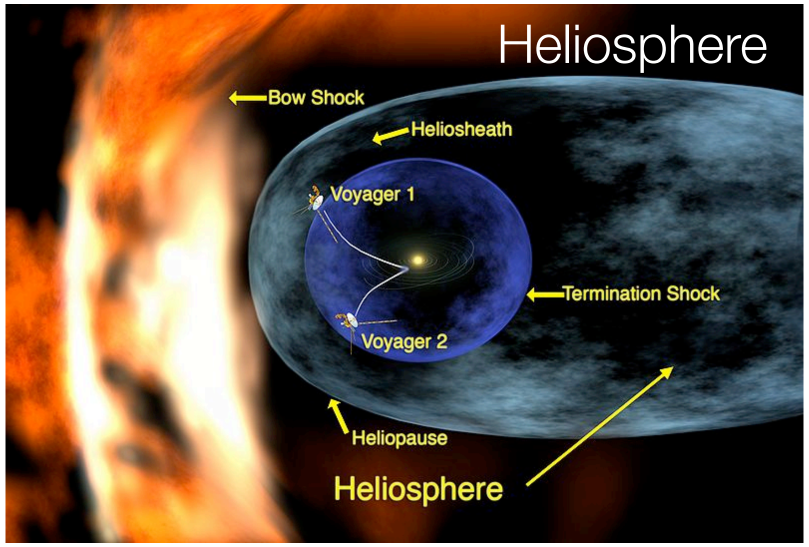

(3 TeV - 140 TeV) < 200 AU - 10^4 AU >

low energy cosmic ray anisotropy in arrival direction

Nagashima et al., J. Geophys. Res., Vol 103, No. A8, Pag. 17,429 (1998)

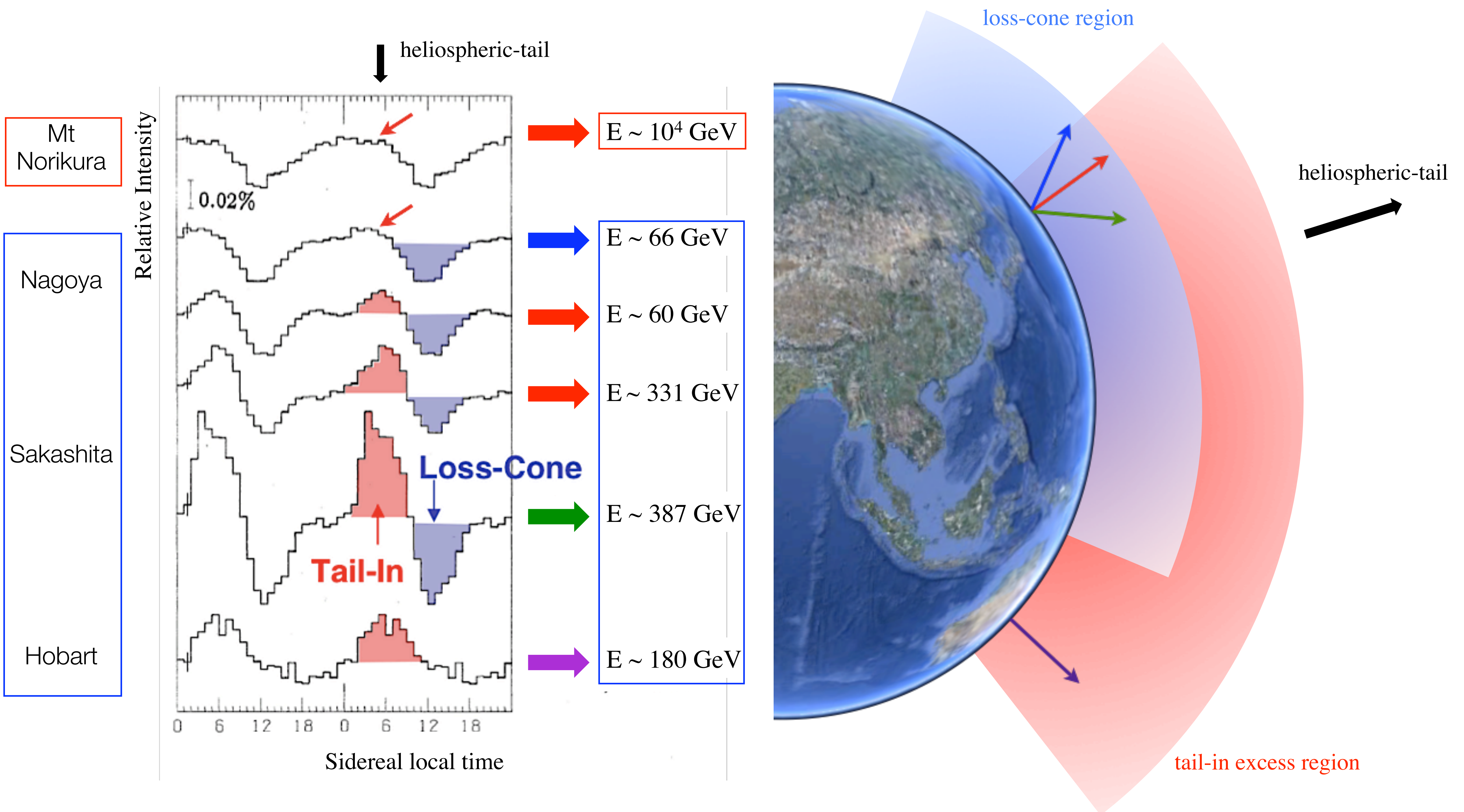

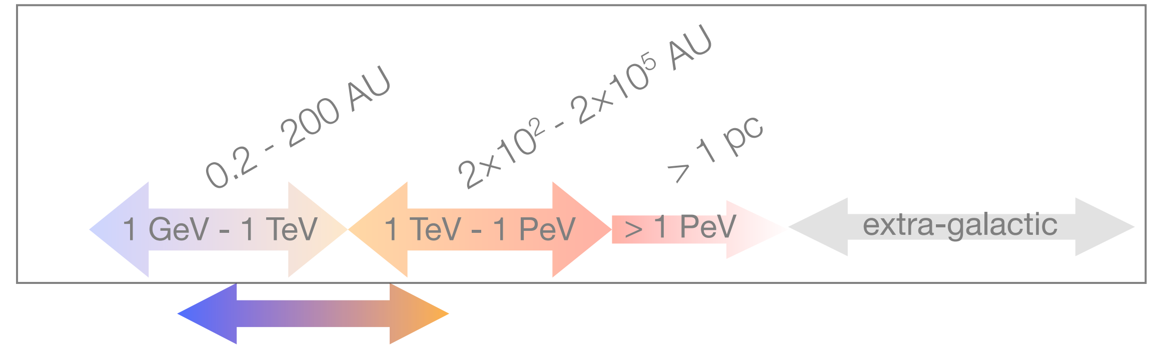

cosmic ray anisotropy

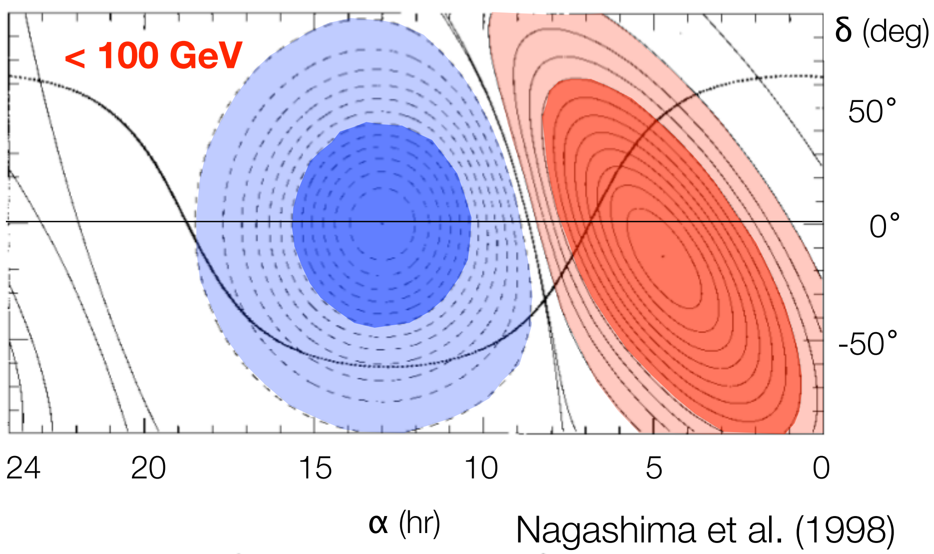

Nagashima et al. (1998)
Hall et al. (1999)

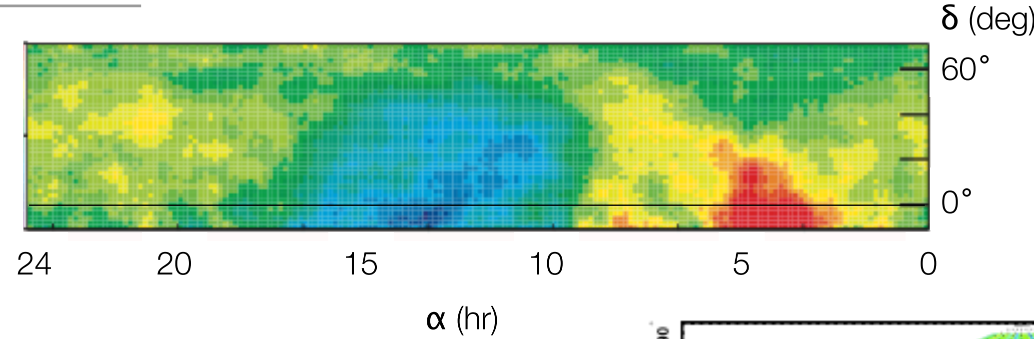

4 TeV
Tibet ASγ
Amenomori et al. (2006)

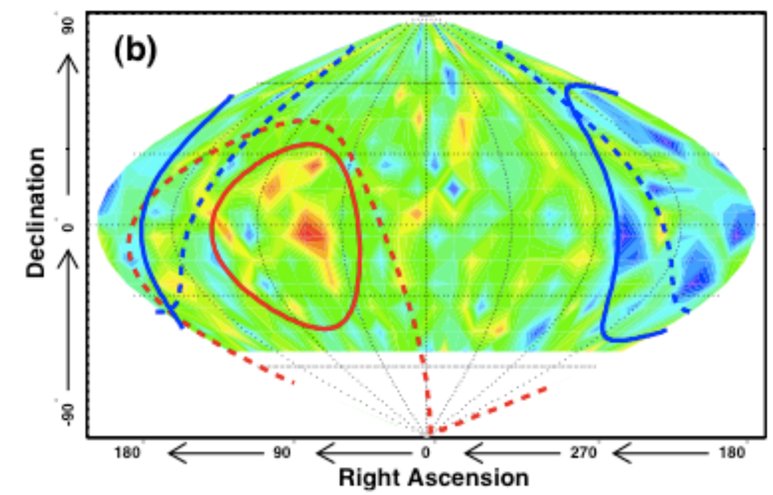

10 TeV
Super Kamiokande
Guillian et al. (2007)

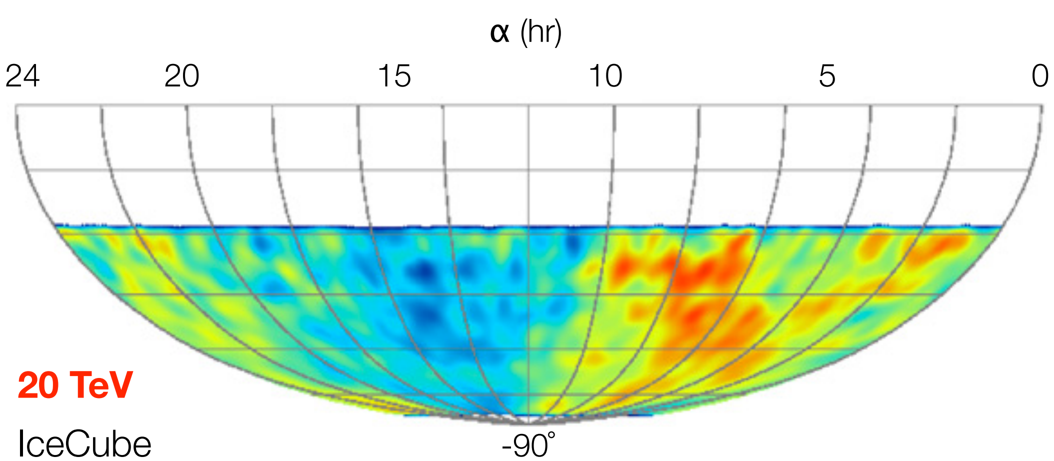

20 TeV
IceCube
Abbasi et al. (2010)

4 TeV
ARGO-YBJ
Zhang et al. (2009)

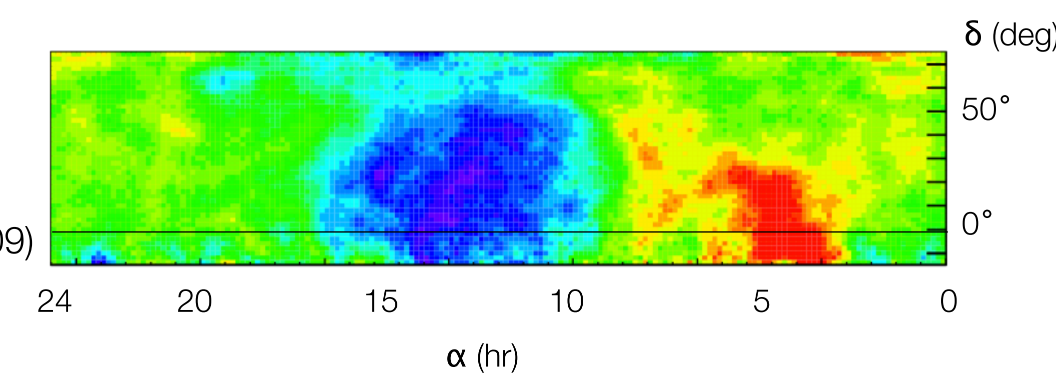

5 TeV
Milagro
Abdo et al. (2009)

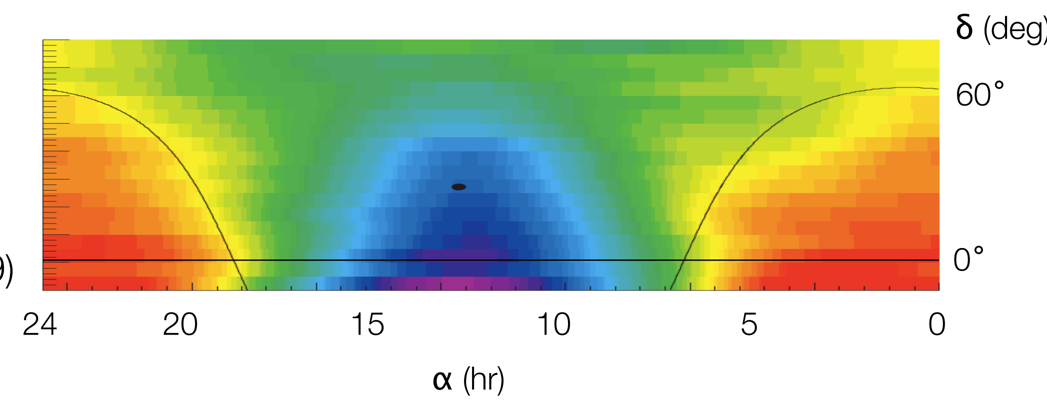

equatorial coordinates

cosmic ray anisotropy large scale
energy dependency

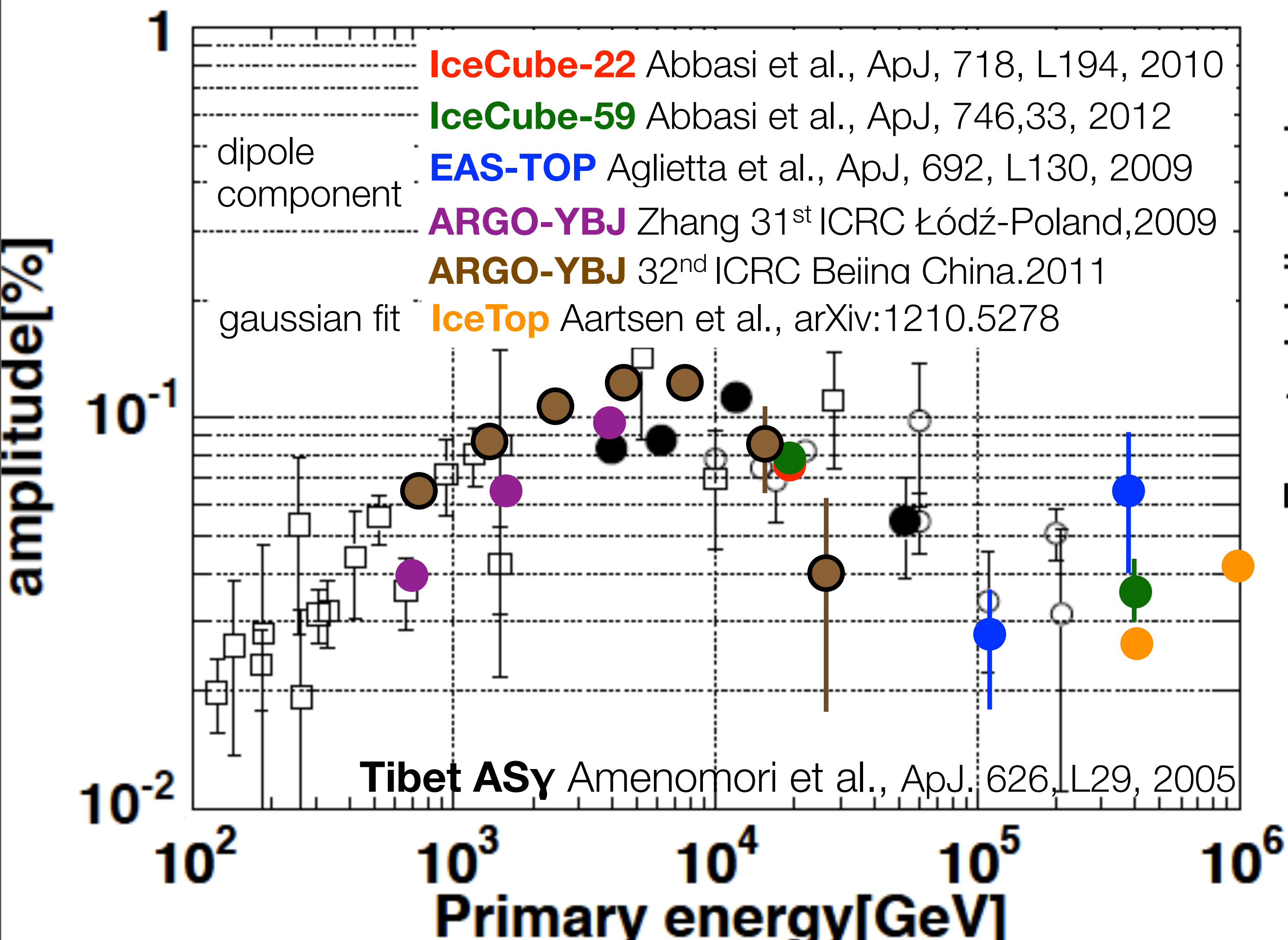

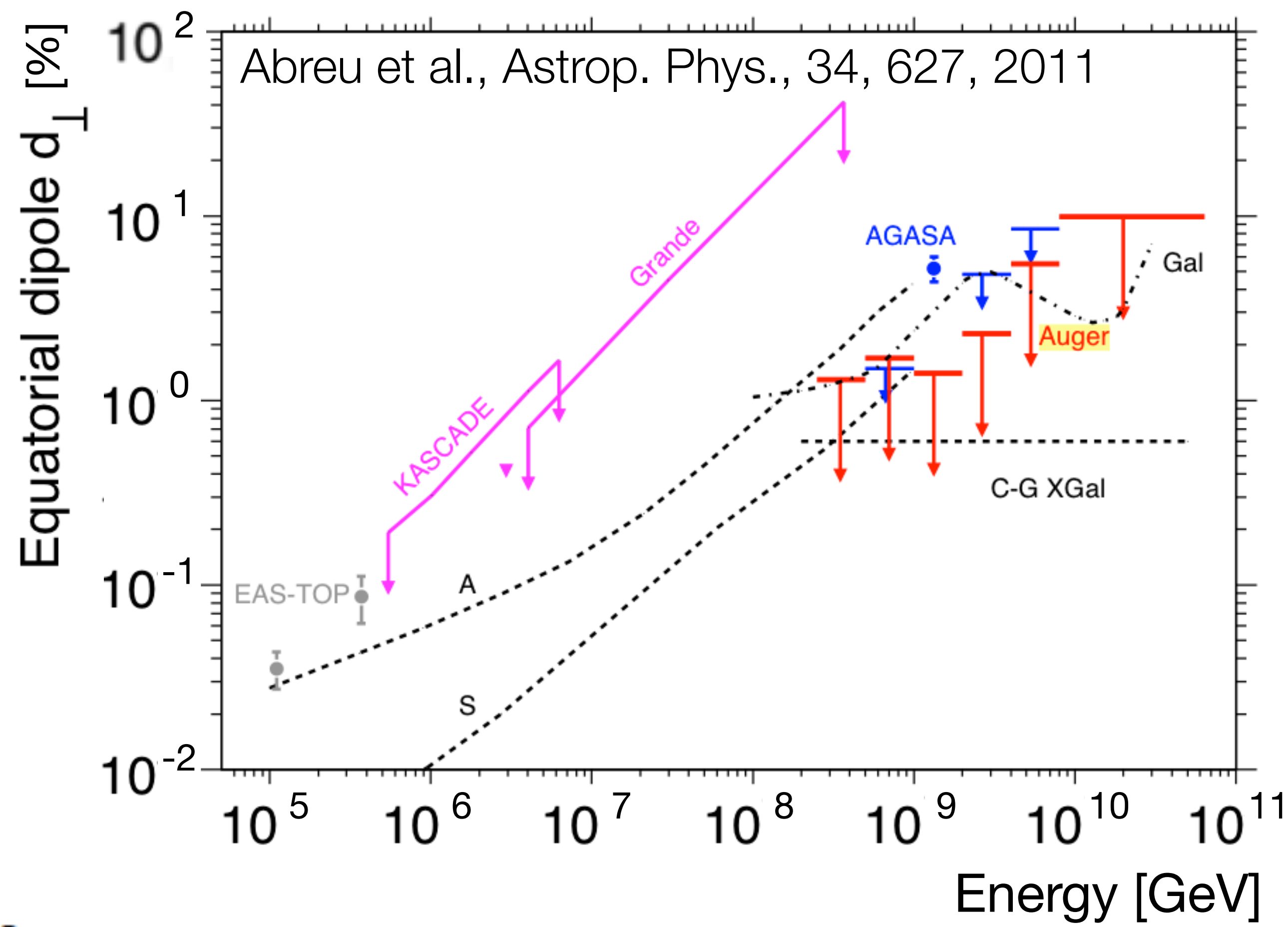

$$\delta A = \left| \sum_{SNR} \frac{eD(E)}{c} \cdot \frac{\vec{\nabla}\phi_{CR}}{\phi_{CR}}(E) \right|$$ anisotropy amplitude ~ 10^{-4}-10^{-3}

$$D(E) \approx (3-5) \times 10^{28} \cdot E^{0.3-0.6} \quad [cm^2 s^{-1}]$$ diffusion coefficient

$$\Rightarrow \delta A \propto E^{0.3-0.6}$$ anisotropy increases vs energy

cosmic ray anisotropy
angular scale structure

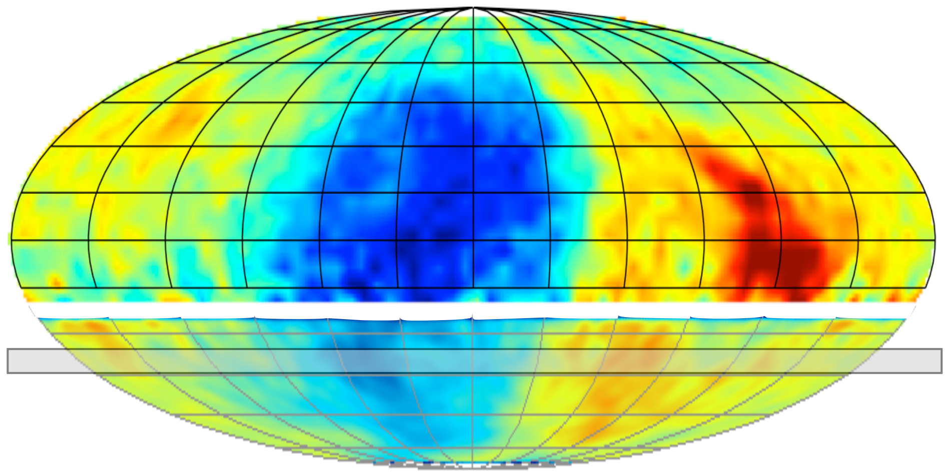

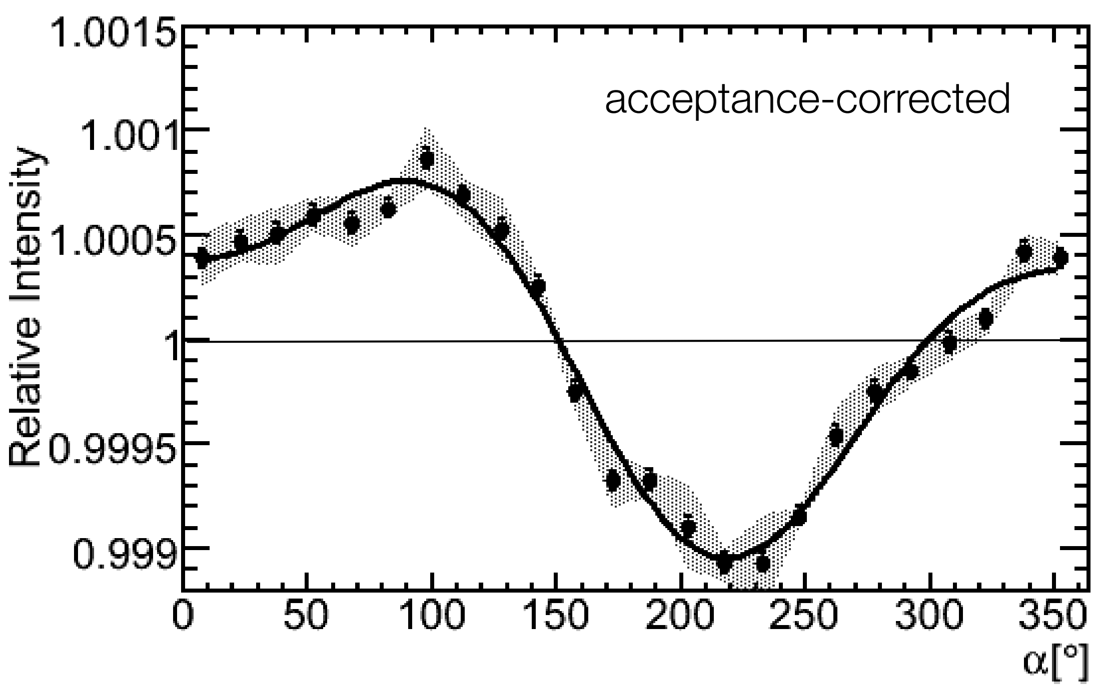

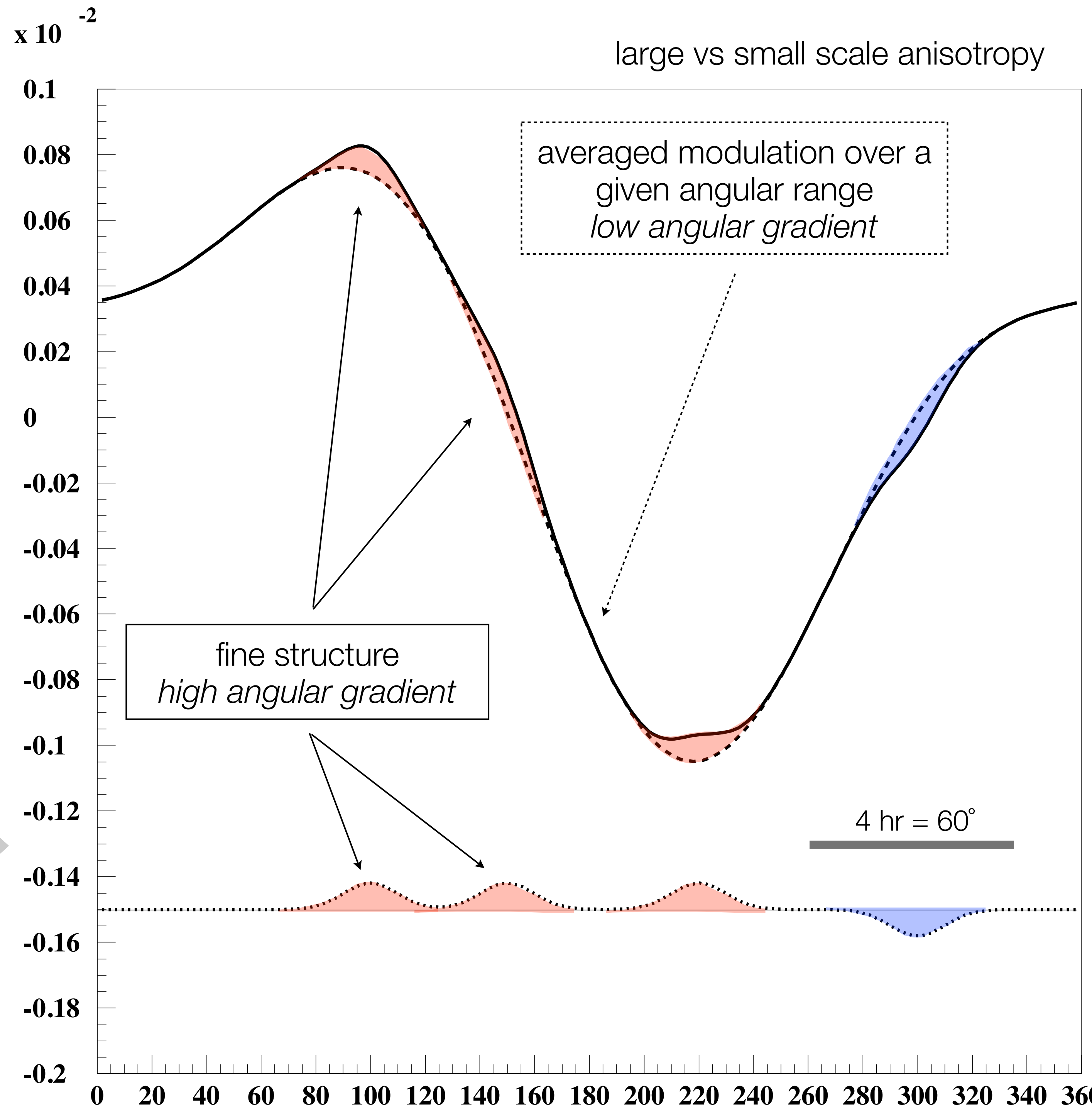

Paolo Desiati

cosmic ray anisotropy small scale
IceCube

relative intensity

raw map

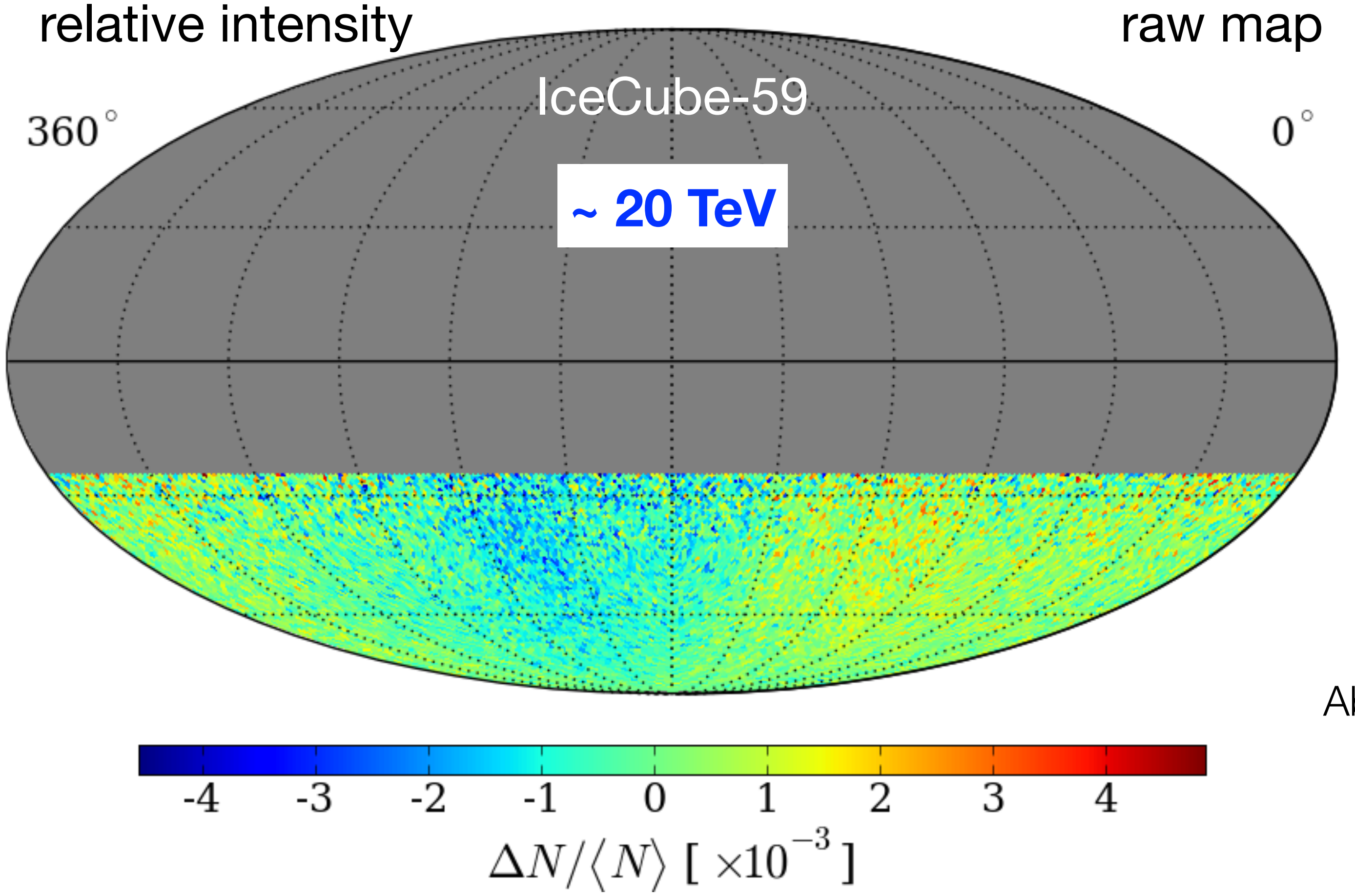

χ^2/ndf = 14743.4 / 14187

Pr(χ^2Indf) = 0.05%

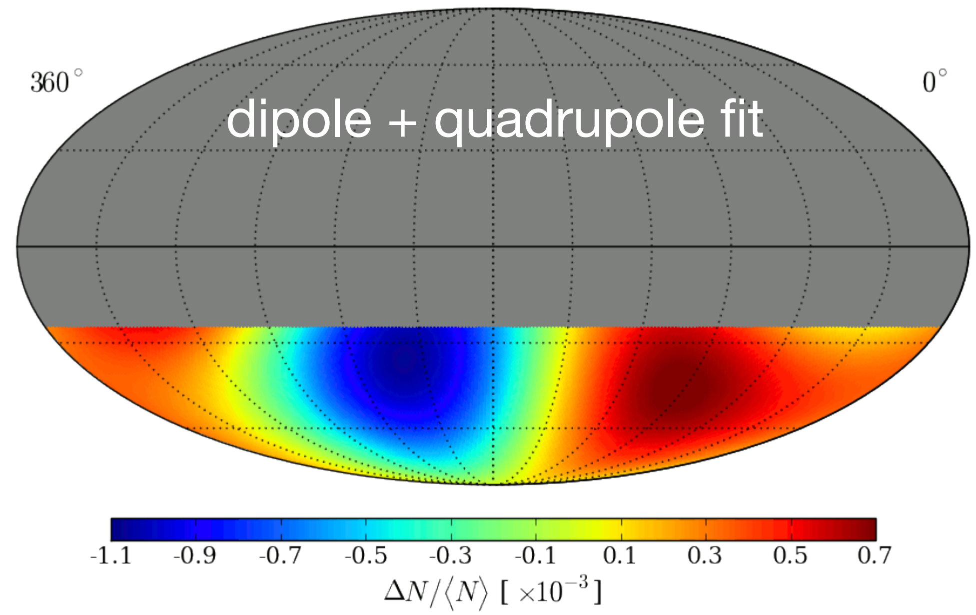

Abbasi et al., ApJ, **740**, 16, 2011

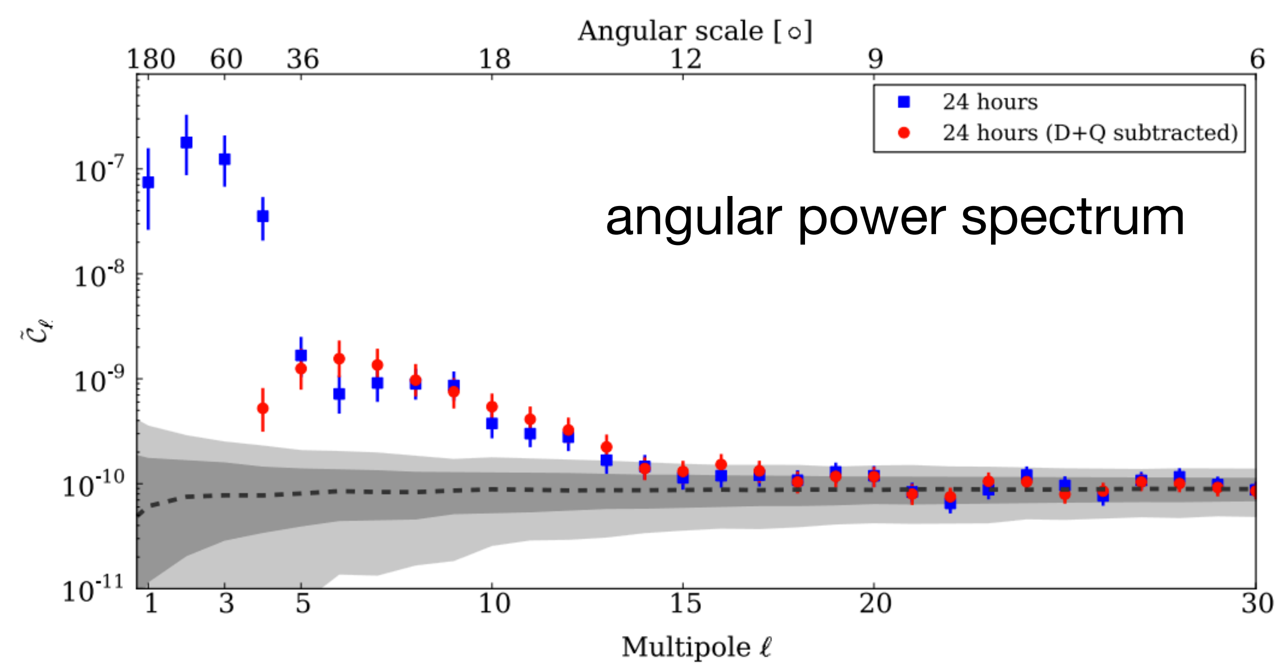

sky map contains correlations at several angular scales

in gray 60% and 95% of simulated isotropic bands

large and small scales *separated* @ ~20 TeV ?

cosmic rays observations
all-particle spectrum

Pamela
Adriani et al. (2011)

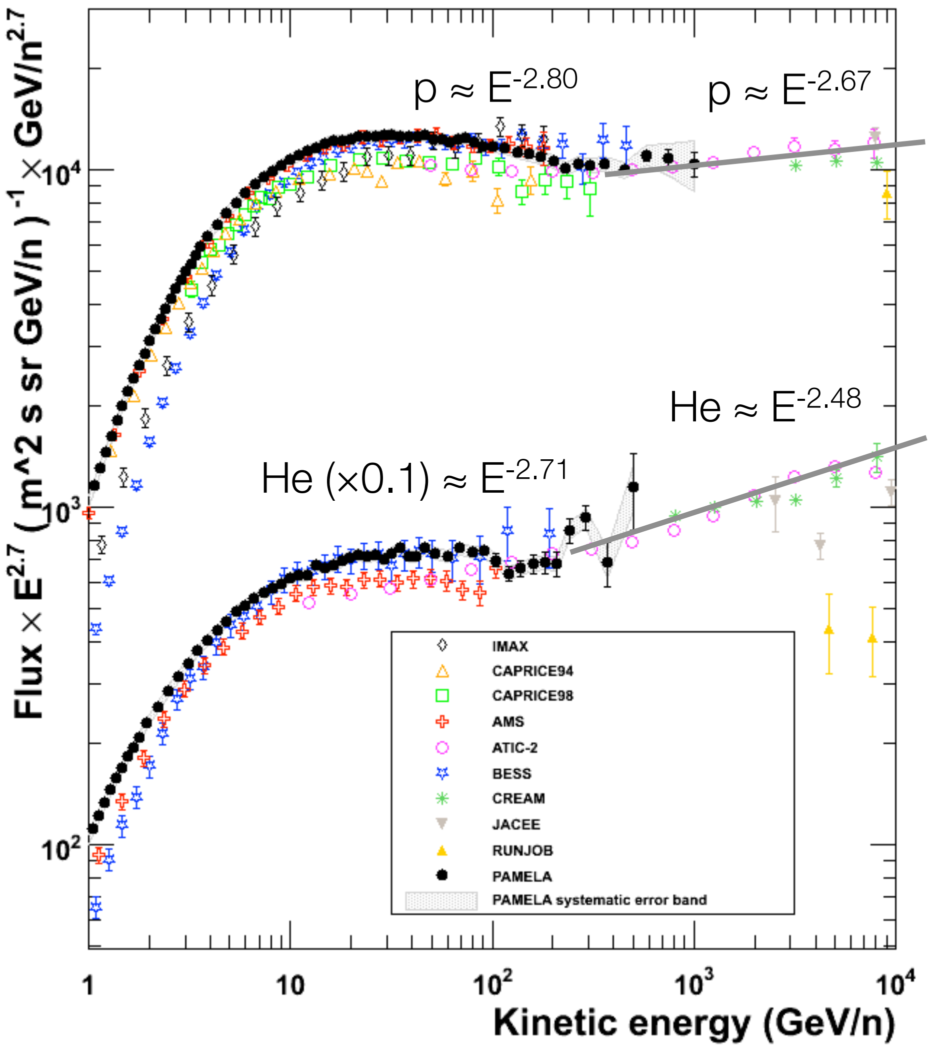

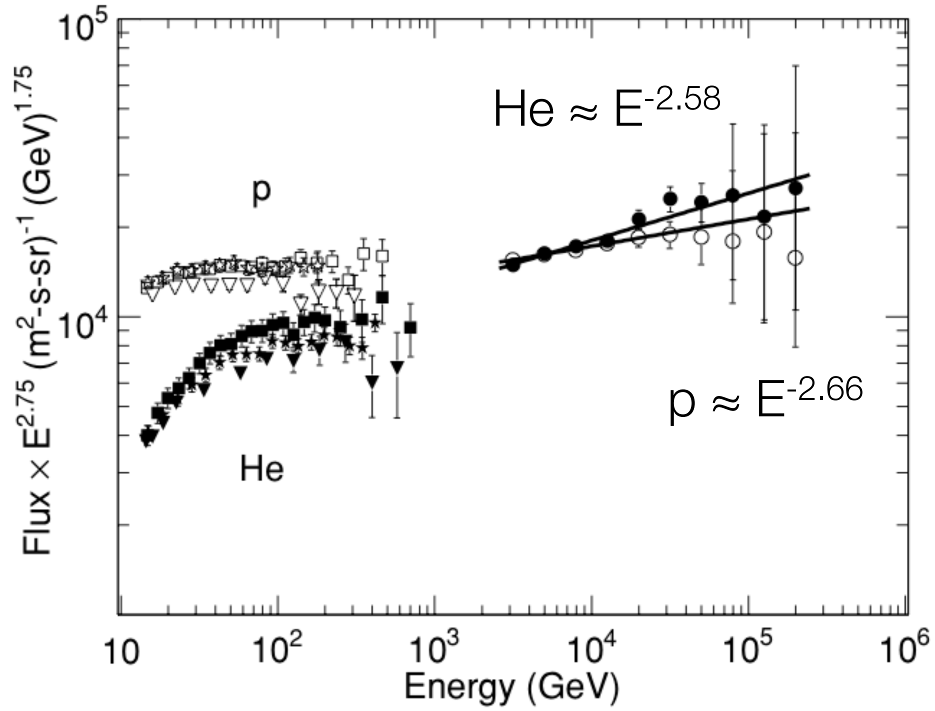

CREAM
Ahn et al. (2010)

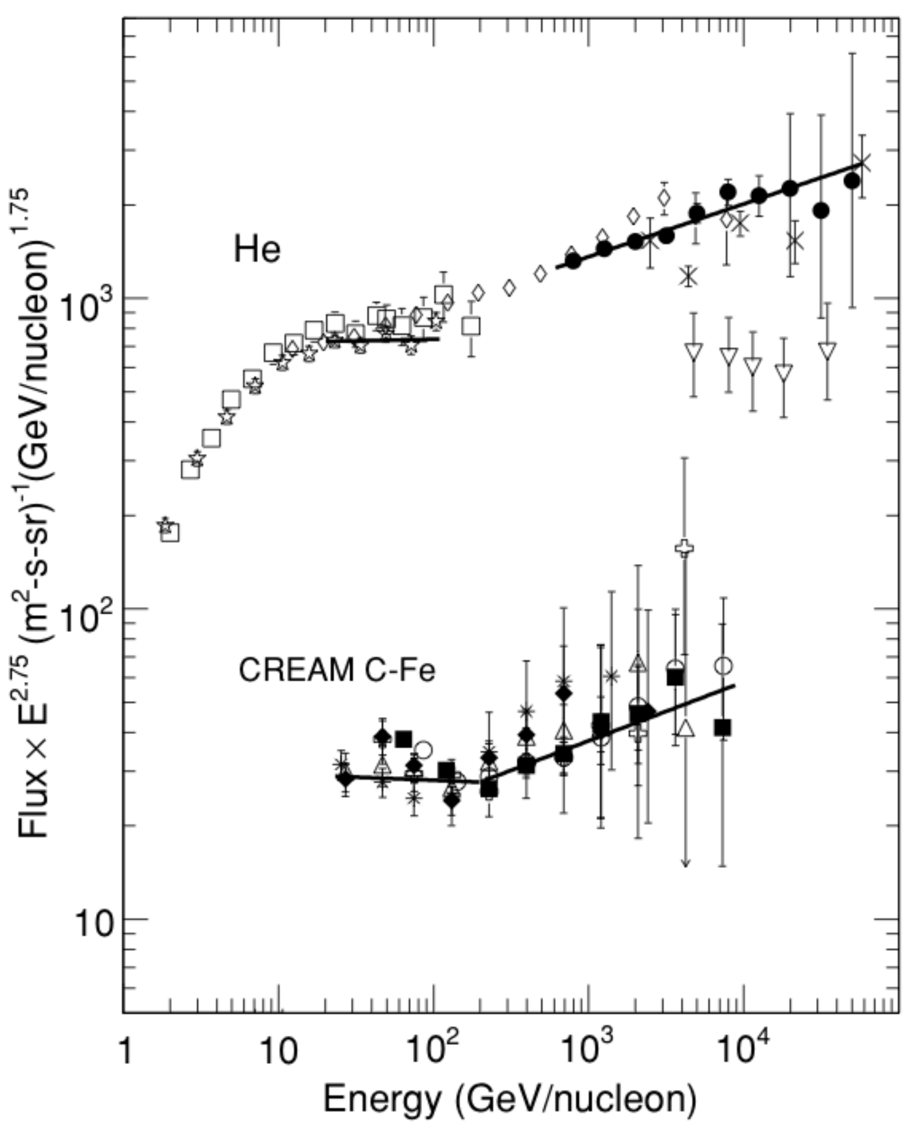

origin of spectral hardening ?

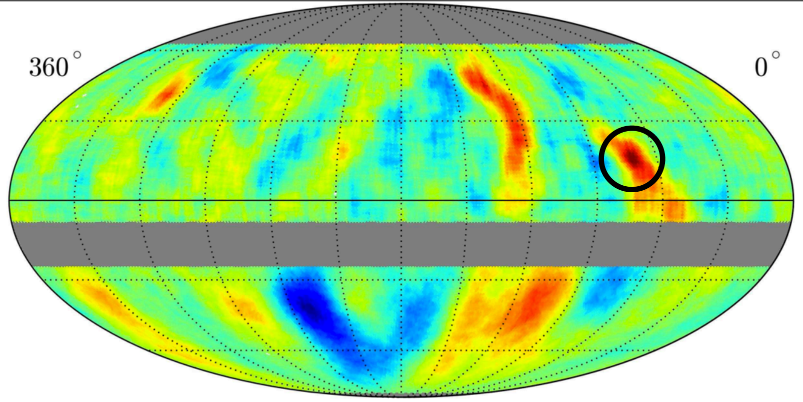

Lazarian & PD, ApJ, 722, 188, 2010

- magnetic polarity reversals due to the 22-year solar cycles produces large scale sectors
- converging of turbulent magnetic field lines can trigger reconnection and make it fast
- magnetic mirror @ single reconnection as site of acceleration (test particle)

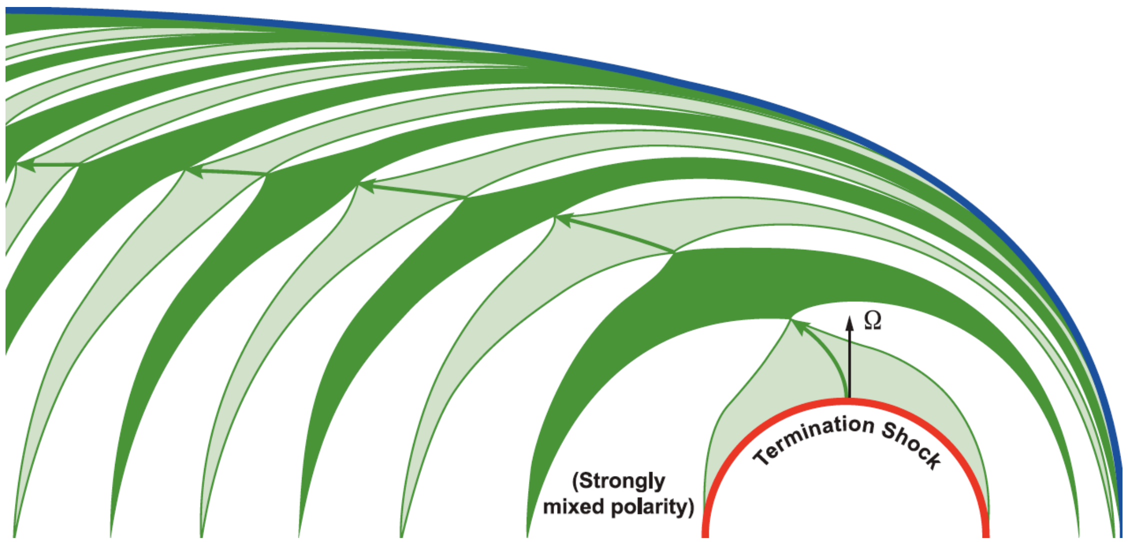

Sweet (1959) & Parker (1957)

Lazarian & Vishniac, ApJ, 517, 700 (1999)

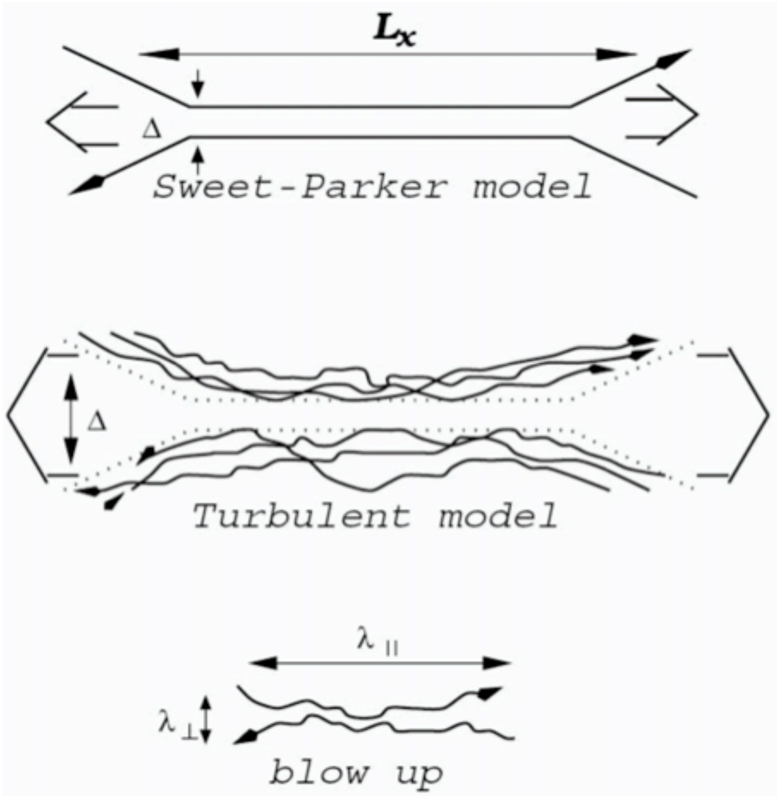

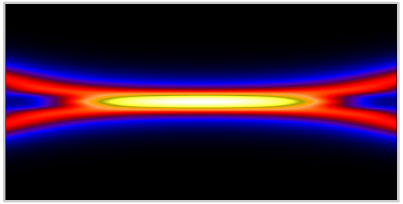

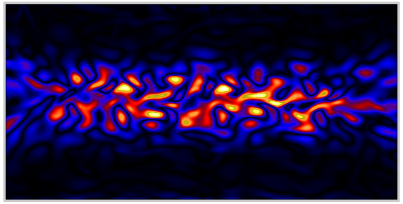

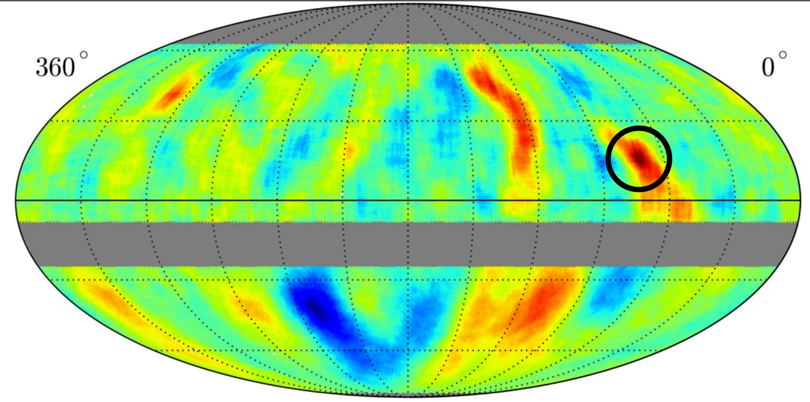

stochastic magnetic reconnection

Lazarian & PD, ApJ, 722, 188, 2010

- magnetic polarity reversals due to the 22-year solar cycles produces large scale sectors
- converging of turbulent magnetic field lines can trigger reconnection and make it fast
- magnetic mirror @ single reconnection as site of acceleration (test particle)
- 1st order Fermi acceleration

$$N(E)\,dE \sim E^{-5/2}\,dE$$

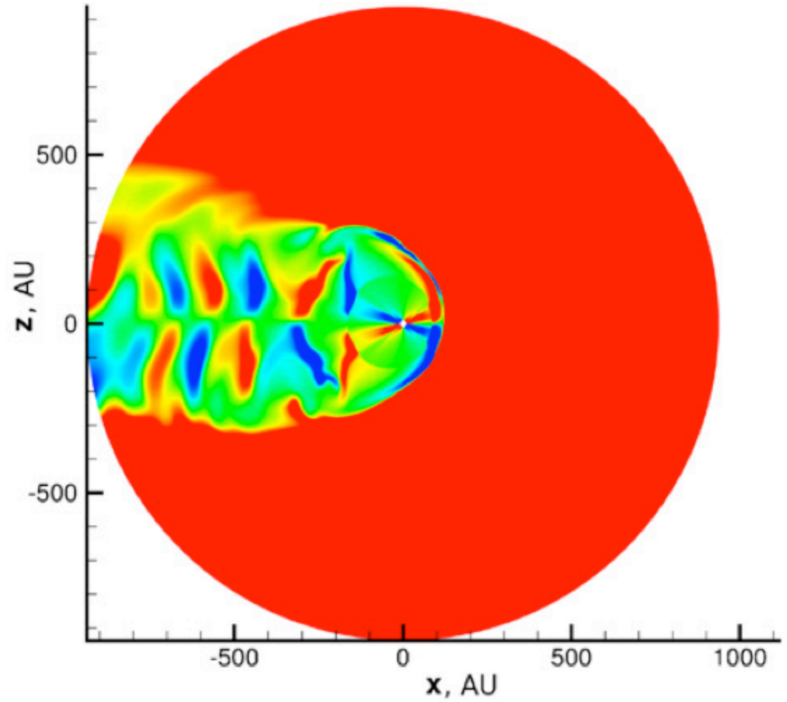

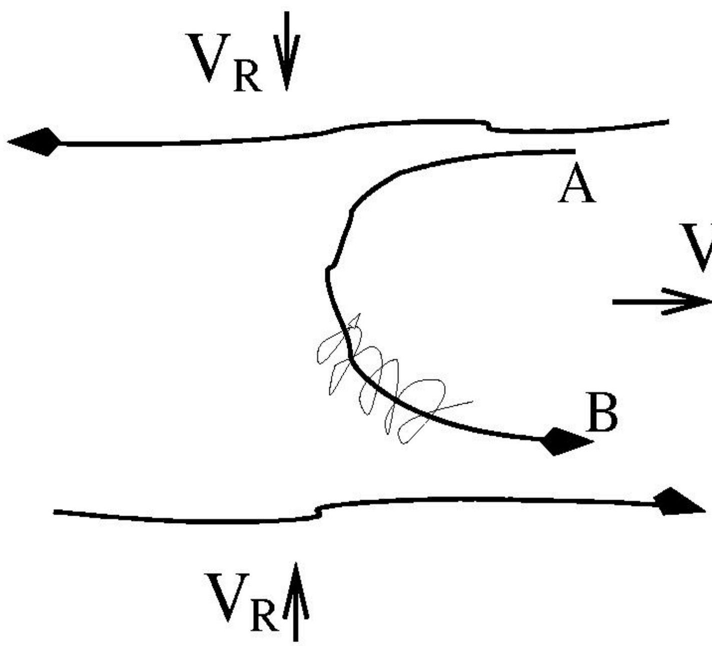

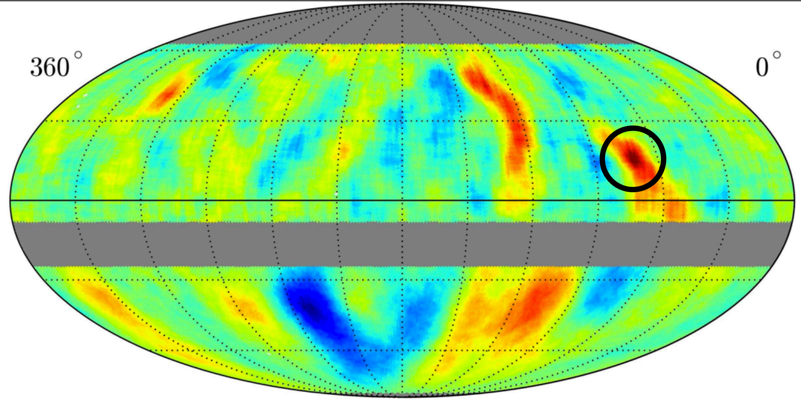

stochastic magnetic reconnection

Kowal et al., ApJ 735, 102 (2011)

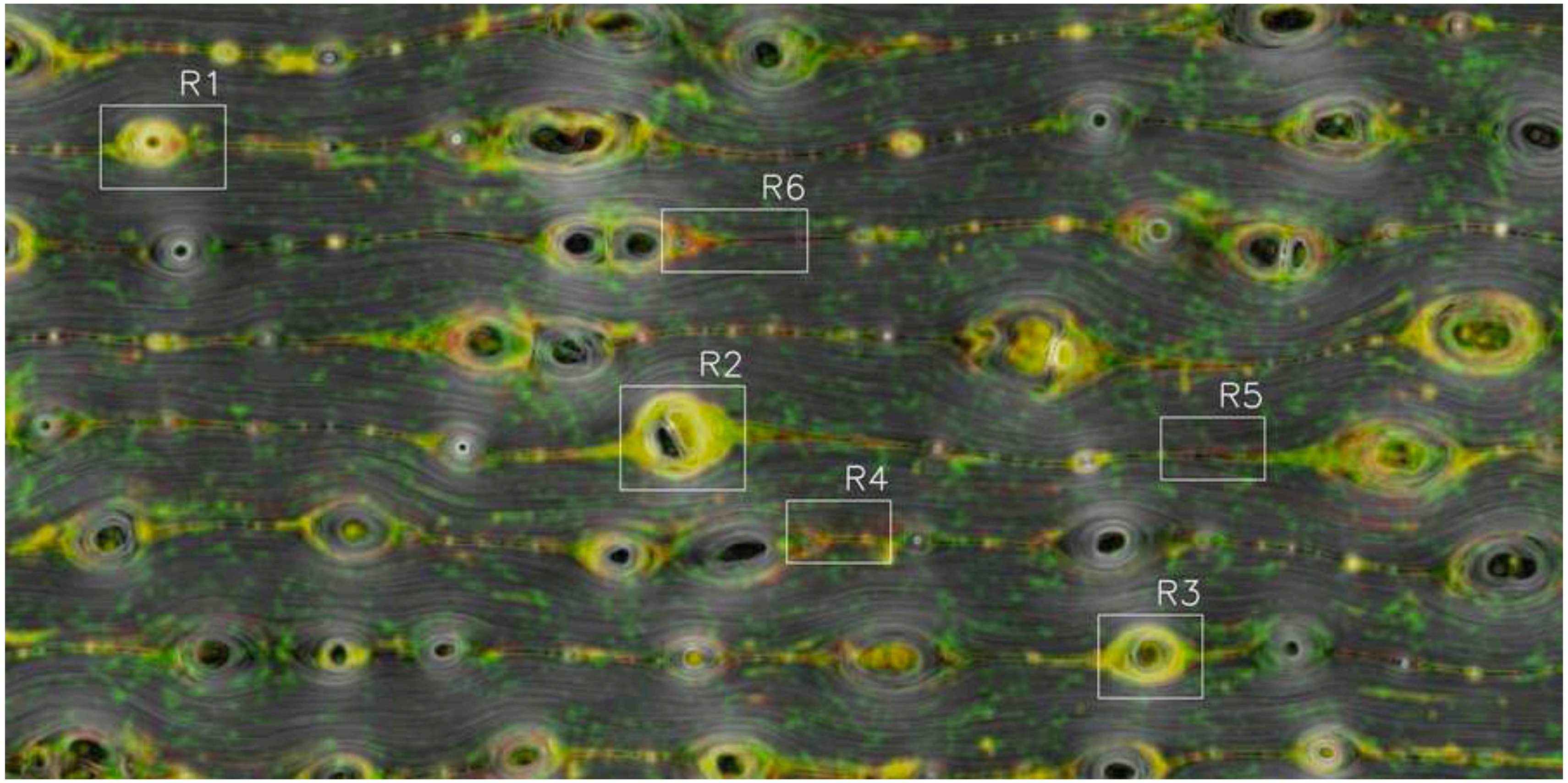

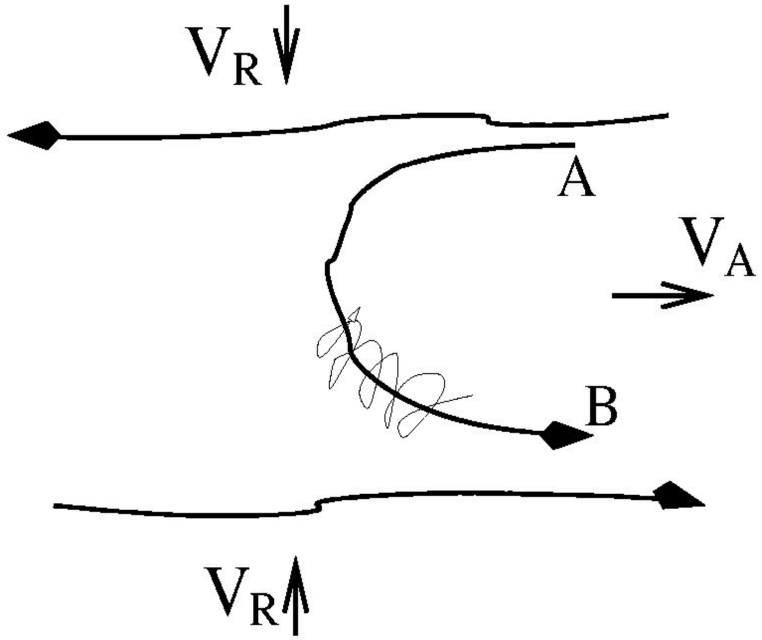

$$N(E)\,dE \;\sim\; E^{-5/2}\,dE$$

stochastic magnetic reconnection

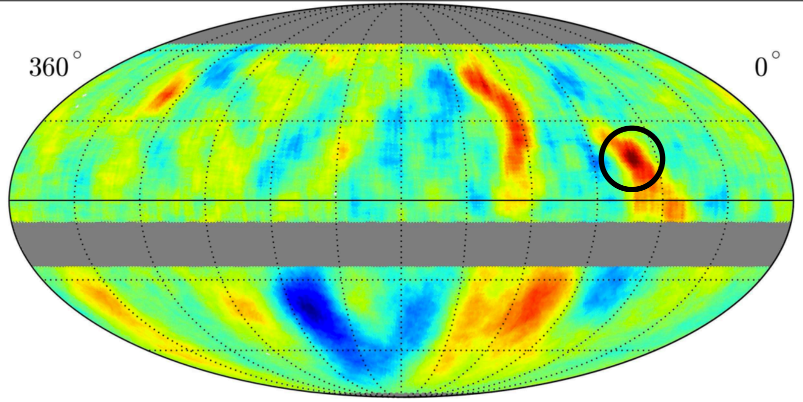

Kowal et al., ApJ 735, 102 (2011)

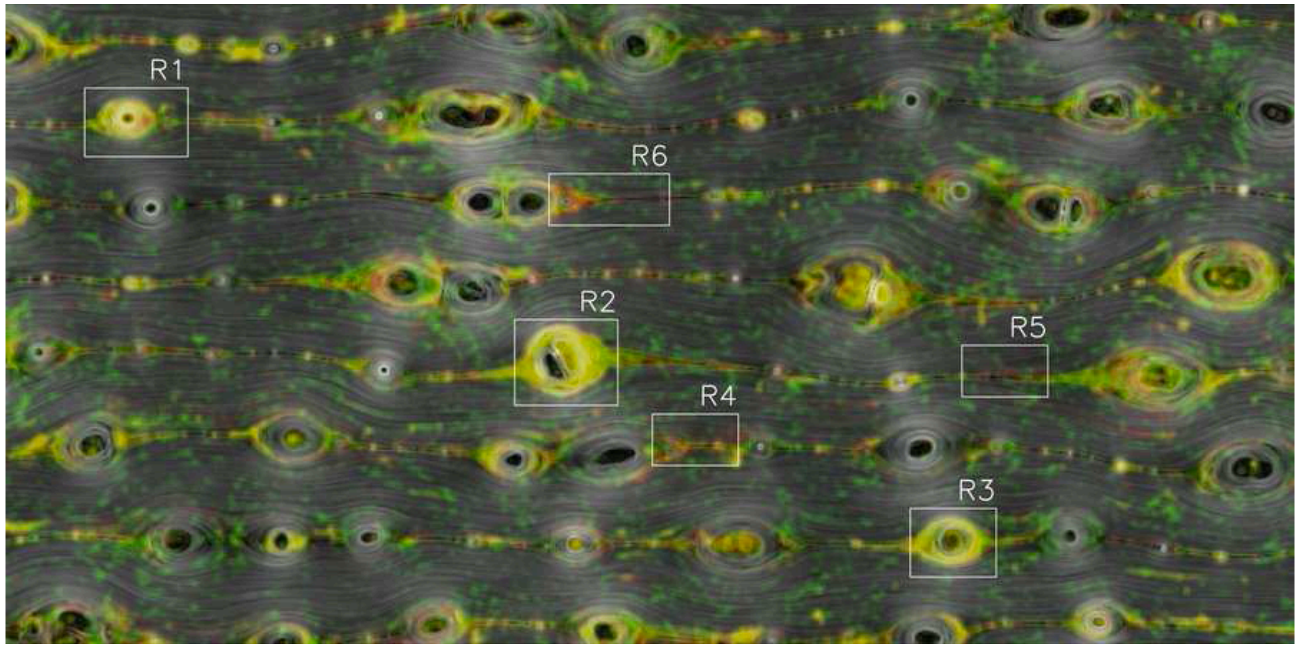

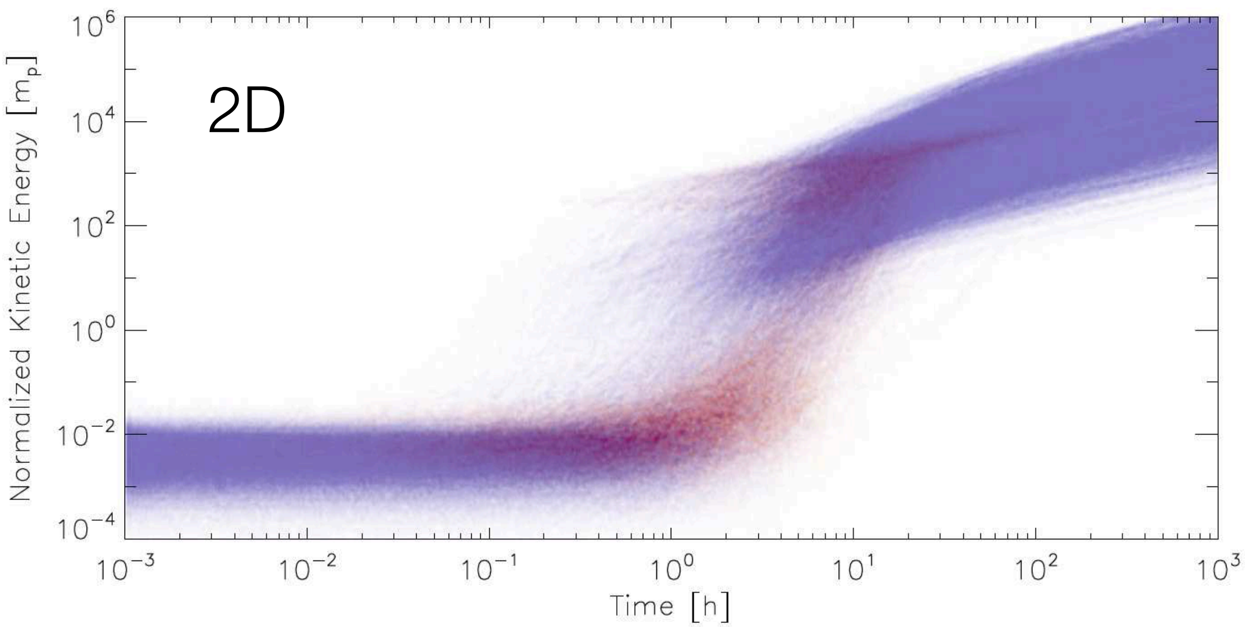

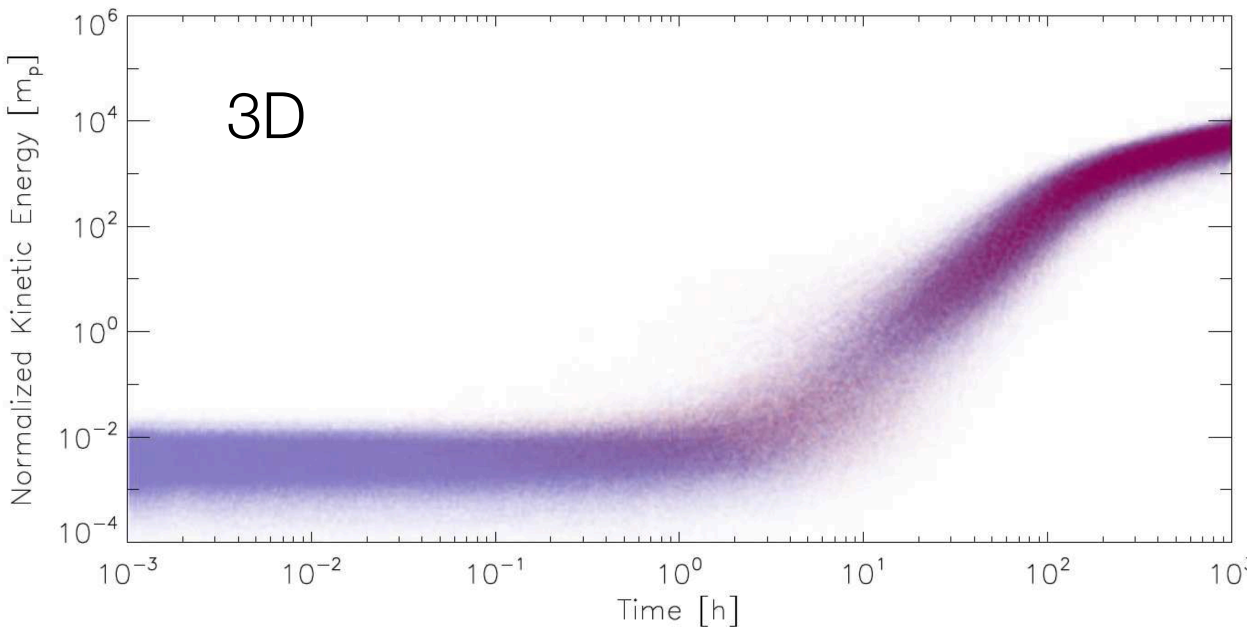

$V_\perp > V_\parallel$

$V_\parallel > V_\perp$

stochastic magnetic reconnection

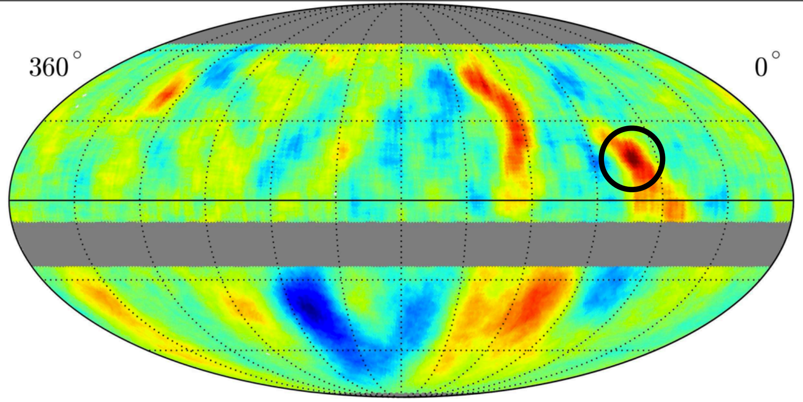

- 2nd order Fermi acceleration is dominant in purely turbulent plasmas with no converging magnetic flow

Kowal et al., PRL 2012

- if converging flow occurs 1st order Fermi acceleration is the most important

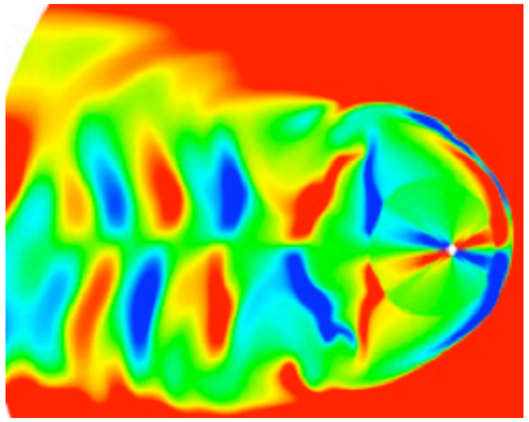

- acceleration by reconnection is efficient if scattering does not isotropize particles. Scattering expected to be minimal along the tail line of sight

$$E_{max} \approx 0.5 \left(\frac{B}{1\,\mu G}\right) \left(\frac{L_{zone}}{100\,AU}\right) TeV \approx 0.5\,-\,6\,TeV$$

- cosmic rays re-accelerated as long as trapped in large scale reconnection regions

spectral feature associated to anisotropy

Abdo A.A. et al., Phys. Rev. Lett., 101, 221101 (2008)

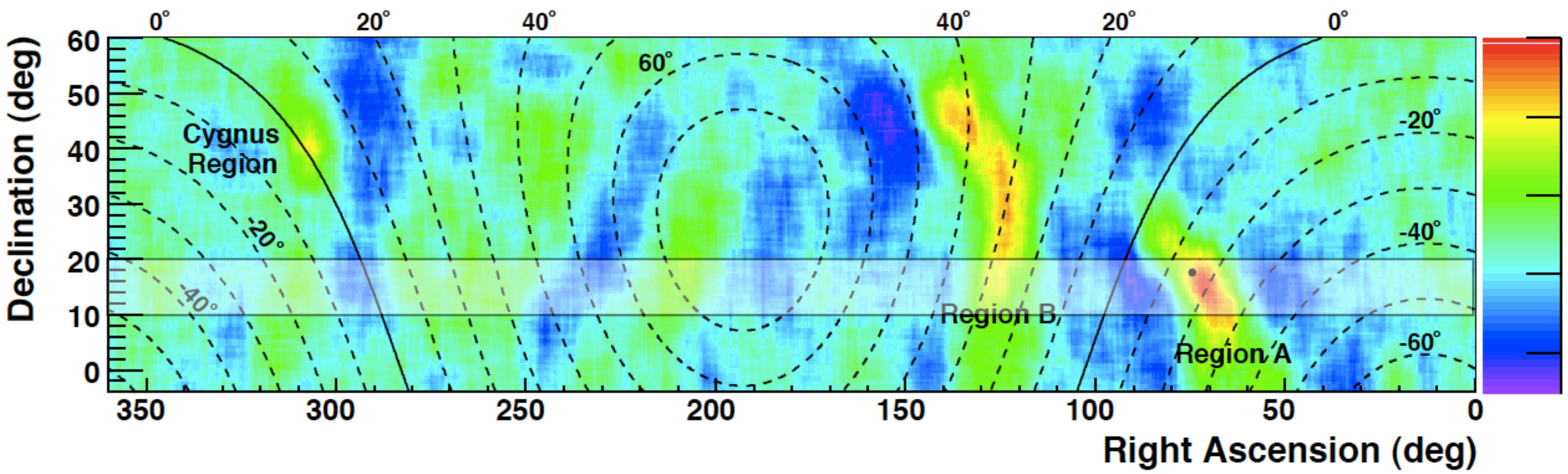

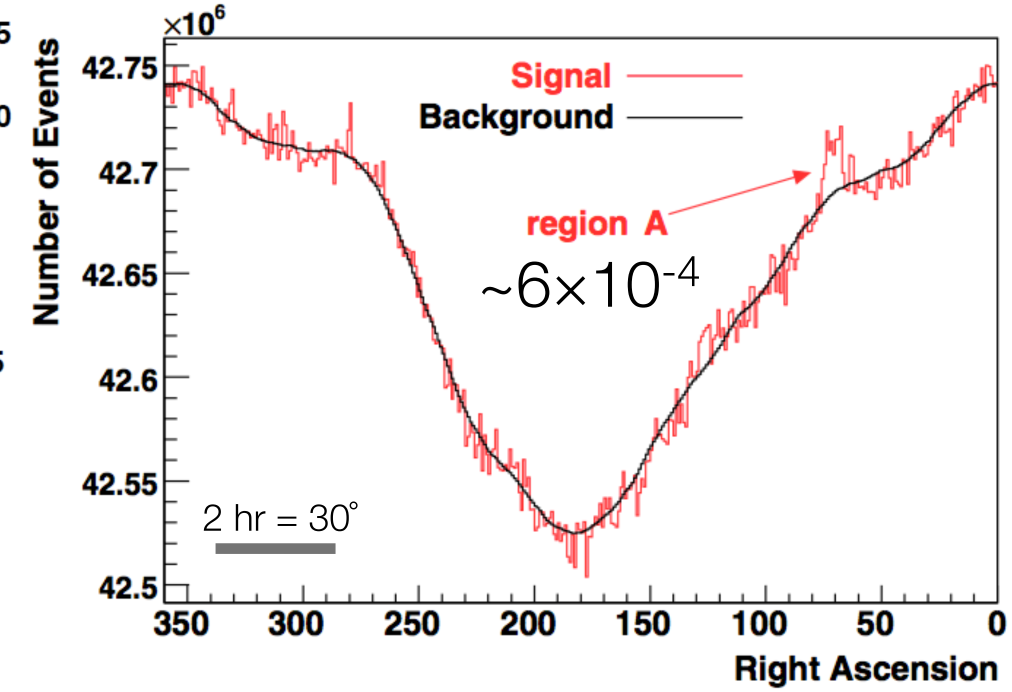

Milagro

γ < 2.7 at 4.6 σ level
E_c = 3 - 25 TeV

E_{flux}(10GeV-10TeV) ~ 10^{-9} - 10^{-8} erg cm^{-2} s^{-1} (γ = 2.7 - 2.0)

$\langle P_{re\text{-}acc} \rangle$ ~ 10^{20} - 10^{22} erg s^{-1}

$\langle P_{solar\ wind} \rangle$ ~ 10^{27} erg s^{-1} (Parker, 1962)

PD, Lazarian, NPG, **19**, 1, 2012

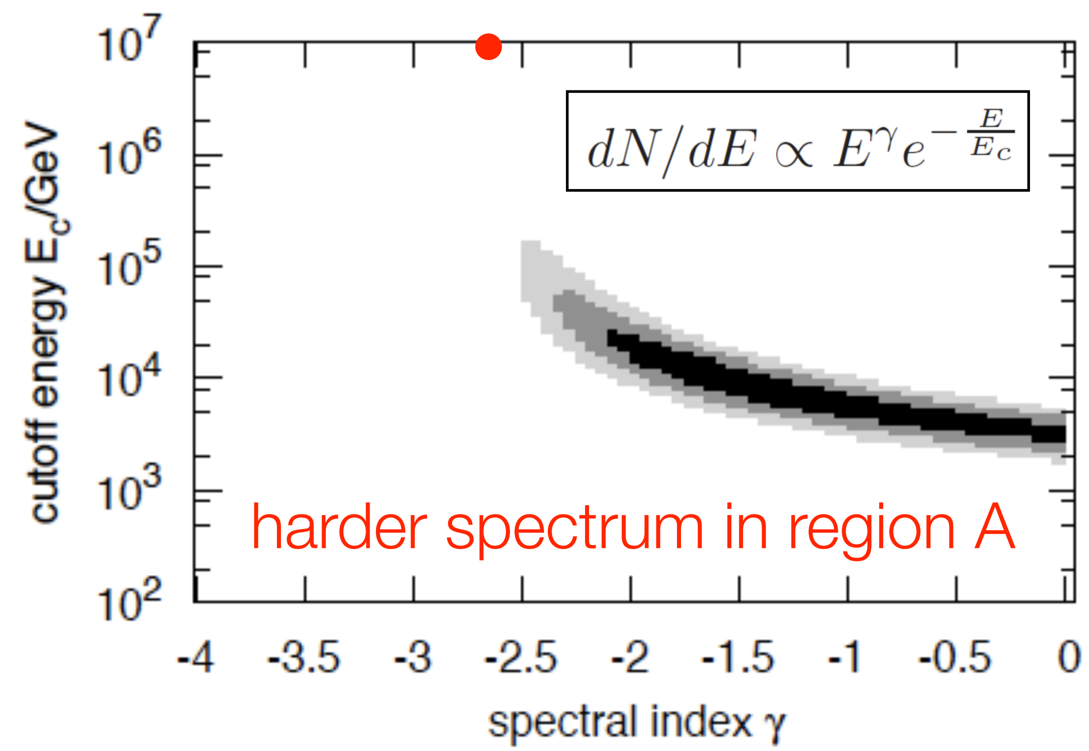

cosmic ray anisotropy
astrophysical origin ?

- stochastic effect of recent nearby CR sources
  - influences spectrum and global arrival direction
  - diffusive scenarios to explain observed features

Dorman+ 1985
Ptuskin+ 2006
Erlykin & Wolfendale 1997, 2001, 2006
Sveshnikova+ 2013
Blasi & Amato 2011, 2012
Pohl & Eichler 2012

Salvati & Sacco 2008
Drury & Aharonian 2008
Salvati 2010

- propagation effects in turbulent ISMF

Battaner+ 2009
Malkov+ 2010

- convection from persistent magnetized flow field from old SNRs

Biermann+ 2012

- breakdown of diffusion regime via scattering with ISMF turbulence

Giacinti & Sigl 2011

- diffusion cannot explain the observed **non-dipolar** topology & **small angular scales**
- limitations on single power-law assumption and spacial dependency of diffusion coeff.

scattering on heliospheric boundary
toy model

PD & Lazarian, ApJ, **762**, 44, 2013

$$N_b = n_{\mathrm{CR}}\, P_s\, R_E^2 \int_{R_H}^{R_H + dR_H} dr \int_0^{2\pi r} dl \int_0^{\infty} \frac{dz}{z^2 + r^2}$$
$$= n_{\mathrm{CR}}\, P_s\, \pi^2\, R_E^2\, dR_H,$$

$$N_d = n_{\mathrm{CR}}\, 4\pi\, R_E^2\, c\, \tau.$$

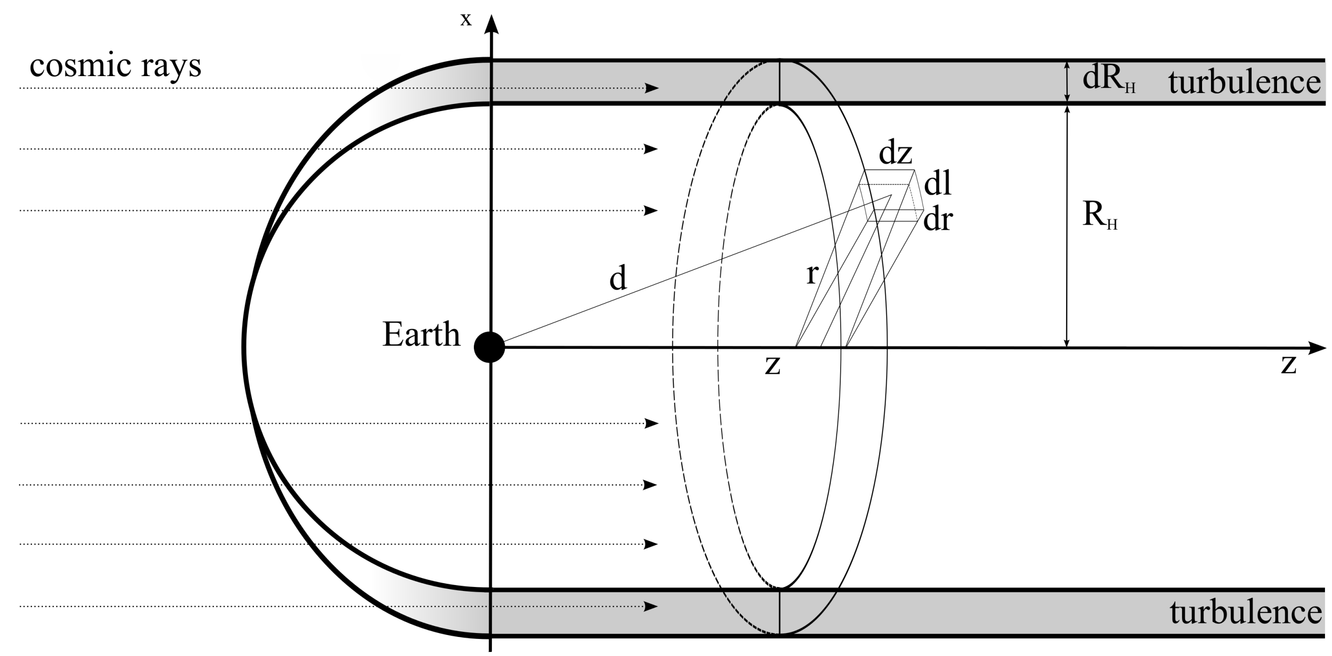

$$\delta = \frac{N_b - N_d}{N_b + N_d} = \frac{N_b/N_d - 1}{N_b/N_d + 1},$$

$$\frac{N_b}{N_d} = \frac{3\pi}{4}\, P_s\, \frac{dR_H}{c\,\tau}.$$

$\delta \gtrsim 0$, $\quad P_s \gtrsim 100/dR_H$

scattering at heliospheric boundary

heuristic model